EXPLORATION OF THE STRUCTURE AND ACTIVITY OF BIMETALLIC CATALYSTS FOR THE DECHLORINATION OF CHLOROCARBONS

by

David Richard Luebke

Bachelor of Science in Chemical Engineering, University of Arkansas, 1998

Submitted to the Graduate Faculty

School of Engineering in partial fulfillment

of the requirements for the degree of

Doctor of Philosophy

University of Pittsburgh

2002

UNIVERSITY OF PITTSBURGH

SCHOOL OF ENGINEERING

This dissertation was presented

by

David R. Luebke

It was defended on

April 15, 2002

and approved by

Vladimir Kovalchuk, Research Professor, Chemical Engineering

Irving Wender, Distinguished University Research Professor, Chemical Engineering

Jorg Wiezorek, Assistant Professor, Material Science and Engineering

Thesis Advisor: Julie d'Itri, Associate Professor, Chemical Engineering

ABSTRACT

Initials _____
Julie L. d'Itri

EXPLORATION OF THE STRUCTURE AND ACTIVITY OF BIMETALLIC CATALYSTS FOR THE DECHLORINATION OF CHLOROCARBONS

David Richard Luebke

University of Pittsburgh

There is increasing demand for technologies that can transform wastes, such as the chlorocarbon byproducts of many industrial reactions, into useful process intermediates or commercial products. While the conversion of chlorocarbons into paraffins is technologically feasible and has been widely studied, there are significant economic incentives to produce olefins. Bimetallic catalysts, in which the metal type and concentration can be used to "tune" catalytic performance, offer considerable promise in this area.

The catalytic performance of PtCu/C with Cu/Pt atomic ratios from 0 and 18 and 0.5 percent weight loading Pt in the reaction of 1,2-dichloroethane dechlorination at 200°C and atmospheric pressure was investigated to understand the molecular

phenomena governing the change in ethylene selectivity with time on stream (TOS). Chapter 3 examines this transient period by varying catalytic pretreatment. It was theorized that alloy formation, not present after standard pretreatment, results in the formation of ethylene at long TOS.

To better understand the molecular phenomena at work with the industrially relevant, carbon-supported catalysts, experiments were undertaken using model silica-supported catalysts. In Chapter 4, a catalytic performance study of a series of these catalysts was undertaken in the dechlorination of 1,2-dichloroethane and complimented by kinetic studies including examination of ethylene hydrogenation, pulse kinetic behavior of the catalysts in dechlorination, and chemisorbtion of CO by FTIR. Large Pt ensembles were found to be present only in catalysts which were ethane selective.

Although a significant improvement over carbon-supported systems, silica-supported catalysts with weight loadings of 0.5 percent Pt proved to be too highly dispersed to allow many techniques to be used. Thus, a series of catalysts was synthesized with 3.0 weight percent Pt, but these catalysts proved to be highly sensitive to exposure to atmospheric moisture. In Chapter 5, the interactions of these catalysts with water are characterized by examining the kinetic performance before and after exposure to water, comparing several types of precursors, and conducting temperature programmed reduction, transmission electron microscopy, and Raman

spectroscopy. The effect of water was attributed to alleviation of the chromatographic separation of metals which occurs during the impregnation procedure.

In Chapter 6, the effect of CO on the catalytic performance of the higher weight loading catalysts was studied. Carbon monoxide was found to split large Pt ensembles in much the same manner as alloy with Cu leading to ethylene selectivity in bimetallic catalysts which would otherwise be selective to ethane.

DESCRIPTORS

Bimetallic	Catalyst
Chlorocarbon	Cu
Ensemble	Kinetic
Mechanism	Pt

FOREWORD

As I complete my Ph.D. work, the conclusion of 22 years of education, I consider it an excellent time to say thank you to a few of the people who have helped me along the way. To my mother...I owe her more than I can ever say. She taught me to think, to dream, and to believe. To my father...who taught me by example what it is to be a man and that sometimes there just isn't any substitute for blood and sweat. To my brother...who challenges me like no one else. To my sister...who taught me that sheer force of will can sometimes make dreams come true.

To my wife...who keeps me sane and makes me strong, who taught me to relax if only a little, who reminds me who I am when I get lost in the quests of the moment, and who tolerates me when no one else can.

To my advisor, Professor Julie d'Itri...who encourages me to get up when I stumble, even if it is occasionally by kicking me, who taught me to ask the right questions, not take the details for granted, and that some of us are at our most creative when we're in over our heads and struggling to figure out where the next breath is coming from. To Professor Vladimir Kovalchuk...who taught me chemistry and to defend my ideas fiercely or not at all. To Gus Sill, Professor Victor Borovkov, Professor Irving Wender, Prof. Jorg Wiezorek, Dr. Kintu Early, Dr. Subodh Deshmukh, Dr. Lalith Vadlamannati, Dr. Parag Kulkarni, Minghui Zhang, Vladimir Pushkarev, Debasish Chakraborty, and Dimitry Kazachkin...who have reviewed my work and contributed to it. And to the Department of Energy...who funded my work

TABLE OF CONTENTS

Page

LIST OF TABLES

LIST OF FIGURES

1.0 INTRODUCTION

1.1 Environmental Impact of Chlorocarbons

Chlorocarbons are one of the most versatile and widely used classes of compounds in the industrial world. Used by organic chemists in the laboratory well before the development of the chemical industry, they spread into every aspect of its development. Beyond simple process intermediates and starting materials, chlorocarbons once found use in every aspect of human existence from dry cleaning[(1)*] to warfare[(2)] to childbirth.[(3)] As with so many other aspects of the industrial revolution, the true consequences of the widespread use and disposal of chlorocarbons did not become apparent until a great deal of damage to human health and the environment had already been done.

While the toxicity of chlorocarbons in high doses had never been in doubt,[(2)] it was only with the environmental awakening of the 1960's that full stock began to be taken of the environmental damage wrought by these compounds.[(4)] Revelations about the carcinogenicity of even small doses of certain chlorocarbons brought even industrialists to reduce their resistance to regulations governing their disposal.[(5)] The true breakthroughs came in 1955 and 1972 with the passage of the Clean Air Act and Clean Water Act and with the founding of the Environmental Protection Agency in 1970.[(6)] After nearly a hundred years of industrial use, chlorocarbon emission and disposal would at last be monitored in earnest.

---

* Numerical References Superior to the Line refer to Bibliography

The discovery of the depletion of the stratospheric ozone layer in the 1970's brought an even stricter wave of regulation on chlorocarbons. While not as harmful as chlorofluorocarbons, it was rightly proposed that chlorocarbons were capable of providing the necessary free chlorine for the ozone depletion reaction.[7] This led to regulations calling for an eventual ban on many types of chlorocarbons. Successive waves of legislation could do little to abate the problem which already existed, however.

Because of the difficulty and expense of chlorocarbon disposal, by the 1980's when these laws were being passed, huge stockpiles of chlorocarbon-containing wastes, now classified as hazardous or toxic, existed in locations all over the country. Many of these stockpiles, including hazardous, toxic, and mixed radioactive wastes still exist today,[8] and a great deal of research has gone into their safe disposal and abatement of the pollution caused by leakages.[9]

Even as science struggles to deal with the mistakes of the past, it must look forward to the future. Chlorocarbons are now and will remain for the foreseeable future important to the industrial processes which power our society. It is important then to think not simply about destruction of the chlorocarbon wastes that already exist but about the prevention of further creation of these wastes. By focusing not on chemistry which facilitates the conversion of chlorocarbon byproducts to useful industrial intermediates, scientists have the opportunity to stop the problem at its source by ending once and for all the need for chlorocarbon disposal. With that in mind, the goal of this work has been to advance the basic scientific knowledge of molecular-level events on catalysts for the conversion of chlorocarbons to more useful, less toxic olefins.

1.2 Activity and Selectivity of Bimetallic Catalysts

The ability of noble metals to transform chlorocarbons into paraffins is well known.[10] The exceptional hydrogenation ability of these metals makes them both extremely resistant to Cl poisoning and less than attractive as catalysts for the production of olefins.[11] Bimetallic catalysts, in which the metal type and concentration can be used to "tune" catalytic performance, offer considerably more promise in this area.

Addition of a second metal to a noble metal catalyst alters catalytic performance to an extent not accountable by a simple superposition of monometallic properties.[12-16] One possible interpretation of this behavior is a change in the electronic properties of each component due of alloy formation. In a second interpretation, the formation of alloys changes the geometry of the available sites either by formation of entirely new alloy structures or by limiting the ensemble size of each component metal.[17] Alteration of either the electronic or geometric properties of an active site can result in changes in the adsorption energetics of reactants and products resulting in higher activity[18] or the suppression of side reactions resulting in higher selectivity.[19-20]

Hall and Emmett were among the first to explain catalytic phenomena based on these electronic modification in alloys of group 8 and 1B metals. Referencing the earlier work of Dowden,[21] they interpreted changes in catalytic properties in terms of alteration of electronic state by donation of electron density from the group 1B metal to the incompletely filled d band of the group 8 metal.[22-23] Sinfelt provided further insight into this and other early work in the area in his 1977 monograph on the subject.[24] Later, Rodriguez, Campbell, and Goodman explored this issue by examining shifts in electron

binding energy and CO desorption temperature when Ni, Cu, and Pd were deposited on single crystals of various transition metals. They proposed a simple model by which occupied states of the electron-rich metal hybridize with empty states of the electron-poor metal.[25-26] Rodriguez and Goodman have also reviewed other similar work.[27] Other researches have gone farther in exploring the electronic effect of one metal on another. Dumesic and coworkers, for example, have shown that the addition of Sn significantly alters the adsorption energies of various compounds including ethylene on Pt.[28-29]

One can imagine many possible geometric effects from changes in particle size on a noninteracting support[30] to occupation by a second metal of low coordination sites on the surface of the first. Recent thought, however, groups these effects into two categories. The theory of ensemble sites holds that metal atoms assembled in particular arrays on the surface constitute the active sites in bimetallic catalysts. It also encompasses the idea of dilution in its assertion that a certain number of contiguous atoms of a particular type are necessary for a given elementary step to take place. This theory has been developed by Satchler and coworkers in a several papers over the last half century, and those and other works have been reviewed.[17] De Jongst, Ponec, and Gault theorized that this sort of geometric phenomenon takes place in Pt-Cu reforming catalysts. A change in mechanism was believed to occur from one requiring several sites in the presence of a Pt-rich alloy to one requiring only a single site in the Cu-rich alloy.[31]

Another way of interpreting geometric effects involves what have come to be known as steric interactions. In this view, surface alloys of very particular confirmation

develop in ways which lead to the blockage of active sites on one metal by another. Koel and coworkers have attributed changes in the olefin chemisorption behavior of Pt-Sn single crystals to the formation of new surface alloys which lack Pt three-fold hollow sites.[32-33] Chorkendorff and coworkers propose similar explanations for the activity modifications observed in their studies of methane dissociation[34-35] and methanol synthesis[36-38] over modified and unmodified Cu single crystals. Various researchers including Goodman and coworkers have suggested that atoms at step edges and other low coordination sites which are highly active are the first to be displaced on the addition of a second metal to a monometallic surface.[39]

The understanding of these concepts in combination with a variety of experimental results leads to an advancement in the understanding of bimetallic systems for the conversion of chlorocarbons.

1.3 Scope of the Thesis

The work presented in this thesis focuses on the conversion of 1,2-dichloroethane in the presence of excess hydrogen over supported, Pt-Cu catalysts. Chapter 2 describes the equipment and experimental procedures used in the investigation. A transient period in the selectivity of carbon-supported, Pt-Cu systems with 0.5 percent Pt weight loading is examined in Chapter 3 by comparison of catalytic performance after various pretreatments. Studies of silica-supported systems with 0.5 percent Pt weight loading using Fourier-transform infrared spectroscopy (FTIR) and kinetic techniques including pulse kinetics and ethylene hydrogenation are the subject of Chapter 4. Chapter 5 probes

the effect of water on silica-supported Pt-Cu catalysts with Pt weight loadings of 3.0 percent prepared from chloride and nitrate precursors by examining kinetic behavior as well as using techniques not available on lower weight loading catalysts such as transmission electron microscopy (TEM) and Raman spectroscopy. On these same catalysts, the role of each metal is examined using flow and static kinetic studies and FTIR in Chapter 6.

2.0 EQUIPMENT AND EXPERIMENTAL SETUP

Work presented in this thesis is based on experimental research. The design of equipment that could accurately and reliably measure the important parameters in the experiments was critical to the results obtained in this investigation. A variety of experimental techniques were used to measure catalyst performance, study molecular adsorption, and characterize catalysts and support materials. This chapter describes the experimental equipment used for the different techniques and the calibration procedures followed. In order to highlight the relevant procedures in each chapter, details of the specific experiments performed are presented in the individual chapters.

2.1 Equipment

2.1.1 Reaction System for Catalytic Performance Measurements

The catalytic performance measurements were carried out at atmospheric pressure in a stainless-steel flow reaction system. A flow diagram for the reaction system is shown in Figure 2.1. The entire system is compactly arranged on a movable cart which allowed for easy positioning. The system interfaced with house electric lines to supply power to the various instruments and electronics, with gas tank lines routed from a common tank-holding area, and vent lines that were routed from the system to a constant air velocity laboratory exhaust system. Gases used in this study were at room temperature and were drawn from individual gas tanks. For gases such as He, H_2, and N_2 (Praxair, 99.999%) and others such as HCl and C_2H_4 (Praxair, 99%+) tanks were

equipped with dual stage pressure regulators that reduced typical tank pressures of ~ 2000 psi to line pressures of ~ 100 psi. The 1,2-dichloroethane (Sigma-Aldrich, 99.8%) was metered into the system by flowing He through a saturator containing the liquid. A constant concentration in this stream was ensured by holding the saturator at a constant temperature of 0°C using a recirculating cooling system. Each gas line was equipped with a check valve, which prevented back-mixing due to pressure fluctuations, and a 0.5 or 2 micron filter. Gaseous reactants were metered using mass flow controllers (MFC, Brooks Instruments model 5850E) and mixed prior to entering the reactor. An electronic unit regulated the power supply and flow readouts from the MFCs. Prior to entering the reactor a 3-way needle valve controlled the space velocity of the reaction mixture. All lines downstream of the reactor were heated to ~ 50 ^{o}C to minimize the condensation of reactants due to pressure increase. This also minimized the possibility of high molecular weight chlorocarbons formed during the reaction plugging the tubing.

The reactor was a 4 mm i.d. quartz U-tube with a 10 mm i.d. section that contained the porous quartz frit to support the catalyst powder. The reactor was attached to the feed system via two glass-to-metal CAJON fittings and could be removed easily for loading the catalyst samples. The reactor zone containing the catalyst was heated by an electric furnace and the catalyst temperature was measured and controlled with an accuracy of ± 1 K using a temperature controller (Omega model CN2011). The catalyst temperature was measured by an Omega type J thermocouple placed in a 1mm i.d. quartz sleeve that was in contact with the quartz frit in the reactor. This thermocouple also supplied the “measured variable” to the temperature controller which operated in a

feedback PID loop to control the heat input to the electric furnace surrounding the reactor.

The reactor effluent was analyzed by on-line GC and, when necessary, GC/MS to identify the reaction products. The GC (Varian 3300 series) was equipped with a 15 ft 60/80 Carbopack B/5 % Fluorocol packed column (Supelco) and a flame ionization detector (FID) capable of detecting concentrations > 1 ppm for all chlorocarbons and hydrocarbons involved in this study. The on-line HP GC/MS system consisted of an HP 5890 series II plus GC (also equipped with a Fluorocol column) connected to an HP 5972 Mass Selective Detector. Gaseous samples of the reactor effluent were injected in the GC column using an automatic, 6-port sampling valve equipped with a 100 μL sample loop. In addition, the GC/MS used a 3-way splitter valve at the GC and MS interface (shown in Figure 2.2) to reduce sample volume entering the MS. This arrangement provided acceptable MS chamber pressures and adequate sample volume for accurate analysis. Both the GC and the GC/MS were interfaced to separate computers running HP Chemstation and MS Chemstation software, respectively. All raw data output from GC or GC/MS measurements could be processed using these software packages and converted to kinetic parameters such as concentration, conversion, and selectivity.

2.2 Instrument Calibration

Calibration of metering devices such as MFCs as well as analytical instruments was performed following manufacturer guidelines. General procedures for calibrating equipment are outlined below along with a few specific examples.

2.2.1 Temperature Controllers

Depending upon the type of thermocouple used and the range of operation, the temperature controllers needed to be calibrated. The controller was calibrated by the manufacturer when assembled. To ensure accuracy, a calibration was also performed before experiments began. A thermometer placed in the furnace gave the actual temperature which was compared to the temperature readout on the controller. The necessary calibrations equation between thermocouple readout and thermometer reading were thus determined. No such equation was required for this research, the discrepancy being within the controller accuracy of +/-1 K.

The PID (proportional, integral and differential) control parameters for the controller were set as explained in the manual. This ensured faster and better control of the temperature and reduced oscillations and overshooting, especially when step changes were imposed.

2.2.2 Mass Flow Controllers

MFCs are factory calibrated for specific gases. To ensure accuracy, a calibration was performed before experiments began. Though it was found that the calibrations for the MFCs do not change sufficiently with time to introduce errors beyond the design accuracy, it was considered good practice to calibrate mass flow controllers at regular intervals (i.e. whenever new equipment was connected or tubing was changed or rearranged, etc). Furthermore, it was always observed that the calibrations obtained for

MFCs had good linearity (correlation factor >99.5%). Even between two calibrations, random checks were performed to helped avoid any error in flow. This was done prior to or even during an experiment by switching the flow momentarily through the bubble flow meter and measuring the flow rate.

To calibrate a MFC, the gas flow is passed through an empty reactor. The idea is to perform the calibration with the system under conditions as close as possible to those which will be used in the experiment. Use of an empty reactor mimics the experimental conditions to some extent. The procedure described below refers to a single gas, but the calibration should be performed independently and individually for all gases following the same procedure. Figure 2.4 shows the typical fit for He flows using a He MFC.

The tank regulator delivery pressures were set to the following values: 80 psig for He, 50 psig for H_2 and 50 psig for N_2 which was used as a carrier gas in the GC. The three-way valve placed downstream was switched so that the gas flowed through the bubble flow meter. The soap solution in the bulb of the flow meter was used to wet the flow meter walls. The MFC reading was set to a given value using the knob on the front panel of its control unit. The flow was measured through the bubble flow meter three times using a stopwatch. The average of the three readings was considered. This procedure was repeated for different MFC settings and the average flow was measured each time. A linear fit (correlation factor of >99.5% is acceptable) was achieved between the MFC values and corresponding average flows. Care was taken to calibrate the MFC in the actual range of flows which would be used in experiments.

2.2.3 GC Calibration

To quantify GC areas, the response of the FID detector were determined. This involved developing a calibration function (response factor for the FID) between the detector area observed for a component and its concentration in the stream. The amount of a species entering the GC (and its area) was related to the pressure and volume in the sample loop. The loop volume always remained constant but the pressure varied depending upon the flow rate and other factors such as back pressure.

The carrier gas and reactants were mixed appropriately to achieve the desired concentrations. Three injections were made each with the gases flowing through the bypass and then through the reactor. The procedure was repeated at the end of the experiment to note and account for the change in the flow. A deviation in the areas of <10% of the average area was deemed acceptable for the current work. The response factor was thus directly determined.

As calibration depends upon the GC settings as well, it was necessary to record several parameters. It was also required to note the retention times since the component was identified by retention time during the experiment. Figure 2.5 showed the change in FID response over time for a constant-concentration GC injection sequence. It was necessary to ensure that the GC response remained within +/- 5 % of the desired concentration.

2.3 Concerns and Cautions

The following list outlines the essential procedures, which must be performed before, during, and after conducting an experiment.

- The system should be checked for leaks after new connections. This is possible with the use of a leak detector liquid for atmospheric pressure systems and by using a MS for the vacuum system.
- Conditioned GC and GC/MS columns should be used, and timely checks for retention times and response factors should be performed.
- Different sets of spatulas, reactors, and thermocouple-wells should be used for different catalysts.
- Instruments should be allowed to stabilize before taking each reading (at least 5 min between each injection to GC, 1 min with the valve in the "Load" position and about 5 min after changing the flow using a MFC).
- Material Safety Data Sheets (MSDS) should be obtained for every reactant used and every major product being formed in the reaction.
- Caution should be exercised while handling hazardous gases such as H_2 and HCl.
- Vent lines should be checked frequently to ensure leak-free operation and a list of possible effluents from reaction studies should always be maintained.
- Safety reviews of equipment and experiments should be made frequently, and designing improvements to make laboratory operations safer should be an ongoing effort in every graduate student's work.

- The GC, GC/MS, and reaction system should be maintained properly. The oil in the vacuum pump should be replaced every six months. The filters for the house air should be checked regularly.

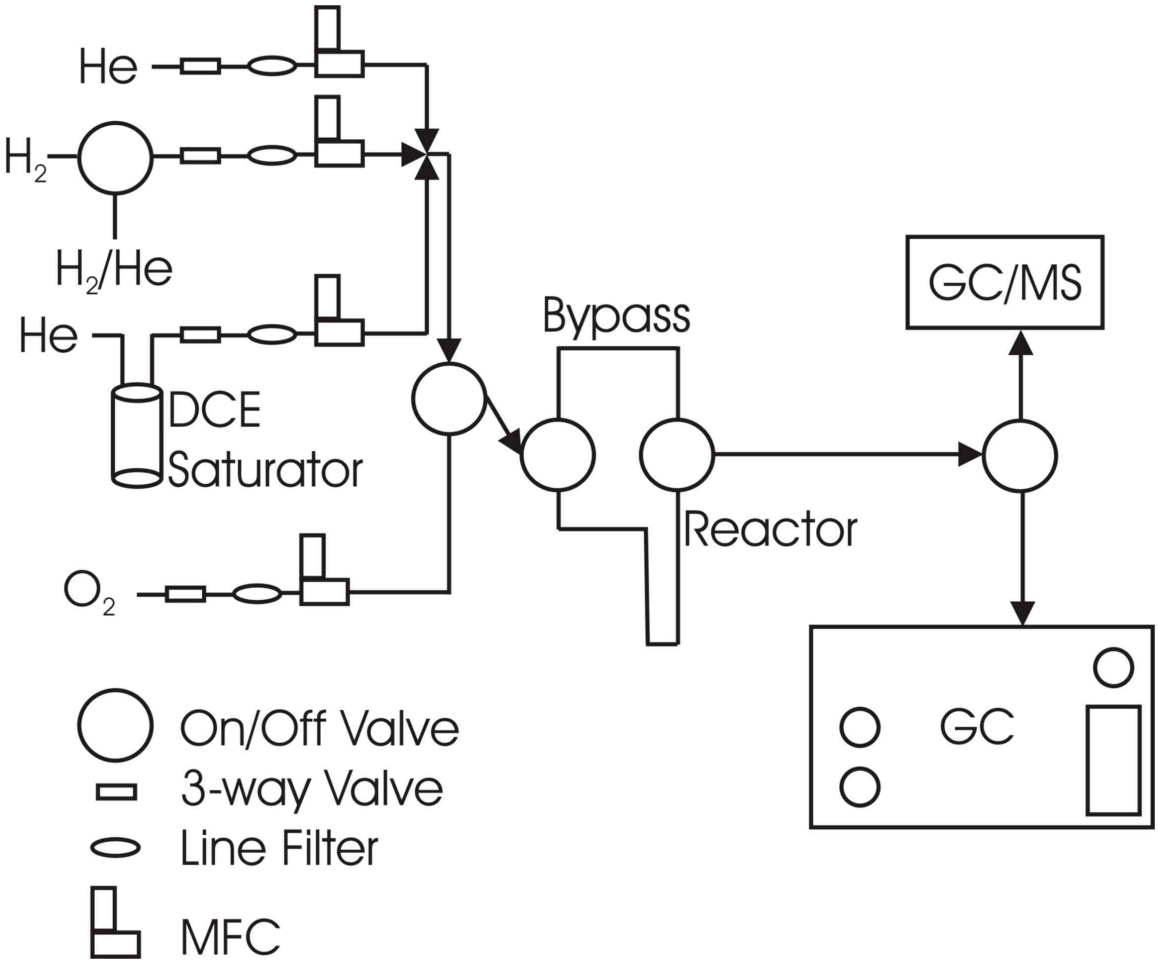

Figure 2. 1 Reaction system for flow kinetics measurements.

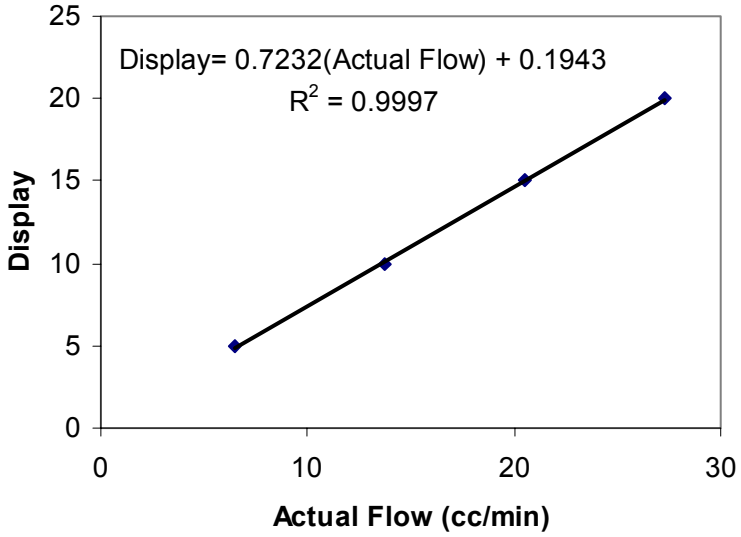

Figure 2. 2 Calibration curve of MFC for diluent He controller.

3.0 HYDRODECHLORINATION OF 1,2-DICHLOROETHANE CATALYZED BY PT-CU/C: EFFECT OF CATALYST PRETREATMENT

3.1 Introduction

There is an ongoing interest in developing new routes to convert chemicals that are usually considered as byproducts into industrially valuable products. A technologically relevant example is the hydrogen-assisted dechlorination of multiply-chlorinated hydrocarbons into completely or partially dechlorinated olefins.[40-45] These investigations have shown that supported bimetallics containing Pt or Pd are selective catalysts for the conversion of vicinal alkyldi- and trichlorides, such as 1,2-dichloroethane, 1,2-dichloro- or 1,2,3-trichloropropane, into olefins and chlorolefins in the presence of H_2. One of the most selective catalysts is PtCu supported on activated carbon.[40,42]

Earlier investigations[42] have shown that PtCu/C catalysts exhibited steady state selectivity toward ethylene in the 1,2-dichloroethane dechlorination in excess of 70%, but selectivity was significantly lower at early time on stream (TOS). It was hypothesized that the increase in ethylene selectivity with TOS was the result of an increase in the degree of alloying under reaction conditions.[46] Prior to the beginning of the reaction, the catalysts consist of the mixture of monometallic Pt, monometallic Cu and bimetallic PtCu particles. Thus, at early time on stream the Pt sites catalyze the formation of ethane from 1,2-dichloroethane with a sufficiently high turnover frequency (TOF) that ethane is

the major product. As the reaction proceeds, more complete alloying of Pt and Cu takes place to form mixed PtCu sites that are selective toward the formation of ethylene.

The objectives of the present paper are to test the hypothesis that alloying Pt and Cu, or in other words surface composition of bimetallic PtCu particles, determines the catalytic performance of Pt-Cu/C in the reaction of 1,2-dichloroethane hydrogen-assisted chlorine elimination. Three of the catalysts tested earlier,[42] namely monometallic Pt/C and two bimetallic PtCu/C catalysts (Cu/Pt atomic ratio 1:1 and 3:1) were selected for these investigations, and the degree of alloying was varied by varying the catalyst pretreatment. The choice of the bimetallic catalysts was motivated by the fact that Pt1Cu3/C has the most pronounced transient behavior, whereas both the Pt/C and Pt1Cu1/C exhibited little selectivity change with TOS with only small amounts of ethylene formed.

3.2 Experimental

3.2.1 Catalyst Preparation and Characterization

The catalysts were prepared by pore volume impregnation of activated carbon (BPL F3, Calgon Carbon) with aqueous solutions of $H_2PtCl_6 \cdot 6H_2O$ (Alfa, 99.9%) or $H_2PtCl_6 \cdot 6H_2O$ and $CuCl_2 \cdot 2H_2O$ (MCB Manufacturing Chemists, 99.5%) as described elsewhere.[42] The concentrations of the metals in the impregnating solutions were adjusted to provide metal loadings of 0.50% for Pt/C, 0.49% Pt + 0.16% Cu, and 0.50%

Pt + 0.49% Cu. The bimetallic catalysts had Cu/Pt atomic ratios of 1:1 (Pt1Cu1) and 1:3 (Pt1Cu3), respectively.

The fractions of Pt atoms exposed following reduction at 350°C for 1 h for Pt/C, Pt1Cu1/C, and Pt1Cu3/C, obtained from CO chemisorption performed on an ASAP 2010 Chemi instrument (Micromeritics), were 26.5, 52.4 and 41.5%, respectively.[42]

3.2.2 Catalytic Experiments

Kinetics experiments were conducted at atmospheric pressure in a stainless-steel, flow reaction system equipped with a quartz microreactor (10 mm i.d.) in which the catalyst was supported on a quartz frit. Gaseous reactants and pretreatment gases (He, H_2, Praxair, 99.999%; HCl, Liquid Carbonic, 99.0%) were metered using mass flow controllers (Brooks Instruments model 5850E), and mixed prior to entering the reactor. The 1,2-dichloroethane (Sigma-Aldrich, 99.8%) was metered into the system by flowing He through a saturator containing the liquid. A constant concentration in this stream was ensured by holding the saturator at a constant temperature of 0°C using a recirculating cooling system. The reaction temperature was 200±1°C, and the catalyst was maintained at that temperature using an electric furnace and a temperature controller (Omega model CN2011). The total flow rate of the reaction mixture consisting of 7,000 ppm CH_2ClCH_2Cl, 36,600 ppm H_2, and the balance He was 41 ml/min.

For all the experiments, the conversion was maintained between 4-5%. This was accomplished by varying the amount of catalyst in the reactor from 80 mg to 100 mg.

This range in catalyst weight corresponded to a space velocity range of 8967 to 7174 h^{-1}. (Space velocity is defined as the ratio of volumetric flow rate of total gas mixture to the volume of the reactor occupied by catalyst). All reactions were run to steady state which, for the purposes of this investigation, was defined by a conversion change of less than 0.2% in 5 h and a change in selectivity of less than 1%. The reaction products were monitored online using a gas chromatograph (Varian 3300 series) equipped with a 10 ft 60/80 Carbopack B/5 % Fluorocol packed column (Supelco) and a flame ionization detector. The detection limit for all products was 2 ppm. HCl was not quantified in these experiments.

The catalyst samples were pretreated by six different methods, starting from the same drying. The drying process consisted of purging the catalyst with He (30 ml/min) for 5 min at 30°C. The He flow was continued as the catalyst was heated to 130°C at a rate of 6.7°/min. The catalyst was maintained at these conditions for 1 h.

For the first pretreatment, the standard, the He flow was switched after the drying step to a H_2+He flow (17% H_2, 60 ml·min^{-1}). The catalyst was heated to 220°C at 3°/min and held there for 1.5 h. Afterwards, the H_2+He flow was switched to pure He, and the catalyst was allowed to cool to the reaction temperature.

The second pretreatment consisted of heating the catalyst after the drying step in He (50 ml·min^{-1}) to 220°C with the ramp of 3°/min and holding the sample at this temperature for 1.5 h. The catalyst was then reduced at 220°C for 1.75 h in H_2+He flow.

The third pretreatment was the same as the second except the final reduction in the H_2+He flow was omitted.

The forth pretreatment consisted of the standard pretreatment followed by heating to 400°C at a rate of 6°/min in the H_2+He flow. The conditions at 400°C were maintained for 3.5 h before switching the H_2+He flow to pure He and cooling to the reaction temperature. The fifth pretreatment consisted of the standard pretreatment followed by heating the sample to 400°C at a rate of 6°C/min in the He flow, holding at this temperature for 3.5 h and cooling down to the reaction temperature.

The sixth pretreatment was as follows. After the standard pretreatment, the catalyst was exposed to HCl+He flow (10.4% HCl, 30 ml·min^{-1}) at 200°C for 1.5 h. The reactor was purged with flowing He (50 ml·min^{-1}) for 5 min before the reaction was started.

3.3 Results

All three catalysts, Pt/C, Pt1Cu1/C and Pt1Cu3/C do not show significant change in the conversion of 1,2-dichloroethane with TOS and with the method of catalyst pretreatment. Reductive pretreatment resulted in some decrease in the conversion with TOS. For example, with PtCu3/C the conversion decreased from ~5% initially to ~4% after 65 h on stream. An increase in conversion was observed for samples without preliminary reduction. In all cases the change in conversion did not exceed 25% of its initial level. Steady state activity was reached after 5-10 h on stream with the conversion

remaining essentially constant thereafter (not shown). However, after standard pretreatment it took several tens of hours for the bimetallic catalysts to reach the steady state selectivity.

The dynamics of the selectivity change for 1,2-dichloroethane hydrodechlorination catalyzed by Pt/C, Pt1Cu1/C and Pt1Cu3/C after the standard catalyst pretreatment are shown in Figure 3.1. For Pt/C the ethylene selectivity reached approximately 5% in 5 h on stream and remained constant thereafter. However, the selectivity toward ethylene for Pt1Cu1/C increased at the expense of ethane during 40 h from ~5% at early TOS to ~20%. The Pt1Cu3/C also exhibited an approximately fourfold increase in the ethylene selectivity with TOS. The initial selectivity was ~20% and reached ~80% after 65 h on stream.

Pretreatment of the Pt/C with HCl after reduction did not alter the selectivity patterns compared to the behavior observed for the standard pretreatment (Figure 3.2). However, there was a twofold increase in the conversion. This is the only case of significant change in conversion for a catalyst resulting from a pretreatment. For the bimetallic catalysts the HCl pretreatment resulted in almost complete elimination of transient behavior with steady state selectivity toward ethylene of approximately 35 and 95% for the Pt1Cu1/C and PtCu3/C, respectively (Figure 3.2).

Non-reductive pretreatment in a He flow at 220°C resulted in the most significant change in performance of the catalysts compared to that after the standard pretreatment (Figure 3.3). The steady state selectivity toward ethylene for Pt/C increased to ~10%,

whereas Pt1Cu1/C and Pt1Cu3/C showed selectivities of ~75 and ~95%, respectively, compared to 20 and 80% after the standard pretreatment.

The TOS behavior of the Pt1Cu3/C catalyst after three other kinds of pretreatment, reduction at 400°C, reduction at 220°C followed by treating in a He flow at 400°C, and heating in a He flow at 220°C followed by reduction at the same temperature are shown in Figure 3.4. The main feature of these results is a negligible change in selectivity with TOS compared to that after the standard pretreatment, with steady state selectivity within the range of 91 to 95%.

With the exception of Pt/C pretreated with HCl, the steady state TOFs in 1,2-dichloroethane hydrodechlorination did not depend significantly on the type of catalyst pretreatment. For example, the TOFs for the Pt1Cu3/C varied within the range of 0.53 to 0.82 s^{-1}. The highest TOF was obtained with the PtCu3/C after the standard pretreatment. Non-reductive pretreatment with He at 220°C resulted in the lowest TOF. The difference in TOFs is not profound. Apparently, the steady state of the catalyst is determined by the reaction mixture and different pretreatments can only accelerate (to different degrees) approach to steady state.

Figure 3.5 shows TOS performance for the 1,2-dichloroethane hydrodechlorination of the PtCu3/SiO_2 catalyst after the standard pretreatment. After approximately 5 h on stream, the catalyst was reduced again at 220°C for 1.5 h, and the hydrodechlorination reaction was allowed to continue. After 67 h on stream the catalyst was reduced a third time at the same conditions. One can see that with the exception of

the very first point, subsequent catalyst reduction had a negligible effect on the overall catalyst transient behavior.

3.4 Discussion

Although the actual mechanism of the hydrogen-assisted chlorine elimination reaction of 1,2-dichloroethane catalyzed by PtCu bimetallics has not been established, chemical kinetics results have prompted speculation that mixed PtCu sites are responsible for ethylene formation.[42] Indeed, monometallic Pt is not selective toward ethylene (Figures 3.1-3); monometallic Cu is highly selective[42,47] for about one turnover of each Cu site because of its limited ability to activate H_2.[48] Thus, alloying of the metallic components must play a decisive role in determining the catalyst selectivity and motivates our discussion of the factors that affect the formation of alloy particles.

A great problem of bimetallic catalyst preparation by coimpregnation of a support is the possible chromatographic separation of ions as the mixed solution passes through the pore structure.[11] The impact of this effect is expected to be more pronounced for supports with high surface area and narrow pores, such as the activated carbon BPL F3 used in this study (1400 m^2g^{-1} surface area; 2.4 nm average pore diameter[42]). It is likely that the supported chlorides of Pt and Cu are substantially separated after the drying step. Thus, the subsequent reduction of the catalysts at 220°C will reduce the chlorides to metal but it may not be sufficient to form homogeneous PtCu particles. This results in

the dramatically different catalytic performance of the PtCu catalysts after pretreatments favoring alloying of Pt and Cu (Figures 3.1-4).

Chlorides and oxychlorides of many transition metals migrate readily over the surface of oxide and carbon supports at higher temperatures.[46,48] Although in the presence of chromatographic effects microcrystallites of Pt and Cu chlorides may be separated on the support surface after drying PtCu/C catalysts, increasing temperature could result in the formation of mixed PtCu moieties because of accelerated surface diffusion.

Both thermodynamics and kinetics favor the reduction of platinum chlorides by H_2 to the metallic state.[11,48] Hence, at higher temperatures the life time of Pt chloride molecules in the presence of H_2 is not expected to be long. Copper chlorides are more stable and need higher temperature or longer time at lower temperature to be reduced to the metal. However, in the presence of platinum, copper chloride would also reduce rapidly. Carbon supports favor hydrogen spillover,[48] and it seems unlikely that there would be a shortage of dissociated H_2 in close proximity to the $CuCl_x$ moieties even if Pt clusters, the source of dissociated H_2, are quite distant. Thus, if Pt and Cu chlorides in a dry PtCu/C catalyst are not in close proximity to one another the standard pretreatment (Figure 3.1) would not result in significant alloying of Pt and Cu. Both Pt and Cu would reduce to the metallic state quite rapidly, but mobility of the metal atoms over the support surface is significantly lower than that of the metal chlorides.[46,48] Increasing the temperature of the catalyst reduction with H_2 would likely enhance alloying because of

higher diffusion rates of metal atoms at elevated temperatures which result in increased initial selectivity toward ethylene (Figure 3.4).

Because both Pt and Cu chlorides are relatively stable in an inert atmosphere, the treatment of the PtCu/C catalysts in He flow at elevated temperatures could lead to a redistribution of Pt and Cu chloride moieties on the support by surface diffusion. As Pt chlorides are thermally unstable at temperatures above 100°C,[49-50] it is expected that some Pt chlorides will decompose to the Pt metal. The Pt metal sites could serve as a trap for the mobile $CuCl_x$ moieties by catalyzing dissociation of Cu-Cl bonds on the Pt surface. The driving force of this process is ΔH of Pt and Cu alloying.[51] The suggestion that a fraction of the metals in the PtCu3/C catalyst is reduced during the pretreatment in He flow at 220°C is supported by the fact that the samples treated in flowing He show similar initial activity independent of whether the treatment was followed by reduction with H_2.

A phenomenon other than promotion of surface migration of Pt and Cu moieties followed by alloying governs the higher initial selectivity toward ethylene in 1,2-dichloroethane dechlorination after exposure of the pre-reduced PtCu catalysts to HCl at 220°C (Figure 3.2). As was mentioned earlier, the metal atoms have a low rate of diffusion over the support surface. Even though Pt and Cu chlorides are mobile, HCl is incapable of oxidizing Pt or Cu to the chloride because of highly unfavorable thermodynamics.[48,52] However, HCl will induce the enrichment of the surface of bimetallic particles with Cu because of higher energy of Cl interaction with Cu than with Pt.[47,53-54] After exposure of the reduced catalysts to HCl, the outer layer of bimetallic

particles would consist of a Cu-rich PtCu alloy that is selective toward ethylene; the interior of the particle is more Pt-rich.

It is worth noting that unlike Pt1Cu1/C the steady state selectivity of Pt1Cu3/C toward ethylene is almost independent of the catalyst pretreatment with the exception of the standard one (Figures 3.2-4). This observation is also consistent with the idea that alloying governs selectivity change with TOS. At lower Cu/Pt ratios (lower loading) migrating Pt and Cu species have to travel greater distances over the support surface to coalesce and form bimetallic particles after reduction. Hence, selectivity changes resulting from the different abilities of the various pretreatments to favor surface diffusion becomes more pronounced.

The above interpretation does not preclude the role of Cl coverage of the surface of metallic particles in altering catalytic performance. Chlorine is known to suppress the activity of Group VIII metals in olefin[55] and aromatics hydrogenation.[56] The effect of Cl will be discussed later. However, some conclusions can be drawn based on the results obtained. The fact that Pt/C without reductive pretreatment exhibited higher ethylene selectivity than after reduction with H_2 is consistent with the idea that Cl on the surface suppresses the hydrogenation ability of Pt. The Cl coverage of Pt must be higher after heating the catalyst at 220°C in He than after heating in H_2. However, the TOS behavior of Pt1Cu3/C in essentially the same after reduction with H_2 at 400°C and without reduction. Moreover, repeated reductions of Pt1Cu3/C after 5 and 67 h on stream that eliminate Cl accumulated on the active catalyst surface do not influence the transient behavior (Figure 3.5). This suggests that though Cl deposited on the catalyst surface does

inhibit the hydrogenation ability of Pt, this phenomenon does not play a decisive role in determining the selectivity of the bimetallic PtCu catalysts with high Cu/Pt atomic ratios. These catalysts possess high selectivity toward ethylene in 1,2-dichloroethane hydrodechlorination likely due to their specific surface topography as has been hypothesized elsewhere.[42,43]

3.5 Conclusion

The selectivity of Pt/C reduced in H_2 flow at 220°C toward ethylene in 1,2-dichloroethane dechlorination is a weak function of TOS and is less than 5% at steady state. The initial ethylene selectivity of PtCu1/C and PtCu3/C reduced under the same conditions is also low but significantly increases with TOS reaching at steady state value of approximately 20 and 80%, respectively. Pretreatment of the bimetallic catalysts with flowing He at 220°C almost completely eliminates the transient period in the catalysts' performance with steady state selectivity toward ethylene being approximately 75% (PtCu1) and 95% (PtCu3). The pretreatment of the pre-reduced PtCu catalysts with HCl at 220°C also led to elimination of transient behavior and increasing steady state selectivity toward ethylene compared to samples initially reduced at 220°C. The effect, however, was less pronounced. None of the pretreatments influenced catalytic behavior of Pt/C. The results are explained by the formation of mixed $PtCuCl_x$ species by coalescence of migrating Pt and Cu chlorides during non-reductive pretreatment resulting in enhancing alloying of Pt and Cu during the catalysts' subsequent reduction by H_2 or

reaction mixture and by the surface enrichment of PtCu particles with Cu atoms during the pretreatment with HCl.

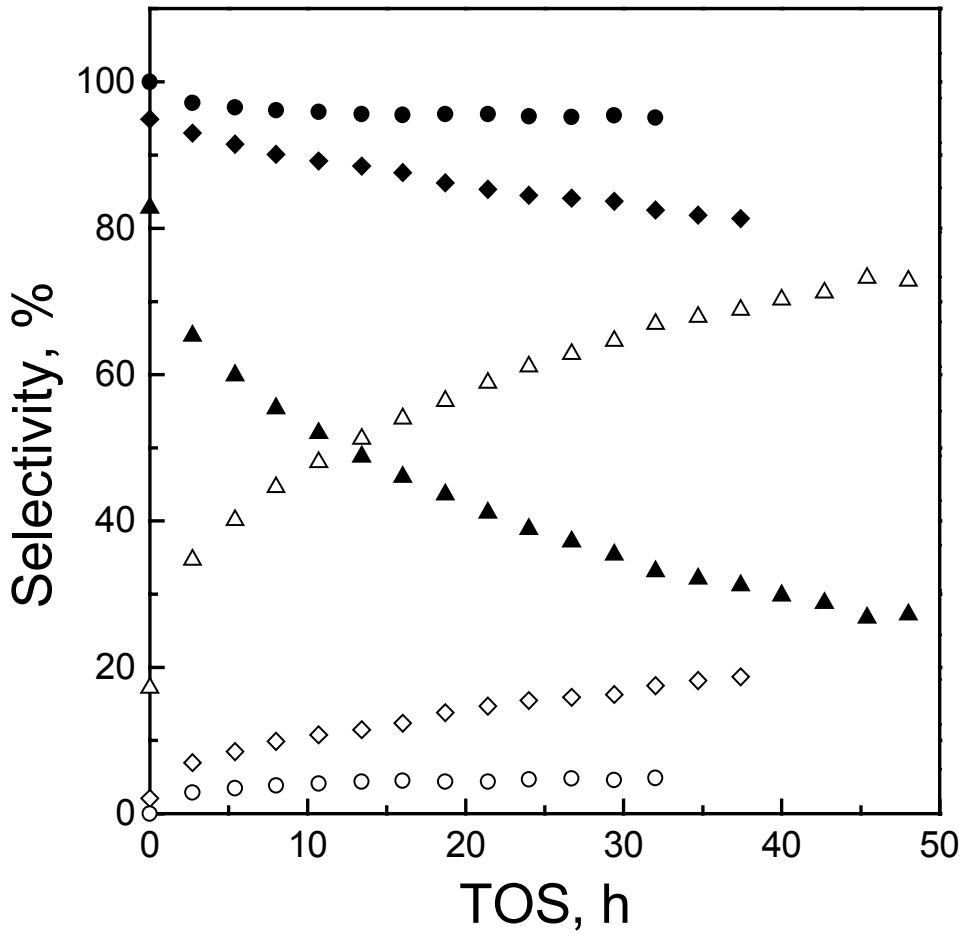

Figure 3. 1 Selectivities toward ethylene (empty symbols) and ethane (filled symbols) vs. TOS for the hydrodechlorination of 1,2-dichloroethane catalyzed by Pt/C (○), Pt1Cu1/C (◊), and Pt1Cu3/C (Δ) after the standard pretreatment.

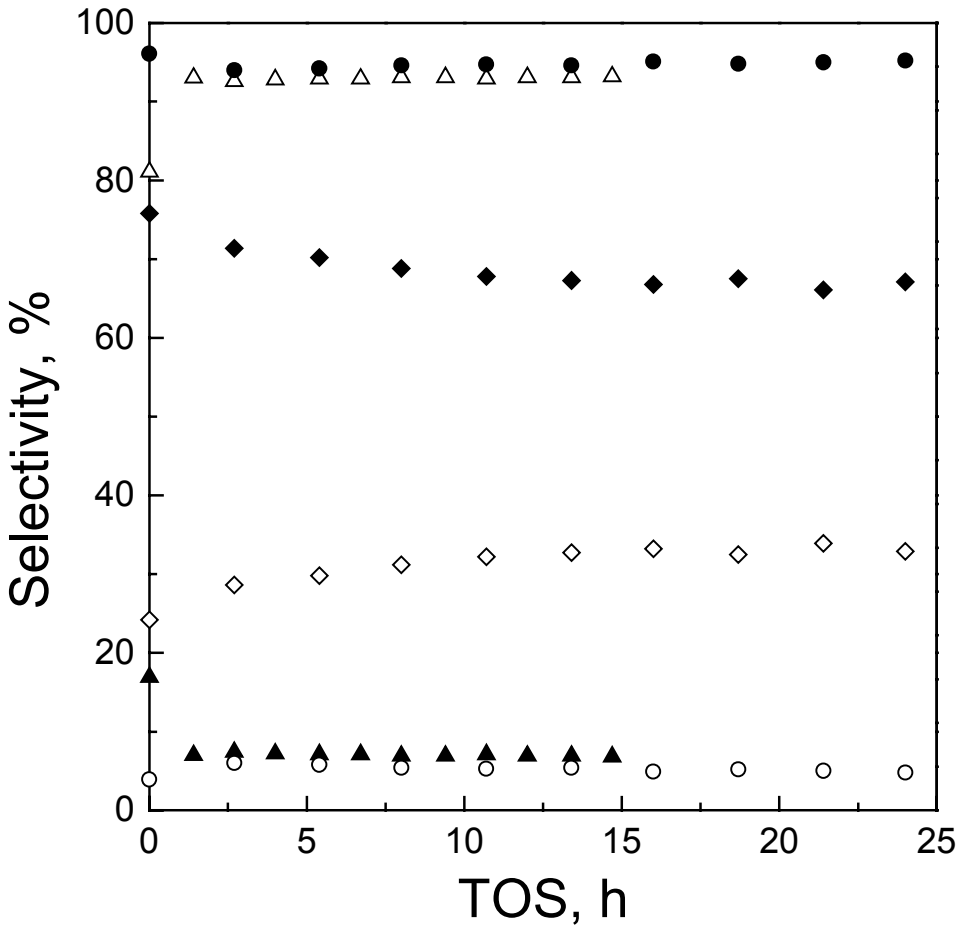

Figure 3. 2 Selectivities toward ethylene (empty symbols) and ethane (filled symbols) vs. TOS for the hydrodechlorination of 1,2-dichloroethane catalyzed by Pt/C (○), Pt1Cu1/C (◊), and Pt1Cu3/C (Δ) after the standard pretreatment followed by treatment with the HCl+He flow at 200°C.

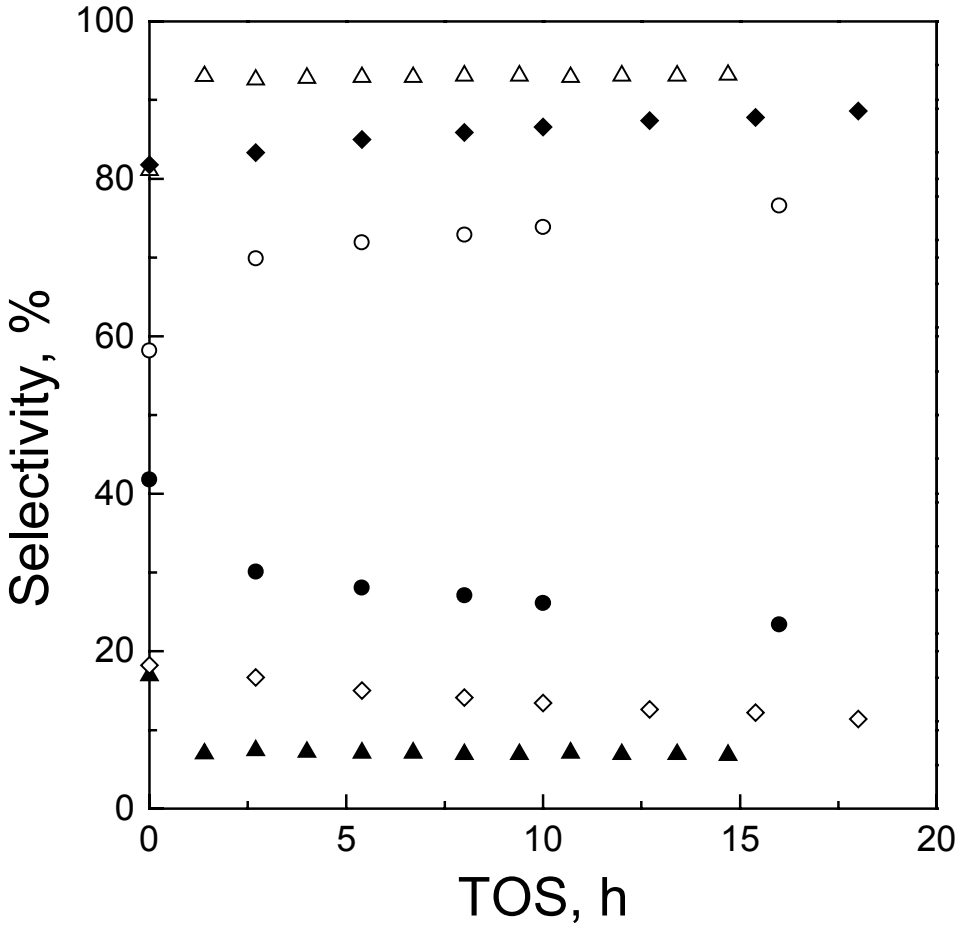

Figure 3. 3 Selectivities toward ethylene (empty symbols) and ethane (filled symbols) vs. TOS for the hydrodechlorination of 1,2-dichloroethane catalyzed by Pt/C (○), Pt1Cu1/C (◊), and Pt1Cu3/C (Δ) after catalyst pretreatment at 220°C in He.

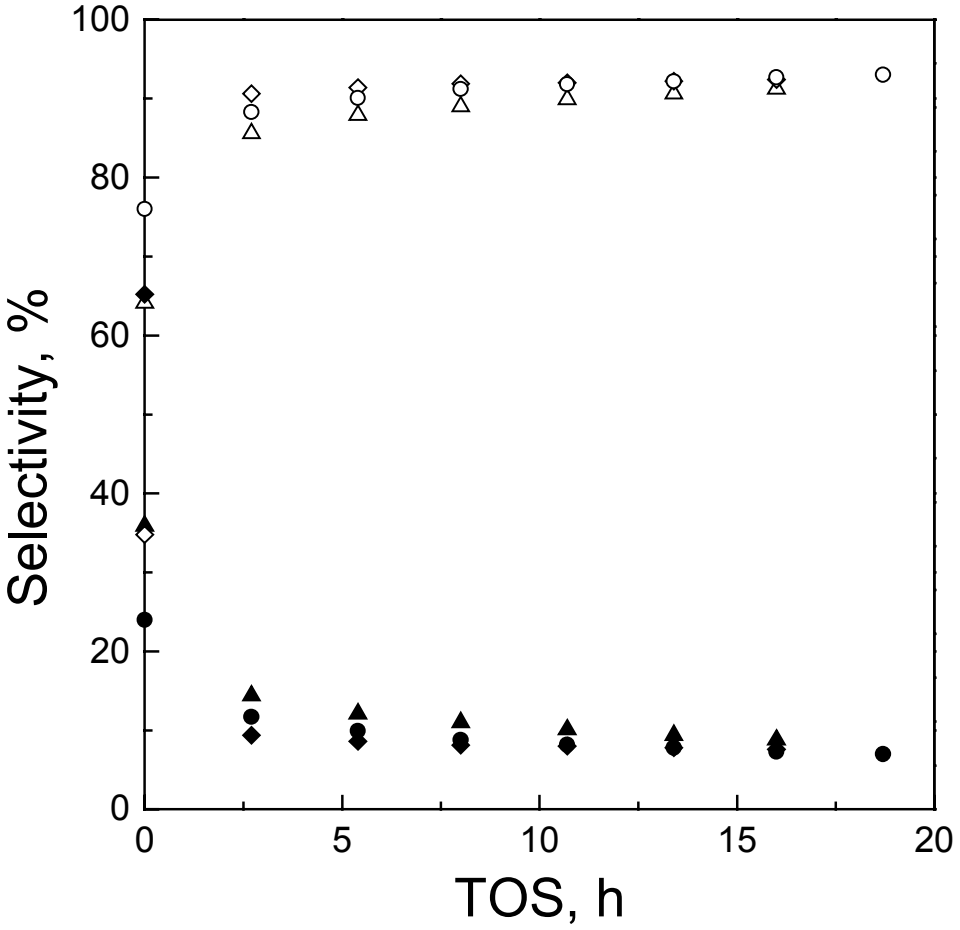

Figure 3. 4 Selectivities toward ethylene (empty symbols) and ethane (filled symbols) vs. TOS for the hydrodechlorination of 1,2-dichloroethane catalyzed by Pt1Cu3/C after treatment of the catalyst sample at 220°C with He flow followed by the reduction at the same temperature (○), reduction at 400°C (◊), and reduction at 220°C followed by the treatment with He flow at 400°C (Δ).

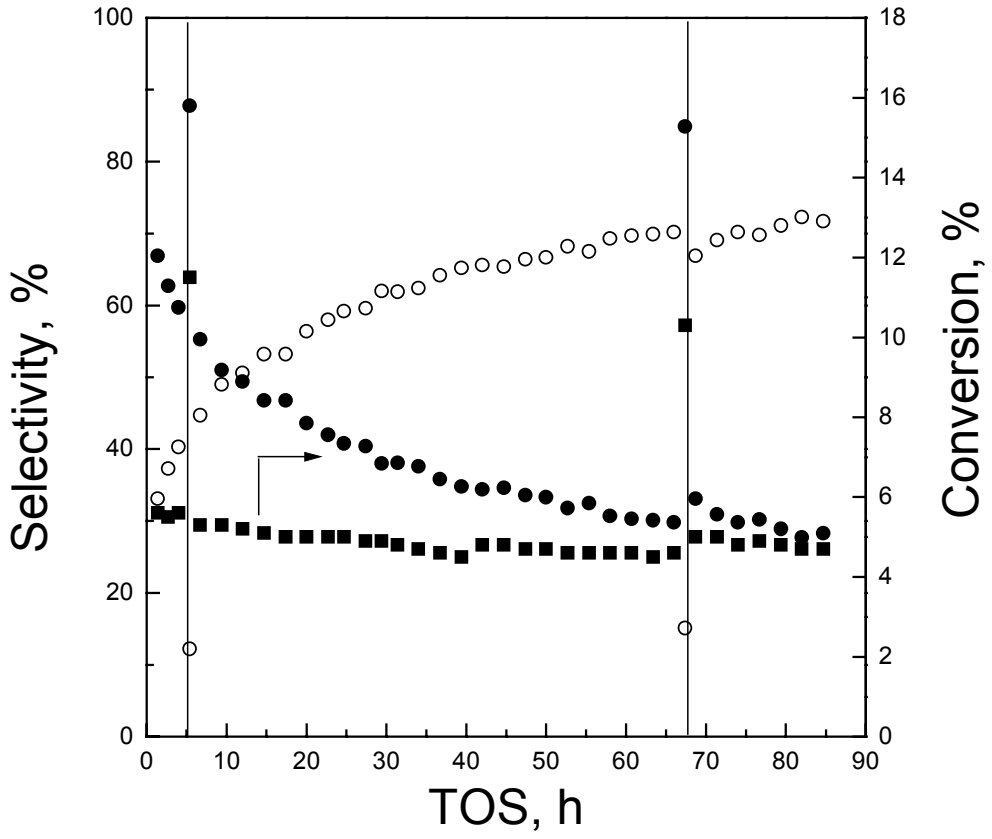

Figure 3. 5 Time on stream performance of the $PtCu3/SiO_2$ in the 1,2-dichlorothane hydrodechlorination after the standard pretreatment, selectivity toward ethylene (○), selectivity toward ethane (●), and conversion (■). After the time indicated by vertical lines the catalyst was reduced again at 220°C for 1.5 h.

4.0 1,2-DICHLOROETHANE REACTIONS: PRODUCTION OF OLEFINS OVER SILICA-SUPPORTED PT-CU CATALYSTS

4.1 Introduction

In an ever more environmentally conscious world, there is increasing demand for technologies that can transform wastes, such as the chlorocarbon byproducts of many industrial reactions, into process intermediates. While the transformation of chlorocarbons into paraffins is relatively straightforward and has been widely studied,[10] there are significant economic incentives to produce olefins. Bimetallic catalysts, which can sometimes be optimized to give the desirable activity traits of both metals, offer considerable promise in this area.

Addition of a second metal to a noble metal catalyst has been shown to alter the activity in ways beyond that which can be explained by a simple superposition of monometallic activities.[12-16] One possible interpretation of this behavior is a change in the electronic properties of each component due of alloy formation. In a second interpretation, the formation of alloys changes the geometry of the available sites either by formation of entirely new alloy structures or by limiting the ensemble size of each component metal.[17] Alteration of either the electronic or geometric properties of an active site can result in changes in the adsorption energetics of reactants and products resulting in higher activity[57] or the suppression of side reactions resulting in higher selectivity.[58-59]

While abundant literature is available for dehydrogenation reactions catalyzed by bimetallic catalysts, there are relatively very few studies which deal with bimetallic catalysts in dechlorination reactions.[41] Earlier work has shown that carbon supported Pt-Cu catalyzes the conversion of 1,2-dichloroethane in excess H_2 to ethylene with a selectivity greater than 90%.[42] The influence of the Pt/Cu atomic ratio on product selectivity in the dechlorination reaction, however, is not yet well understood.

The current work presents the results from a variety of kinetic techniques and FTIR spectroscopic studies to understand the role of each metal on a molecular level in the dechlorination of 1,2-dichloroethane over silica-supported Pt-Cu bimetallic catalysts.

4.2 Experimental

4.2.1 Catalyst Preparation and Characterization

The catalysts were prepared by pore volume impregnation of SiO_2 (Aldrich, 99+%, 60-100 mesh, 300 m^2 g^{-1}, average pore diameter, 150 Å) with a 0.1 N aqueous HCl solution containing $H_2PtCl_6 \cdot 6H_2O$ (Alfa, 99.9%) or a mixture of $H_2PtCl_6 \cdot 6H_2O$ and $CuCl_2 \cdot 2H_2O$ (MCB Manufacturing Chemists, 99.5%), as described elsewhere.[42] The concentrations of the metal precursors in the impregnating solutions were adjusted to obtain metal weight loadings of 0.5% Pt and the corresponding amount of Cu necessary to give the desired Pt/Cu atomic ratio (Table1). The catalyst nomenclature is defined according to the Pt to Cu ratio. For example, a catalyst with Pt to Cu ratio of 1:3 is referred to as Pt1Cu3.

CO chemisorption measurements were carried out using a volumetric sorption analyzer ASAP 2010 Chemi (Micromeritics) to determine the fraction of Pt atoms exposed, as described elsewhere.[42]

4.2.2 Standard Catalytic Experiments: CH_2ClCH_2Cl

The flow kinetics experiments were conducted in a stainless-steel, differential, flow reaction system equipped with a quartz microreactor (10 mm i.d.) in which the catalyst was supported on a quartz frit. The pretreatment gases and gaseous reactants were metered using mass flow controllers (Brooks, model 5850E) and mixed prior to entering the reactor. All gases were 99.999% pure with impurities of O_2, H_2O, and total hydrocarbons not exceeding 4.0, 3.5, and 0.5 ppm, respectively (Air Products). The 1,2-dichloroethane (Sigma-Aldrich, 99.8%, primary impurity: 1,1-dichloroethane) was metered into the system by flowing He through a saturator containing the liquid reactant. A constant inlet concentration was ensured by maintaining the saturator at a constant temperature of 273±1 K using a recirculating cooling system. The catalyst temperature was maintained ±1 K using an electric furnace and a temperature controller (Omega model CN2011). The reaction products were monitored online using a gas chromatograph (Varian 3300 series) equipped with a 10 ft 60/80 Carbopack B/5% Fluorocol packed column (Supelco) and a flame ionization detector. The detection limit for all products was 2 ppm. Hydrogen chloride was not quantified in these experiments.

The catalyst pretreatment consisted of purging the catalyst with He (30 ml/min) for 5 min at 303 K. The He flow was held constant as the catalyst was heated to 403 K at a rate of 6.7 K/min. The catalyst was maintained at these conditions for 1 h before the flow was switched to 20% H_2 + 80% He (50 ml/min). The catalyst was heated to 493 K at a rate of 6.7 K/min and held at 493 K for 1.5 h. The catalyst was then cooled in He (40 ml/min) to the reaction temperature.

The reaction was conducted at 473 K and atmospheric pressure. The total flow rate of the reaction mixture was 41 ml/min and consisted of 7,000 ppm CH_2ClCH_2Cl, 36,600 ppm H_2, and a balance of He. The conversion was maintained in the differential range between 1 and 3%. Approximately 200 mg of catalyst was necessary to achieve this conversion given the described flow rates and temperature.

4.2.3 Standard Catalytic Experiments: Ethylene

Experiments were also performed to test the ethylene hydrogenation rates on selective and unselective catalysts. These experiments were conducted in the flow kinetics system previously described. Pt1Cu1 and Pt1Cu3 catalysts were tested with a reaction mixture consisting of 3250 ppm ethylene, 6500 ppm H_2 and the balance He with a total flow rate of 180 mL/min. The experiments were preformed at room temperature with ~30 mg of catalyst.

4.2.4 Pulse Catalytic Experiments

Another type of kinetics experiment involved the injection of pulses of CH_2ClCH_2Cl into a continuous flow of H_2 and He and will be referred to here as pulse kinetics experiments. These experiments were carried out in the same system used for the standard kinetic experiments described above with only slight modifications required. After the catalyst was pretreated in the standard fashion, a flow of gas identical to that used in the standard kinetic experiments with the omission of CH_2ClCH_2Cl was begun. The system had been modified so that, after passing over the catalyst, the gas passed directly into the GC column. One mL pulses of the CH_2ClCH_2Cl saturated He described above were injected into the flow upstream of the reactor at 40 minute intervals. Conversion was held in the same range as above.

4.2.5 FTIR Spectroscopy Experiments

The infrared spectra were recorded with a Mattson Research Series II FTIR spectrometer equipped with a liquid N_2 cooled MCT detector. The resolution was 4 cm^{-1} and 400 scans were accumulated per spectrum. The IR cell was similar to that described elsewhere.[60] The cell volume was 200 cm^3 and the light pathlength was approximately 15 cm. The cell was equipped with glass stopcocks connected to gas inlet/outlet ports.

The infrared spectra were collected in the transmission mode which mandated the use of thin wafers of the catalyst sample. The self-supporting catalyst wafers (~ 20 mg/cm^2 thick) were prepared by powdering the catalyst material in an agate mortor and

then pressing the powder at 830 atm for 3 min. *In-situ* activation of the sample included drying under dynamic vacuum at 403 K for 1 h and reduction in 100 Torr of H_2 at 673 K for 1.5 h followed by evacuation at 673 K for 1 h and cooling to room temperature. Then the gas phase was evacuated at 493 K to a pressure of 10^{-5} Torr.

The dipole-dipole frequency shifts and singleton frequencies of CO adsorbed on the metals were measured using an isotopic dilution method.[61] Mixtures of ^{12}CO (PraxAir, 99.99%) and ^{13}CO (Isotec Inc., 98%), which varied between 10 and 100% ^{12}CO, were introduced and spectra recorded with particular attention paid to the band for ^{12}CO linearly adsorbed on Pt.

4.3 Results

4.3.1 Catalyst Dispersion

Based on the CO chemisorption measurements, 60% of the Pt atoms were exposed with the reduced silica-supported monometallic Pt catalyst. The bimetallic Pt1Cu1 and PtCu2 had Pt dispersions of ~35%, and for the other PtCu catalysts that had a lower Pt/Cu atomic ratio the dispersion was approximately 10%, independent of the catalyst composition (Table 4.1).

4.3.2 Standard CH_2ClCH_2Cl Kinetics

Both monometallic Pt/SiO_2 and bimetallic $(Pt+Cu)/SiO_2$ catalysts were active for the dechlorination of 1,2 dichloroethane at 473 K to form ethane and ethylene (Table 4.2).

However, under the same conditions the CH_2Cl-CH_2Cl conversion for Cu/SiO_2 was below the detection limit (0.1%). For each catalyst the conversion dropped by 1-2% during the first 0.5 h of reaction after which the rate decreased ~0.05% every 5 h (Figure 4.1-2). All of the catalysts containing Pt exhibited similar steady-state TOFs, based on CO chemisorption (Table 4.2). The highest TOFs were observed for Pt and Pt1Cu1 catalysts.

The catalyst selectivity strongly depended on Pt/Cu atomic ratio (Table 4.2). For the monometallic Pt/SiO_2 the major product was ethane (~83%) and the second major product was monochloroethane (~17%). With Pt1Cu1, ethane and monochloroethane were also the major products, with an ethane selectivity of ~88% and a chloroethane selectivity of ~12%. The characteristic feature for the catalysts with a Pt/Cu atomic ratio $\geq 1/2$ is the absence of ethylene in the reaction products. However, as the Cu content increased the selectivity towards ethylene increased considerably, ranging from 67% on Pt1Cu3 to above 93% on Pt1Cu18 (Table 4.2). It is worth noting that the catalysts with Pt/Cu ratio $< 1/2$ did not produce monochloroethane. Thus, there is a marked difference in the selectivity of the monometallic Pt catalyst, bimetallic Pt/Cu catalysts with atomic ratio $\geq 1/2$ and catalysts with Pt/Cu $< 1/2$.

4.3.3 Standard Ethylene Kinetics

Both the $Pt1Cu1/SiO_2$ and $Pt1Cu3/SiO_2$ catalysts, unselective and selective, respectively, showed similar steady state activities in the hydrogenation of ethylene. At room

temperature, the $Pt1Cu1/SiO_2$ catalyst had a TOF of 0.062 s^{-1}, and the $Pt1Cu3/SiO_2$ catalyst had a slightly higher TOF of 0.176 s^{-1}.

4.3.4 Pulse Kinetics

Catalyst TOFs for the pulse kinetics work were calculated on a per pulse basis. The $Pt1Cu1/SiO_2$ and $Pt1Cu3/SiO_2$ catalysts showed TOFs of $1.332X10^{-5}$ and $3.248X10^{-4}$ CH_2ClCH_2Cl atoms per pulse per exposed Pt atom, respectively. The $Pt1Cu1/SiO_2$ catalyst showed selectivities of approximately 91 percent and 9 percent for ethane and ethyl chloride, respectively (Figure 4.3). The $Pt1Cu3/SiO_2$ catalyst was 100 percent selective toward ethylene (Figure 4.4).

4.3.5 Infrared Experiments

The infrared spectra of CO adsorbed on Pt/SiO_2 and $Pt1Cu3/SiO_2$ catalysts at saturation coverage are shown in Figure 4.3 as spectrum 1 and 2, respectively. In spectrum 1 the band at 2078 cm^{-1} is characteristic of linearly adsorbed ^{12}CO on Pt^0.[62] The bands at 2130 and 2031 cm^{-1} in spectrum 2 have been assigned to linearly adsorbed CO on Cu^0 and Pt^0, respectively.[62] As the ν(CO) adsorbed on Cu^0 and Cu^{1+} are very close, the band assignment was confirmed by the fact that the band at 2130 cm^{-1} disappeared when gas phase CO was evacuated. Unlike CO-Cu^0, the CO-Cu^{1+} adsorption complexes are known to be stable and do not decompose upon evacuation at room temperature.[63]

The position of the absorption band of ^{12}CO on Cu^0 for all of the catalysts was independent of the composition of gaseous ^{12}CO+^{13}CO mixture used in the adsorption experiments and was the same as for the Cu/SiO_2 catalyst. The frequency of ^{12}CO vibration on Pt for Pt/SiO_2 catalyst shifted from 2078 to 2052 cm^{-1} when the ^{12}CO concentration of the ^{12}CO+^{13}CO mixture was decreased from 100 to 0%, but remained almost constant at around 2030 cm^{-1} for the $Pt1Cu3/SiO_2$ catalyst (Figure 4.6). It is noteworthy that the $\nu(^{12}CO)$ band of CO adsorbed on Pt for the $Pt1Cu2/SiO_2$ catalyst was close to that of Pt/SiO_2 for pure ^{12}CO and to that for the $Pt1Cu3/SiO_2$ catalyst at infinite dilution of ^{12}CO with ^{13}CO (Figure 4.6).

4.4 Discussion

Bimetallic Pt-Cu catalysts show olefin selectivity much greater than that of monometallic Pt while maintaining activity beyond that which is possible for monometallic Cu (Table 4.2). Analysis of the possible causes of this synergistic effect gives insight into the molecular level surface interactions between reactant, product, and catalyst and serves to clarify the nature of the active site itself.

Given the character of the dechlorination reaction, the catalyst precursors, and the metals themselves, it is reasonable to somewhat restrict the possible sources of the selectivity trends leading to olefins. Monometallic Pt is highly active if not selective in conversion of 1,2-dichloroethane (Table 4.2), and clearly the possibility exists that the observed selectivity effect arises from modification of the Pt active sites in some fashion due to the presence of the Cu. The “inert” nature of the silica support allows electronic

modification of the active site due to changes in dispersion facilitating more intimate metal/support contact to be ignored.[48]

Electronic modification by chlorine, either residual from the chloride precursors or accumulated during reaction, is a more reasonable possibility. Since Cu is much less able to dissociate H_2 than Pt[64-65] and surface Cl is highly reactive with atomic H,[63] one would expect higher Cl coverage on the bimetallic catalysts containing more Cu. Pulse kinetics experiments allow some examination of this possibility. While comparison of activities observed in pulse kinetics to those observed in simple flow is nontrivial, comparison of selectivities in a system which delivers 40 minutes of hydrogen flow to the catalyst between pulses of chlorocarbon allow examination of the selectivity of the surface with much lower chlorine coverage. If chlorine played an important role in selectivity through electronic modification, it would be expected that catalysts would show different selectivities under pulse conditions. It is found that this is not the case. While the activity of the catalysts is significantly enhanced, even with the greatly reduced chlorine coverage expected in these conditions, $Pt1Cu3/SiO_2$ remains highly selective toward the formation of ethylene (Figure 4.4) indicating that electronic modification by Cl is not the decisive factor in selectivity.

A second possible source of electronic modification of the Pt active site is the Cu itself. CO chemisorption is a widely used tool to probe electronic structure of metals because ν(CO) is very sensitive to the electron density of the adsorption sites.[62] Spectroscopic investigations led Ponec et al. to conclude that for PtCu catalysts an electronic effect, if it existed at all, was slight.[66] However, the results of the present

investigation provide evidence that an electronic interaction between Pt and Cu in the catalysts may exist. The singleton frequencies of CO adsorbed on Pt determined by the isotopic dilution method[66] were 2052 cm^{-1} for monometallic Pt and 2030 cm^{-1} for Pt1Cu1 and Pt1Cu3 catalysts (Figure 4.6). While the Pt1Cu1 catalyst is not selective toward ethylene in 1,2-dichloroethane hydrodechlorination, the ethylene selectivity of the Pt1Cu3 catalyst is 67% (Table 4.2). As the singleton frequency of the Pt1Cu1 and Pt1Cu3 are the same, the selectivity effect on the catalysts in halocarbon dechlorination reaction is probably not caused by an electronic structure change of Pt.

Beyond simple modification of the Pt active site, it now appears that Cu itself takes part in the reaction in some fashion. One possible role of Cu is to facilitate through spillover the desorption of the surface hydrocarbon intermediates before they can be fully hydrogenated to produce ethane. This hypothesis is consistent with the fact that the heat of ethylene adsorption on Cu is much less than that on Pt (18 kcal/mol[67] and 22-30 kcal/mol,[68] respectively). Ethylene hydrogenation results, however, seem to suggest otherwise. Both selective and unselective catalysts show similar activities for ethylene hydrogenation. If ethylene-like intermediates spillover readily enough in the dechlorination reaction to limit the efficiency of Pt sites in hydrogenating them, why would they spillover less quickly in the absence of obstructive surface Cl atoms as in the case of simple ethylene hydrogenation? This is certainly counter intuitive if the role of Cu continues to be interpreted in terms of simple modification of a Pt active site or indirect participation through facilitation of desorption. If, however, the results are interpreted in terms of a shift in active site location away from the Pt centers responsible

for ethylene hydrogenation to more remote Cu sites, a clearer picture of the role of each metal begins to emerge.

A more direct role of Cu in ethylene selective catalysts appears still more likely when the activity of monometallic Cu is more fully explored. Even though C-Cl bond scission in vicinal dichlorohydrocarbons occurs readily on a Cu surface to form an olefin,[69-70] silica-supported Cu did not show dechlorination activity at 200°C with standard pretreatment (Table 4.2), but was activated by 400°C reduction (not shown). The greater amount of chlorine removed by the higher temperature pretreatment was then sufficient to allow the dechlorination reaction to occur, though, at one tenth the rate of the bimetallics. This is most likely because dissociative H_2 chemisorption is activated on Cu surfaces.[71] If the rate of H_2 dissociation on a Cu surface is slower than the rate of C-Cl bond cleavage, the result would be a shift in the rate limiting step. Thus, the catalytic activity is suppressed by this new limiting step and by enhanced Cl poisoning. The catalytic requirement, then, for ready formation of ethylene on Cu sites is simply a sufficient source of dissociated H_2.

Indeed, a close look at CO dipole-dipole interaction results (Figure 4.4) suggests that Pt is in considerably more intimate contact with Cu in the selective Pt1Cu3 catalyst than in the unselective Pt1Cu1 catalyst. The monometallic Pt and Pt1Cu1 have similar $\nu(^{12}CO)$, around 2080 cm^{-1} when pure ^{12}CO is adsorbed, but the band position of adsorbed ^{12}CO shifts to lower wavenumbers as ^{12}CO is diluted with ^{13}CO reaching a value characteristic of the Pt1Cu3 catalyst at infinite dilution (Figure 4.6). This decrease in the $\nu(^{12}CO)$ is due to elimination of dipole-dipole coupling between ^{12}CO molecules as

the concentration of ^{13}CO increases.[26] However, no change in $\nu(^{12}CO)$ occurs when the composition of ^{12}CO+^{13}CO mixture is varied for the Pt1Cu3 catalyst (Figure 4.6). Thus, if Pt ensembles are relatively large in the Pt1Cu1 catalyst, they consist of small ensembles or isolated Pt atoms in the Pt1Cu3 catalyst.

The enhancement in the activity of Cu sites as Pt becomes more intimately associated with them is insufficient to explain the trends in catalytic activity and selectivity. Ethylene is not simply being produced in addition to ethane but replacing it. Hence, the dramatic difference in selectivity toward ethylene between the catalysts with Pt/Cu atomic ratio $< 1/3$ and $\geq 1/3$ can be understood in terms of the C-Cl bond cleavage being a size demanding elementary step.[12,73] If hydrogenolysis of C-Cl bond requires larger Pt ensembles, the reduced production of ethane on PtCu catalysts with Pt/Cu atomic ratio $\leq 1/3$ must be due to deficiency of sufficiently large Pt islands for the bond scission. In this case the role of Cu is to catalyze the C-Cl bond dissociation of adsorbed 1,2-dichloroethane to form surface $\cdot CH_2\text{-}CH_2\cdot$ species that subsequently desorbs as ethylene. Pt is necessary to provide a source of dissociated hydrogen which upon spilling over from Pt sites reduces surface CuCl species to form HCl regenerating catalytically active sites.

4.5 Conclusion

The addition of Cu to Pt supported catalyst alters its selectivity towards ethylene in the dechlorination of 1,2-dichloroethane in the presence of hydrogen. Results obtained

from infrared investigations using isotopic mixtures of ^{12}CO and ^{13}CO, pulse kinetic studies, and ethylene hydrogenation kinetic experiments suggest that Cu has both a geometric and an electronic influence on Pt. Of the two effects, dilution of Pt ensembles by Cu appears to dominate in terms of the selectivity behavior of the bimetallic catalysts. A size demanding C-Cl bond scission is consistent with the experimental observations. As well, it is possible that Pt acts only as a source of dissociated hydrogen while dissociation of C-Cl bond followed by the desorption of ethylene occurs on Cu.

Table 4. 1 Percent weight loadings for Pt and Cu and percent Pt exposed as determined by CO chemisorption for silica supported Pt and Pt-Cu catalysts.

Catalyst	% Pt Weight Loading	% Cu Weight Loading	% Pt Exposed
Pt	0.50	0.00	61
Pt1Cu1	0.50	0.17	33
Pt1Cu2	0.49	0.32	37
Pt1Cu3	0.50	0.48	11
Pt1Cu6	0.49	0.96	15
Pt1Cu9	0.48	1.40	11
Pt1Cu18	0.47	2.70	10

Table 4. 2 Steady state kinetics parameters of (Pt+Cu)/SiO_2 catalysts for the hydrodechlorination of 1,2-dichloroethane.

Catalyst	Conversion %	Selectivity, mole %			Activity μmol/s/g_{cat}	TOF x10^3, s^{-1}
		C_2H_4	C_2H_6	C_2H_5Cl		
Pt	2.7	0	82.8	17.2	60.9	4.0
Pt1Cu1	1.9	0	87.6	12.4	31.2	3.5
Pt1Cu2	2.0	0	92.2	7.8	10.0	1.1
Pt1Cu3	1.3	67.1	32.9	0	4.8	1.9
Pt1Cu6	1.8	86.5	13.5	0	4.5	1.8
Pt1Cu9	1.6	96.2	3.8	0	4.7	1.8
Pt1Cu18	1.6	93.7	6.3	0	5.4	2.1
Cu	0	-	-	-	0	-

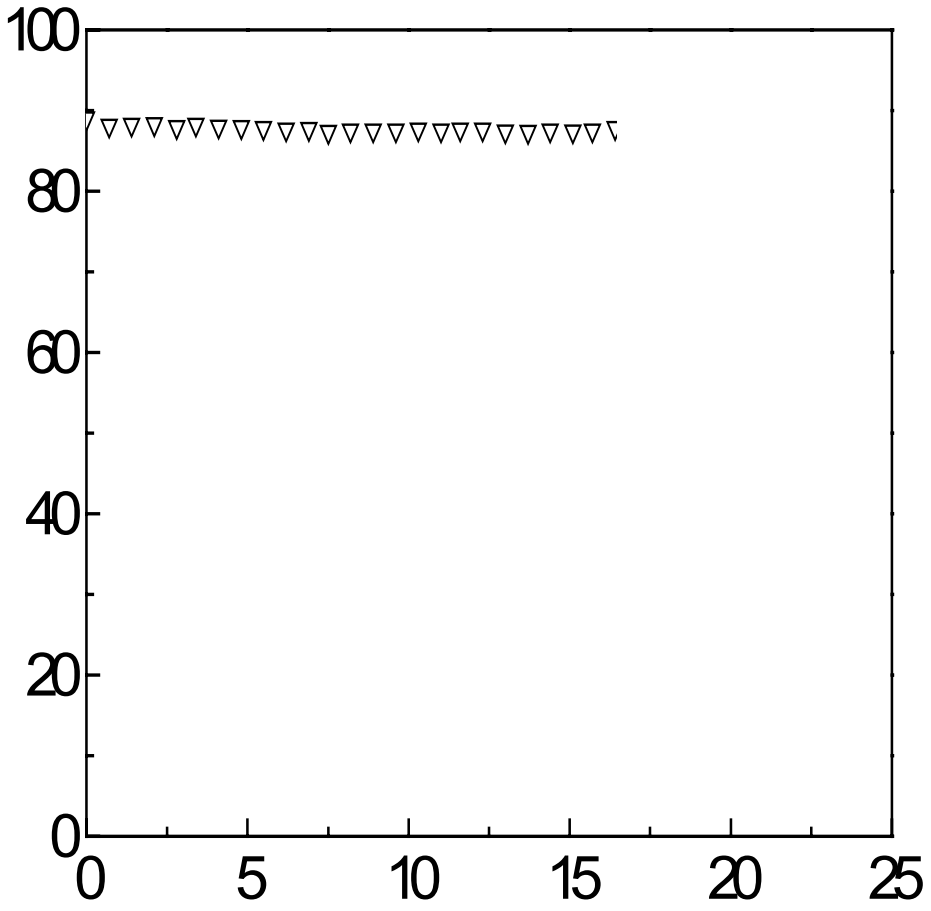

Figure 4. 1 Selectivity vs. time on stream for Pt1Cu1/SiO2 at 200^{o}C. 1 - ethane, 2 - ethylene, 3 - monochloroethane, 4 - conversion.

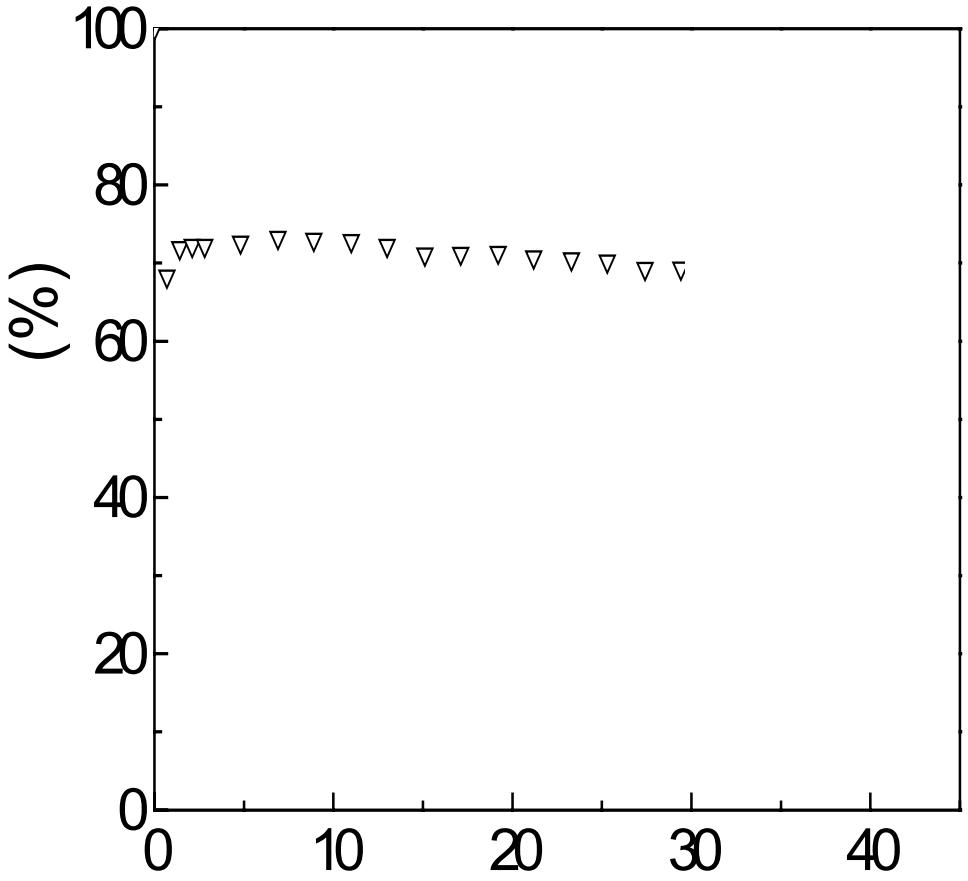

Figure 4. 2 Selectivity vs. time on stream for Pt1Cu3/SiO2 at 200^{o}C. 1 - ethane, 2 - ethylene, 3 - conversion.

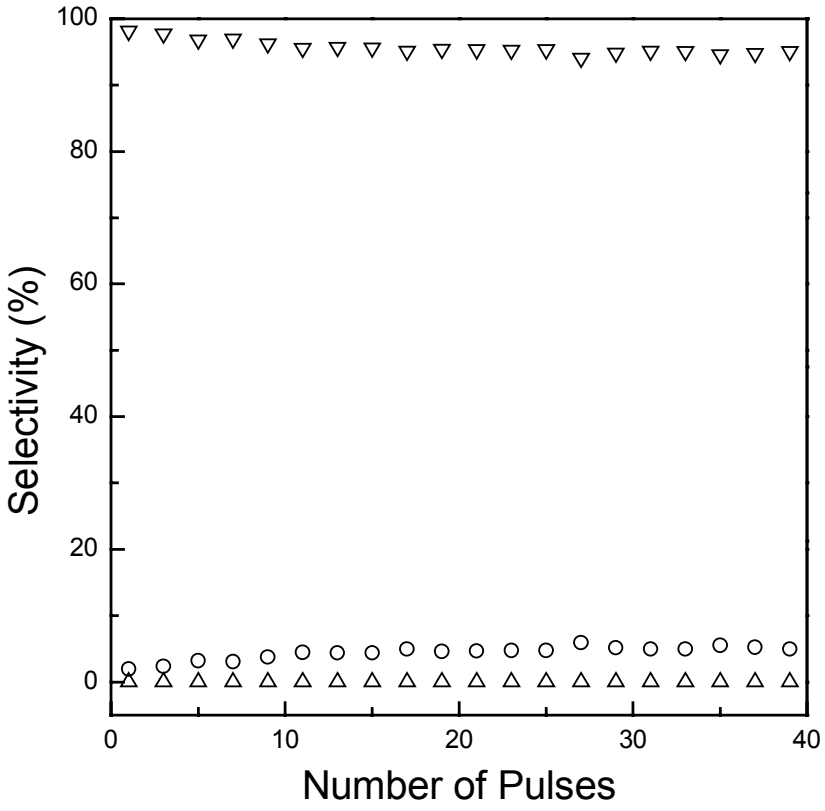

Figure 4. 3 Selectivity vs. pulse number for $Pt1Cu1/SiO_2$ at 200°C. ▼ - ethane, Δ - ethylene, ○ - monochloroethane.

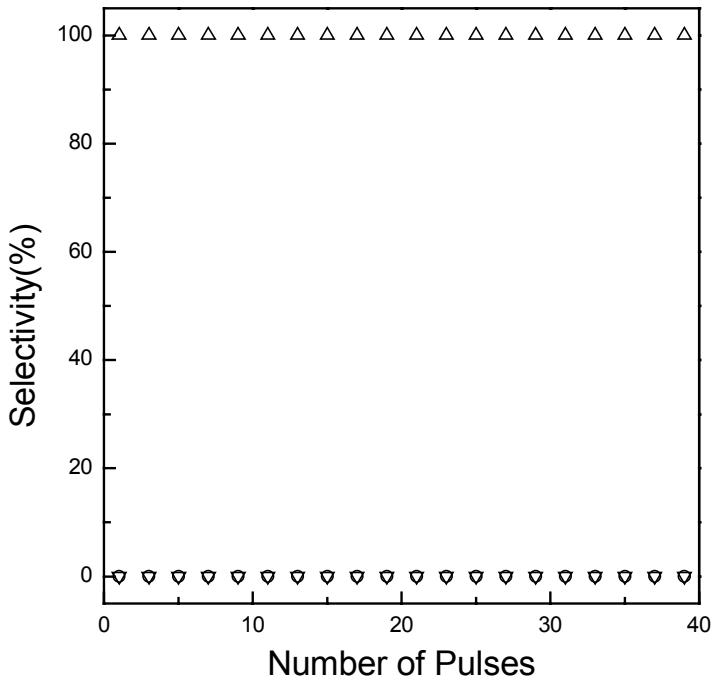

Figure 4. 4 Selectivity vs. pulse number for $Pt1Cu3/SiO_2$ at 200°C. ▼ - ethane, Δ - ethylene, ○ - monochloroethane.

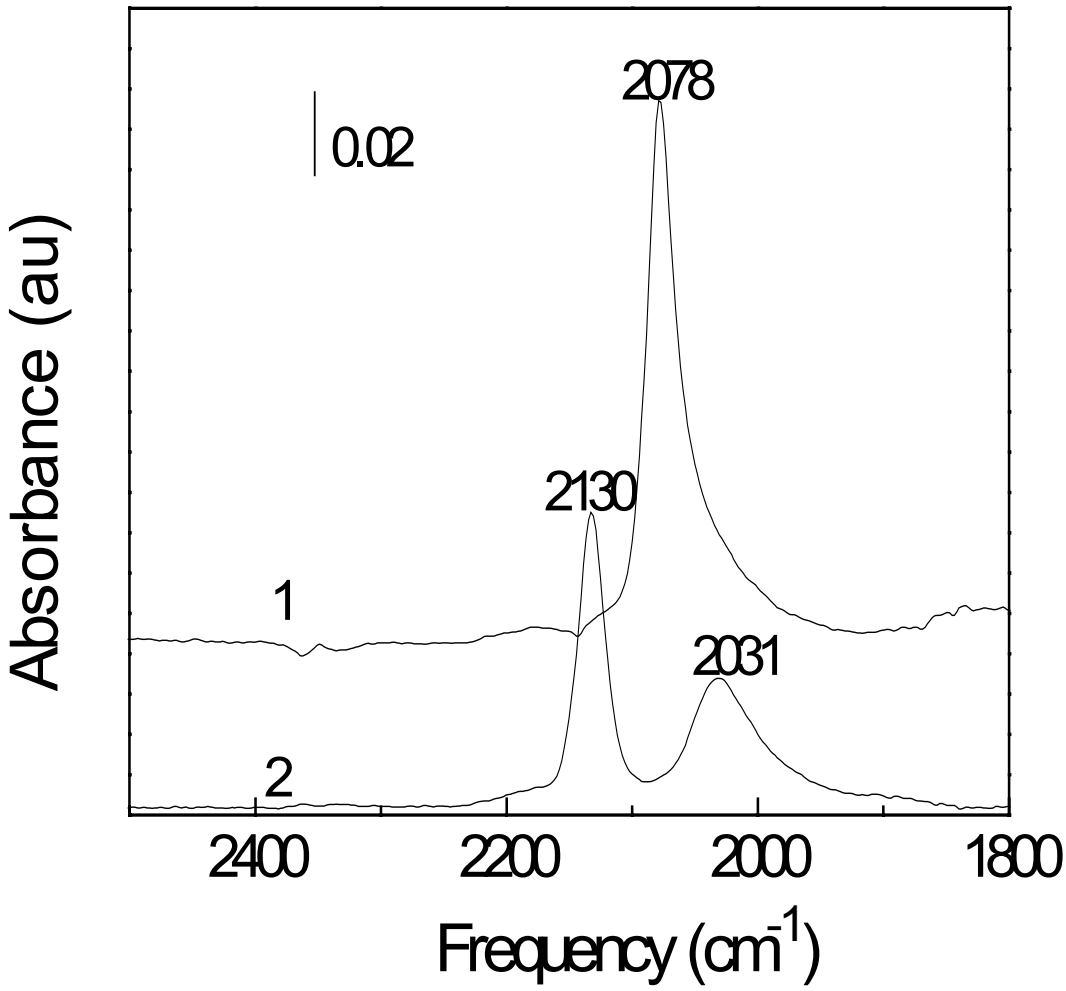

Figure 4. 5 Spectra of ^{12}CO (P = 10 Torr) adsorbed on Pt/SiO_2 (1) and $Pt1Cu3/SiO_2$ (2).

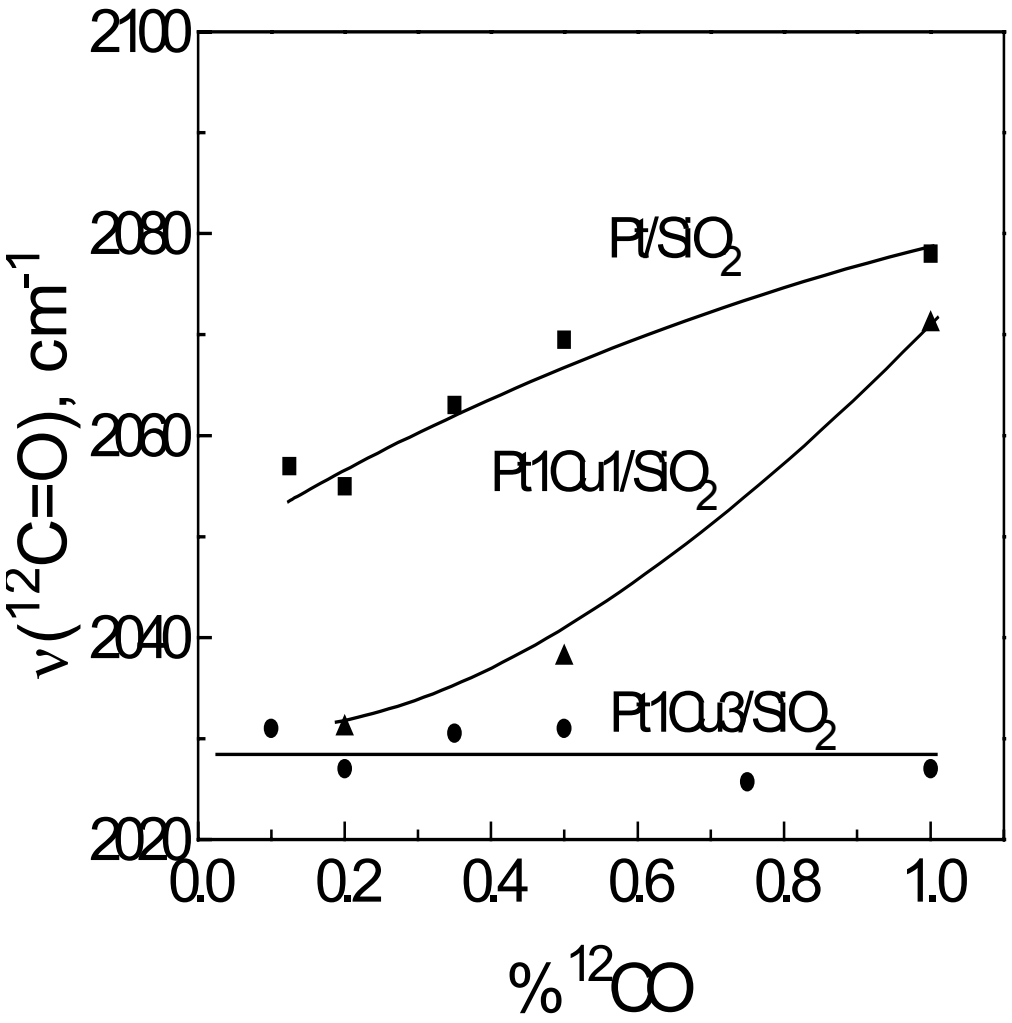

Figure 4. 6 Dependence of $\nu(^{12}C{=}O)$ of ^{12}CO-Pt complexes on the composition of ^{12}CO+ ^{13}CO mixture (P_{total}= 10 Torr).

5.0 MOBILITY OF METALLIC PRECURSORS IN SILICA-SUPPORTED PT-CU SYSTEMS

5.1 Introduction

A critical issue in the performance of supported, bimetallic catalysts is the degree of contact between the metals on the support surface. While spillover effects across the support surface can be significant,[74] the formation of alloy or, at a minimum, bimetallic particles is generally required if performance unique to the bimetallic catalyst, rather than simply a superposition of monometallic performance properties, is to be achieved.[12-14]

The preparation of these bimetallic particles is not always simple and can present an unpleasant choice between a large fraction of bimetallic particles and high dispersion. The simplest and least expensive methods available are those of successive and coimpregnation. These procedures, however, can result in separation of the metal precursors on the support surface due to lack of strong precursor-precursor interactions and chromatographic effects.[11] In order to alleviate these separations and produce alloy particles, high temperature treatments are generally required which tend to result in reduced dispersion. Organometallic[75] and surface controlled reaction[76-78] techniques, which take advantage of the controlled stoichiometric reactions to produce particles with the desired structure and composition, are certainly an alternative, but these methods can be too expensive and complex for industrial use. A possible solution to the problem is the development of low temperature pretreatments capable of enhancing alloying of the metals without causing substantial sintering.

Water, either liquid or in the form of atmospheric humidity, is known to significantly facilitate alloy formation in some catalysts.[79-80] Anderson and coworkers, in particular, were able to use exposure to atmospheric humidity to vary the alloy state of Pt-Cu/SiO_2 catalysts.[82] The current study addresses the interactions of similar catalysts with water using a variety of kinetic and characterization techniques, Raman spectroscopy, and transmission electron microscopy.

5.2 Experimental

5.2.1 Catalyst Preparation and Characterization

Catalysts were prepared from two types of precursors: chloride and nitrate. The chloride-precursor catalysts were prepared by pore volume impregnation of SiO_2 (Aldrich, 99%) with aqueous solutions of $H_2PtCl_6 \cdot 6H_2O$ (Alfa, 99.9%) or $H_2PtCl_6 \cdot 6H_2O$ and $CuCl_2 \cdot 2H_2O$ (MCB Manufacturing Chemists, 99.5%), as described elsewhere.[42] The nitrate-precursor catalysts were prepared by pore volume impregnation of SiO_2 (Aldrich) with aqueous solutions of $Pt(NH_3)_4(NO_3)_2$ (Strem Chemical) or $Pt(NH_3)_4(NO_3)_2$ and $Cu(NO_3)_2 \cdot 6H_2O$ (Fisher Scientific). The impregnation mixtures were allowed were then allowed to equilibrate over night before drying at ambient temperature and pressure for 24 h. A portion of each of the nitrate-precursor catalysts was then calcined at 500^{o}C in lab air to remove precursor species and leave only insoluble Pt and Cu oxides on the surface.[11] All other catalysts were dried at 100^{o}C in lab air. The concentrations of the

metal precursors in the impregnating solutions were varied to give the metal weight percents shown for each of the dry catalysts in Table 5.1.

After preparation the catalysts were divided into batches of approximately 500 mg and stored in tightly-sealed glass vials. Some samples of each type of "fresh" catalyst were exposed to water for varying periods of time from 10 min to 30 days. The procedure for exposing a catalyst to liquid water consisted of placing two drops of distilled water into the catalyst vial, shaking for 1 minute, and repeating the first two steps. Another catalyst sample was exposed to laboratory air for 30 days to determine the effect of atmospheric moisture.

For reference, catalysts will be referred to by Pt:Cu atomic ratio followed by a parenthetical annotation to show the type of precursor and pretreatment, i.e. Pt(Cl) denotes a monometallic Pt catalyst prepared from chloride precursors, Pt1Cu1(Cl-fr-cal) denotes a catalyst with a Cu:Pt atomic ratio of 1 prepared from nitrate precursors and calcined at 500^{o}C in air, and Pt1Cu3(Cl-fr, H_2O) denotes a catalyst with a Cu:Pt atomic ratio of 3 prepared from nitrate precursors, left uncalcined, and exposed to water for 5 days.

5.2.2 Catalytic Experiments

Kinetics experiments were conducted at atmospheric pressure in a stainless-steel, flow reaction system equipped with a quartz microreactor (10 mm i.d.) in which the catalyst was supported on a quartz frit. Gaseous reactants and pretreatment gases (He,

H_2, Praxair, 99.999%) were metered using mass flow controllers (Brooks Instruments model 5850E), and mixed prior to entering the reactor. The 1,2-dichloroethane (Sigma-Aldrich, 99.8%) was metered into the system by flowing He through a saturator containing the liquid. A constant concentration in this stream was ensured by holding the saturator at a constant temperature of 0°C using a recirculating cooling system. The reaction temperature was 200±1°C, and the catalyst was maintained at that temperature using an electric furnace and a temperature controller (Omega model CN2011). The total flow rate of the reaction mixture consisting of 7,000 ppm CH_2ClCH_2Cl, 36,600 ppm H_2, and the balance He was 41 ml/min.

For all the experiments, the conversion was maintained between 2-3%. This was accomplished by varying the amount of catalyst in the reactor from 1 mg to 1 g. All reactions were run to steady state which was defined by a conversion change of less than 0.2% in 5 h and a change in selectivity of less than 1%. The reaction products were monitored online using a gas chromatograph (Varian 3300 series) equipped with a 10 ft 60/80 Carbopack B/5 % Fluorocol packed column (Supelco) and a flame ionization detector. The detection limit for all products was 2 ppm. HCl was not quantified in these experiments.

The catalyst samples were pretreated by four different methods, starting from the same drying procedure. The drying process consisted of purging the catalyst with He (30 ml/min) for 5 min at 30°C, continuing the He flow as the catalyst was heated to 130°C at a rate of 6.7°C/min, and maintaining the catalyst at these conditions for 1 h.

For the first pretreatment, the standard, the He flow was switched after the drying step to a H_2+He flow (17% H_2, 60 ml·min^{-1}). The catalyst was heated to 220°C at 3°C/min and held there for 1.5 h. Afterwards, the H_2+He flow was switched to pure He, and the catalyst was allowed to cool to the reaction temperature.

The second pretreatment consisted of heating the catalyst after the drying step to 220°C with the ramp of 3°C/min and holding the sample at this temperature for 1.5 h. The catalyst was then reduced in H_2+He flow at 220°C for 1.75 h in H_2+He flow.

The third pretreatment consisted of the standard pretreatment followed by heating to 400°C at a rate of 6°C/min in the H_2+He flow. These conditions were maintained for 3.5 h before switching from H_2+He flow to pure He and cooling to the reaction temperature. The fourth pretreatment consisted of the standard pretreatment followed by heating the sample to 400°C at a rate of 6°C/min in the He flow, holding at these conditions for 3.5 h and cooling to the reaction temperature in He flow.

5.2.3 TEM Experiments

Transmission electron microscopy studies were conducted using a JEM2010 (JEOL) electron microscope with a resolution of 0.14 nm and an accelerating voltage of 200 kV capable of distinguishing metal particles as small as 10 Å on the support surface. Catalysts were pretreated in the kinetics system described above then placed in tightly-sealed glass vials for transport to the microscopy system. Catalysts were tested after standard pretreatment, the treatment with 400^{o}C reduction described above, and exposure

to water followed by standard pretreatment. Sample preparation consisted of hand grinding under ethanol for 20 to 60 s followed by further dispersion with ultrasound at 35 kHz. Drops of the suspension were then placed on gold grids for examination. Digital Fourier-analysis (FFT) was used to clarify the HREM shown in Figure 5.14. Metals present in a given particle were identified using microdiffraction to measure the fcc spacing in the particle. An example of these diffractograms is shown as Figure 5.15. The mean diameter of all particles observed, D_m, and the summation of the cubes of the diameters of all particles observed divided by the summation of the squares of the diameters, D_{ss}, were calculated from measurements taken of more than 100 particles per sample.

5.2.4 TPR Experiments

Temperature programmed reduction experiments were carried out in a stainless steel, flow system similar to that used in the kinetics experiments. The gas stream leaving the reactor was monitored using a mass spectrometer (Balzer, TCP 121) with a channeltron detector operated at a chamber pressure of 10^{-5} Torr which was monitored using a PKR250 gauge.

The reactor was loaded with 100 mg of catalyst, and the reducing flow (10% H_2, 20 ml/min) started. The catalyst was purged for 30 min before heating from room temperature to 500^{o}C at a rate of 8^{o}C/min. The product stream was analyzed for H_2 uptake and HCl and Cl_2 formation.

5.2.5 EXAFS Experiments

EXAFS experiments were performed on X-ray beamline 4-1 at the Stanford Synchrotron Radiation Laboratory (SSRL) at the Stanford Linear Accelerator Center, Stanford, California. The storage ring energy was 3 GeV, and the ring current was 60–100 mA. Each powder sample was pressed into a wafer with a C-clamp and loaded into the EXAFS cell. The sample mass was calculated to give an absorbance of about 2.5 at the Pt L_3 and Cu K absorption edges. After standard pretreatment, the sample was aligned in the X-ray beam. The EXAFS data were collected in transmission mode after the cell had been cooled to nearly liquid nitrogen temperature. The data were collected with a Si(220) double crystal monochromator that was detuned by 20% to minimize effects of higher harmonics in the X-ray beam. The samples were scanned at energies near the Pt L_3 (11564 eV) and Cu K (8979 eV) absorption edges.

The EXAFS data were analyzed with experimentally and theoretically determined reference files. The former obtained from EXAFS data for materials of known structure. The Pt–Pt, Pt–$O_{support}$, Cu–$O_{support}$, and Cu–Cu interactions were analyzed with phase shifts and backscattering amplitudes obtained from EXAFS data for Pt foil, $Na_2Pt(OH)_6$, CuO, and Cu foil, respectively. The Pt–Cu and Cu–Pt interactions were calculated on the basis of the crystallographic data reported for $Cu[Pt_3(CO)_3(PPh_3)_3]_2$ by use of the FEFF software package.

The EXAFS data were extracted from the raw spectra with the XDAP software package. Data representing each sample were the average of six scans. The raw EXAFS

data obtained at Pt L_3 edge were analyzed with a maximum of 16 free parameters over the ranges $3.0 < k < 15.0$ Å^{-1} (k is the wave vector) and $0.0 < r < 4.0$ Å where k is the wave vector and r is the distance from the adsorbing atom. The statistically justified number of free parameters, n, was approximately 31, as estimated from the Nyquist theorem, $n = (2\Delta k \Delta r/\pi) + 1$, where Δk and Δr represent the k and r ranges used to fit the data. The raw EXAFS data obtained at the Cu K edge were analyzed with a maximum of 16 free parameters over the ranges $3.0 < k < 15.0$ Å^{-1} and $0.0 < r < 4.0$ Å. The statistically justified number of free parameters, estimated as described above, was approximately 31.

The data analysis was carried out using a difference file technique. The reliable parameters for the high-Z (Pt, Cu) and low-Z contributions ($O_{support}$) were determined by multiple-shell fitting in r space and k space with application of k^1 and k^3 weightings. Because data were obtained at both the Pt L_3 and Cu K edges, it was possible to determine the Pt-Cu distance, coordination number, and Debye-Waller factor from the data at each edge and evaluate the internal consistency of the fitting results.

5.2.6 Raman Spectroscopy

The Raman spectra were acquired using a Renishaw System 2000 confocal Raman spectrometer equipped with a Lieca DMLM microscope and a 514.5-nm Ar^+ ion laser as the excitation source. A low laser power of 5-25 mW at the source was used to prevent sample damage. An Olympus x50 objective was used to focus the unpolarized laser beam to a <3 μm spot on the sample surface and to collect backscattered light. Ten

scans were accumulated for each spectrum in the 100-4000 cm^{-1} region with a resolution better than 4 cm^{-1}. The *in situ* Raman measurements were carried out at atmospheric pressure in a THMS 600 heating-cooling Raman cell from Lincam Scientific. The desired He flow rate was maintained within ± 1 cm^3/min using Brooks mass flow controllers (model 5850E). About 100 mg of catalyst sample was layered on a thin microscope slide and the slide was mounted in the cell. Spectra were recorded for Pt1Cu3(Cl) with no pretreatment and after 5 days exposure to H_2O followed by drying at 130^oC for 2 h.

5.3 Results

5.3.1 CO Chemisorption

The fractions of Pt atoms exposed following reduction at 350°C obtained from CO chemisorption performed on an ASAP 2010 Chemi instrument (Micromeritics) are shown in Table 5.2.[42]

5.3.2 Catalytic Experiments

All the catalysts tested showed activities in the range 0.155 and 0.010 μmol/gm/s, Pt(Cl) being the most active, and Pt1Cu6(Cl, H_2O) being the least. The catalysts also showed a steady decrease in activity with increasing Cu content. This effect was most pronounced in the catalysts prepared from chloride precursors and not treated with H_2O in which

Pt1Cu6(Cl) was 89 percent less active than Pt(Cl) (Table 5.3). No correlation between decreasing activity and increasing selectivity is observed.

The catalysts prepared from chloride precursors were the only ones to be affected by the addition of water. Significant changes in neither activity nor selectivity were observed in nitrate-precursor catalysts after the addition of water were observed (Tables 5.4-5). For the chloride precursor catalysts, ethylene selectivity enhancements from 0 to 66 percent and from 0 to 90 percent were observed for Pt1Cu3(Cl) and Pt1Cu6(Cl), respectively, while neither catalyst showed significant changes in activity (Table 5.3).

Pt1Cu3 catalysts prepared from chloride precursors and nitrate precursors with calcination shows differing changes when exposed to alternative pretreatments. When the catalyst was dried in He at 220^{o}C instead of the usual 130^{o}C, the chloride precursor catalyst began to display an ethylene selectivity of 73 percent rather than the usual 0, but the activity was reduced by 45 percent. The nitrate precursor catalyst showed no change in selectivity. The activity, however, increased by 39 percent. When the a 400^{o}C reduction step was added after the standard reduction, the activity decreased by 40 and 14 percent for chloride and nitrate precursor catalysts, respectively. The ethylene selectivity of the chloride precursor catalyst was also increased from 0 to 46 percent, but no enhancement was observed for the nitrate precursor catalyst. The same 400^{o}C treatment, when H_2 was eliminated, caused no selectivity change but raised activity by 25 and 19 percent for the chloride and nitrate precursor catalysts, respectively.

Time was required for the changes caused by water to take place. A Pt1Cu6(Cl) catalyst exposed to water then immediately dried and reduced showed no change in

selectivity. The same catalyst exposed to water and allowed to equilibrate for 5 or 20 days displayed the changes in selectivity discussed earlier (Table 5.7).

5.3.3 TEM

The particle size distributions for all catalysts was monomodal and narrow (Figure 5.1-9). Catalysts prepared with the standard pretreatment showed the greatest degree of uniformity regardless of atomic ratio. All catalysts pretreated in this way had more than 60 percent of the particles in a range of less than 20 Å (Figures 5.1, 5.4, and 5.7). The addition of water or 400^{o}C reduction resulted in a greater degree of variation in particles size with no more than 50 percent of particles falling in the same 10 Å size range.

Under standard pretreatment, particles rarely (two or fewer per sample) exceed 60 Å in diameter regardless of atomic ratio. The addition of water does not serve to efficiently produce these "large" particles. All water-exposed catalysts have fewer than 3 percent of their particles in this range. Catalysts reduced at 400^{o}C, however, were observed to have as much as 10 percent "large" particles (Figures 5.1-9).

Another way of characterizing the uniformity of catalyst particles is by comparing D_{ss} to D_m. In a catalyst with greater particle size deviation, the D^3 sum will dominate the D^2 sum and lead to larger values of D_{ss}. After standard pretreatment, D_{ss} and D_m differ by 26, 10, and 17 percent for Pt(Cl), Pt1Cu1(Cl), and Pt1Cu3(Cl), respectively. After addition of water followed by standard pretreatment, they differ by 6, 24 and 17 percent,

respectively. After reduction at 400°C, they differ by 24, 22, and 25 percent, respectively (Table 5.8).

Monometallic Pt catalysts prepared from chloride precursors were made up of slightly distorted spherical Pt particles regularly distributed over the support surface regardless of pretreatment. All particles showed distinct microdiffraction fringes with fcc structure d_{111}=2.27 Å. A small number of agglomerate particles having diameters near the average were observed.

The Pt1Cu1(Cl) and Pt1Cu3(Cl) catalysts also exhibited uniformly distributed metal particles, a small fraction of which are agglomerates. Prior to exposure to H_2O, both catalysts consisted primarily of metallic particles near the average observed diameter with fcc structure d_{111}~2.27 Å. A much larger number of smaller, amorphous objects (~5Å) were observed on the support surface. After exposure to water, neither catalyst showed any change in the observed size and crystal structure of the metallic particles. In the Pt1Cu3 catalyst, however, a thin amorphous layer (5-10 Å thick) was observed on the metallic particles. Reduction of the Pt1Cu1(Cl) and Pt1Cu3(Cl) catalysts at 400°C resulted in some sintering, the mean diameter changing by 11 and 28 percent for PtCu1(Cl) and Pt1Cu3(Cl), respectively, and the formation of particles which showed fcc structure with d_{111} ranging from 2.09 to 2.27 Å. No amorphous layer was observed on the surface of these particles.

5.3.4 TPR

The only reduction product of the catalysts was HCl. Hydrogen uptake profiles are shown in Figure 5.16. The reduction profile of Cu(Cl) consists of two peaks at 372^{o}C and 464^{o}C, respectively. The reduction profile of Pt1Cu3(Cl) shows peaks at 220^{o}C and 291^{o}C, respectively. The reduction profile of Pt(Cl) consists of three joined peaks at 198^{o}C, 233^{o}C, and 274^{o}C, respectively.

5.3.5 EXAFS

Coordination numbers did not change significantly with the addition of water. The Pt-Pt, Pt-Cu, and Cu-Pt coordination changed by 47, 45, and 76 percent in the absence of water and 41, 39, and 72 percent in the presence of water, respectively, from Pt1Cu1(Cl) to Pt1Cu6(Cl) (Tables 5.9-10).

5.3.6 Raman Spectroscopy

The spectrum of the fresh Pt1Cu3(Cl) catalyst showed couplets with peaks at 216 and 247 cm^{-1} and 318 and 344 cm^{-1}, respectively, as well as a single peak at 407 cm^{-1}. After treatment with H_2O for 5 days followed by drying at 130^{o}C for 2h, the couplet at 216 and 247 cm^{-1} disappeared , and the couplet at 318 and 344 cm^{-1} degraded to a single broad peak at 331 cm^{-1}. At the same time, a new peak appeared at 287 cm^{-1} (Figure 5.17).

5.4 Discussion

In the examination of a heterogeneous catalyst, it is always questionable to what degree the support and dispersion effects dominate the intrinsic activity of the metal. The catalysts under investigation show no selectivity toward ethylene under standard pretreatment conditions even at a Cu:Pt ratio of 6. Previously, a series of identical chloride precursor catalysts with the exception of weight loading were shown to produce increasing amounts of ethylene, approaching 100 percent, with increasing Cu:Pt atomic ratio.[43] A similar trend is observed in the high weight loading catalysts currently under consideration in the presence of water. It has been previously theorized that Cu-rich Pt-Cu alloy particles are responsible for the production of ethylene in Pt-Cu bimetallic catalysts.[42-43,83] Given the potential industrial applicability of a phenomenon which allows alloys to form on the surface while maintaining high dispersion, it is interesting to investigate the specific effect of water on these catalysts.

One technique capable of examining the catalyst precursors in their unreduced form is Raman spectroscopy. Prior to the addition of water, Pt and Cu precursor species appear to be largely separated in the bimetallic catalysts. For the Pt1Cu3(Cl) catalyst, strong Raman couplets at 216/247 cm^{-1} and 318/344 cm^{-1} corresponding to the symmetric and asymmetric stretching vibration of the Cu-Cl[84] and Pt-Cl[85] bonds, respectively, are observed as well as a single band at 407 cm^{-1} corresponding to bond deformation for Cu-Cl[19] (Figure 5.17). The presence of these bands indicates a particle size in excess of 25 Å, and the lack of significant shifts from the literature values and the presence of new

bands suggests that the Pt and Cu chloride species are present separately and not as mixed chlorides.[87]

Similarities in activity and selectivity of catalysts reduced at 400°C to that of catalysts which have been exposed to water seem to suggest that structural similarities could be present as well. In the unreduced Pt1Cu3(Cl) catalyst, Raman spectroscopy shows considerable degradation of the bands observed in the fresh catalyst once water is added. One explanation is redistribution of the precursor species to form particles less than 25 Å in diameter.[87] These particles would fall below the detection limit for Raman resulting in peak degradation similar to that observed. Microscopy makes this seem unlikely, however, since it observes no difference in the size of reduced Pt particles in H_2O exposed catalysts. A second possibility arises from the appearance of a new band at 287 cm^{-1}. This band has not previously been observed, but situated between the stretching vibrations of the Pt-Cl[84] and Cu-Cl[85] bonds, it offers the suggestion of a Cl atom bridged between Pt and Cu. Kawashima and coworkers observed the appearance of a similar band when a portion of the Pt in a complex bridged structure was replaced with Cu.[89] Raman, then, suggests the formation of more intimately associated Pt and Cu precursor species on the support surface, a state known to often lead to the formation of alloy particles.[11]

Microscopic images give evidence for considerable alteration of the post-reduction surface after the addition of water, but in a fashion distinct from that observed on catalysts reduced at 400°C. Reduced Pt particles, i.e. particles having fcc structure with d_{111}=2.27 Å, with diameters near 30 Å and amorphous objects approximately 5 Å in

diameter look probable. In bimetallic catalysts treated with water, however, a film of amorphous material 5 to 10 Å thick covers these particles. An illustration can be seen in Figure 5.12b. This structure is explainable through a series of steps which begin with the mixed chloride particles suggested by the Raman experiments. Upon addition of H_2 at 220^{o}C, most of the Pt is reduced as shown by the TPR experiments (Figure 5.16). Because of high, metallic surface tension of 1700 mN/m[89] and weaker interaction with Cl than Cu,[13] Pt would likely segregate upon reduction. Henry and coworkers have shown that the presence of electronegative adsorbates such as Cl leads to segregation and particle rounding in Pd-Cu catalysts.[90] The Cu in contact with Pt is partially reduced (Figure 5.16), but the remaining surface chlorine prevents alloy formation by forcing the surface to remain enriched in Cu (Figure 5.16).[13] Even in the absence of Cl, Brongersma and Sparnaay have observed surface enrichment of Cu on Pt-Cu bimetallic catalysts.[91] Any Cu which was reduced oxidizes immediately when exposed to air.[92] As in the absence of water, Cu not in close contact with Pt does not reduce (Figure 5.16), explaining the presence of 5 Å amorphous $CuCl_2$ particles in both catalysts. This sequence is illustrated in Figure 5.19.

Before a discussion of the mechanics of the effect of water can begin, it must first be established why Pt and Cu are initially found in separate particles. Separation of metals precursors because of differences in migration rates through catalyst pores has long been known to be a major problem with coimpregnation techniques.[11] Since H_2PtCl_6 and $CuCl_2$ differ significantly in their state in solution, i.e. Cu forming a positively charged species and Pt a negative one, it is expected that they migrate into the

pores at differing rates resulting in chromatographic separation upon drying of the catalyst, an effect illustrated in Figure 5.20. These chromatographic separations could result in a catalyst consisting primarily of monometallic Pt and Cu particles after reduction. Catalysts displaying this sort of separation would likely possess regions rich in Cu and Pt precursor particles, respectively, leading to significant separation between metallic Pt and Cu particles after reduction.

After initial drying, water added to the catalyst could fill the pores and result in reformation of the original impregnating solutions. Since liquid diffusion rates are several orders of magnitude larger than surface diffusion rates,[93] this condition would allow migration through the liquid phase to alleviate chromatographic separations. This hypothesis is consistent with the finding that the effect of water on selectivity is not instantaneous but requires several days, the time required for migration of the precursor solution species in the pores, for full effect (Table 5.3). The lack of effect on catalysts with different precursor species, which naturally have different solubilities and migration rates, suggests that the effect is dependent upon the ability of the migrating species to dissolve in water, i.e. no water effect whatsoever on the highly insoluble oxides[94] present after calcinations and a greatly reduced one on nitrate precursor catalysts. The condensation of atmospheric humidity inside the pores to form a liquid film similar to the solution discussed above explains the effect of exposure to atmosphere on these catalysts (Figure 5.21).

5.5 Conclusion

Exposure to laboratory air before reduction significantly enhances the ethylene selectivity of chloride-precursor, Pt-Cu catalysts. An even greater selectivity enhancement, as much as 66 percent, is observed when these catalysts are exposed to small amounts of liquid water for more than 3 days prior to reduction. Similar, though less pronounced, selectivity changes are observed after reduction of the catalyst at 400^{o}C.

Experiments in which the time of water exposure was varied show that the alterations of the surface is not instantaneous. Changes in the water effect when nitrates and oxides are present on the surface instead of chlorides suggest that the effect of water is related to solubility which is consistent with a mechanism involving the alleviation of chromatographic separation of precursor species produced during preparation.

Table 5. 1 Weight percent metal loadings for the dry catalysts.

	Cu:Pt Atomic Ratio	Chloride-precursor		Nitrate-precursor (Uncalcined)		Nitrate-precursor (Calcined)	
		Cu	Pt	Cu	Pt	Cu	Pt
Pt	0	0	2.3	N/A	N/A	0	3.0
Pt1Cu1	1	0.9	2.8	N/A	N/A	N/A	N/A
Pt1Cu3	3	2.7	2.7	2.6	2.7	2.9	3.0
Pt1Cu6	6	5.1	2.6	4.9	2.5	5.8	3.0
Cu	∞	2.9	0	N/A	N/A	N/A	N/A

Table 5. 2 Fraction of Pt exposed after reduction of catalysts at 350^{o}C.

	Chlorine-containing	Chlorine-free (Uncalcined)	Chlorine-free (Calcined)
Pt	.43	N/A	
Pt1Cu1	.06	N/A	N/A
Pt1Cu3	.03		
Pt1Cu6			

Table 5. 3 Ethylene selectivities and TOFs for catalysts prepared from chloride precursors after standard pretreatment with and without 5 day exposure to water prior to pretreatment.

	Fresh Catalyst		Catalyst with H_2O Exposure	
	TOF (μmol/gm/s)	Ethylene Selectivity	TOF (μmol/gm/s)	Ethylene Selectivity
Pt(Cl)	0.155	0	0.092	0
Pt1Cu1(Cl)	0.085	0	0.019	4
Pt1Cu3(Cl)	0.020	0	0.023	66
Pt1Cu6(Cl)	0.017	0	0.010	90

Table 5. 4 Ethylene selectivities and TOFs for catalysts prepared from nitrate precursors and calcined to leave insoluble oxide species on the surface pretreated under standard conditions with and without long-term exposure to water prior to pretreatment.

	Fresh Catalyst		Catalyst with H_2O Exposure	
	TOF (μmol/gm/s)	Ethylene Selectivity	TOF (μmol/gm/s)	Ethylene Selectivity
Pt(Cl-fr-cal)	0.073	0	0.062	0
Pt1Cu1(Cl-fr-cal)	N/A	N/A	N/A	N/A
Pt1Cu3(Cl-fr-cal)	0.022	0	0.018	2
Pt1Cu6(Cl-fr-cal)	0.015	3	0.013	10

Table 5. 5 Ethylene selectivities and TOFs for catalysts prepared from nitrate precursors pretreated under standard conditions with and without long-term exposure to water prior to pretreatment.

	Fresh Catalyst		Catalyst with H_2O Exposure	
	TOF (μmol/gm/s)	Ethylene Selectivity	TOF (μmol/gm/s)	Ethylene Selectivity
Pt(Cl-fr)	N/A	N/A	N/A	N/A
Pt1Cu1(Cl-fr)	N/A	N/A	N/A	N/A
Pt1Cu3(Cl-fr)	0.041	0	0.038	0
Pt1Cu6(Cl-fr)	0.022	20	0.021	0

Table 5. 6 Ethylene selectivities and TOFs for Pt1Cu3 catalysts prepared from chloride precursors and from nitrate precursors with calcination pretreated under varying conditions.

	Chlorinated Precursors		Non-chlorinated Precursors	
	TOF (μmol/gm/s)	Ethylene Selectivity	TOF (μmol/gm/s)	Ethylene Selectivity
220°C Treatment before Reduction	0.011	73	0.036	0
400°C Reduction	0.012	46	0.019	0
400°C Treatment after Reduction	0.027	0	0.027	0

Table 5. 7 Ethylene selectivities and TOFs for Pt1Cu6(Cl) catalysts exposed to 4 drops of water and left for varying times in sealed glass vials.

Time (days)	TOF (μmol/gm/s)	Ethylene Selectivity
0	0.015	0
5	0.010	90
20	0.011	89

Table 5. 8 D_m and D_{ss} of catalysts prepared from chloride precursors determined by microscopy after standard pretreatment, exposure to water followed by standard pretreatment, and standard pretreatment followed by 400°C reduction (Å).

	Standard		H_2O + Standard		400°C Reduction	
	D_m	D_{ss}	D_m	D_{ss}	D_m	D_{ss}
Pt(Cl)	20.3	27.6	27.9	29.8	28.0	37.0
Pt1Cu1(Cl)	30.9	34.4	30.0	39.4	34.3	44.1
Pt1Cu3(Cl)	26.2	31.6	31.0	37.5	33.5	44.4

Table 5. 9 Coordination numbers for the PtL_3 edge observed by EXAFS for chloride-precursor catalysts with and without exposure to water.

	Coordination Number	
	Pt-Pt	Pt-Cu
Pt1Cu1(Cl)	7.4	3.3
Pt1Cu1(Cl-H_2O)	6.9	3.5
Pt1Cu6(Cl)	3.9	6.0
Pt1Cu6(Cl-H_2O)	4.1	5.7

Table 5. 10 Coordination numbers for the CuK edge observed by EXAFS for chloride-precursor catalysts with and without exposure to water.

	Coordination Number	
	Cu-Cu	Cu-Pt
Pt1Cu1(Cl)	N/A	3.7
Pt1Cu1(Cl-H_2O)	N/A	3.6
Pt1Cu6(Cl)	8.3	0.9
Pt1Cu6(Cl-H_2O)	7.8	1.0

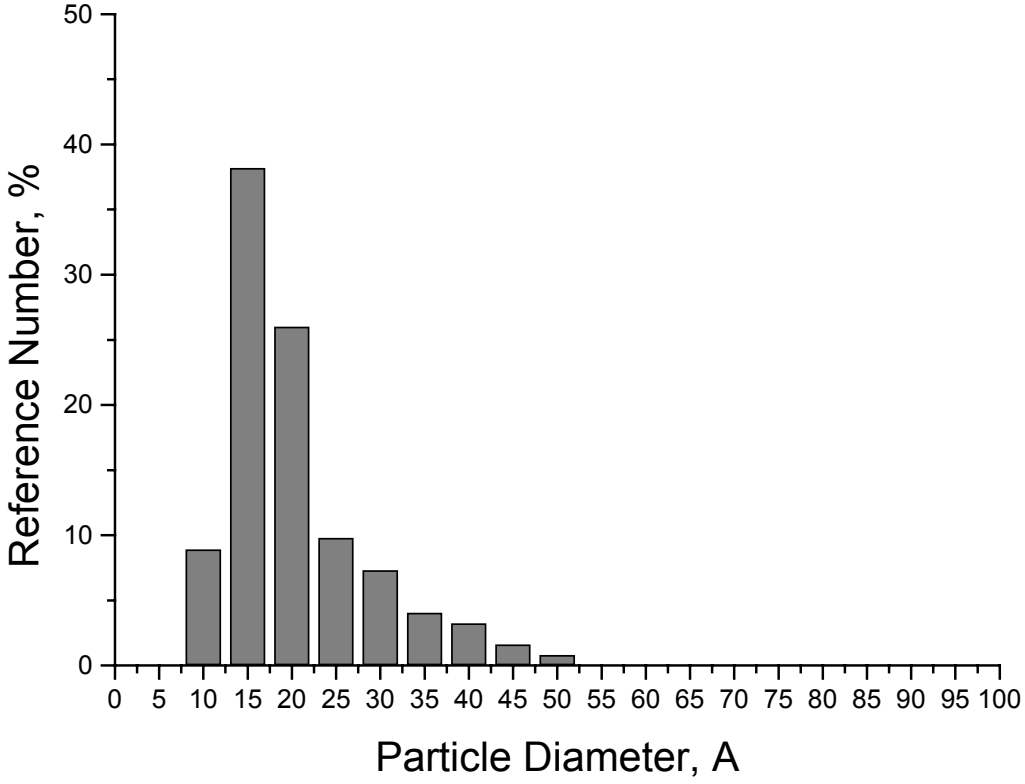

Figure 5. 1 Particle size distribution (Å) for a Pt(Cl) catalyst pretreated under standard conditions.

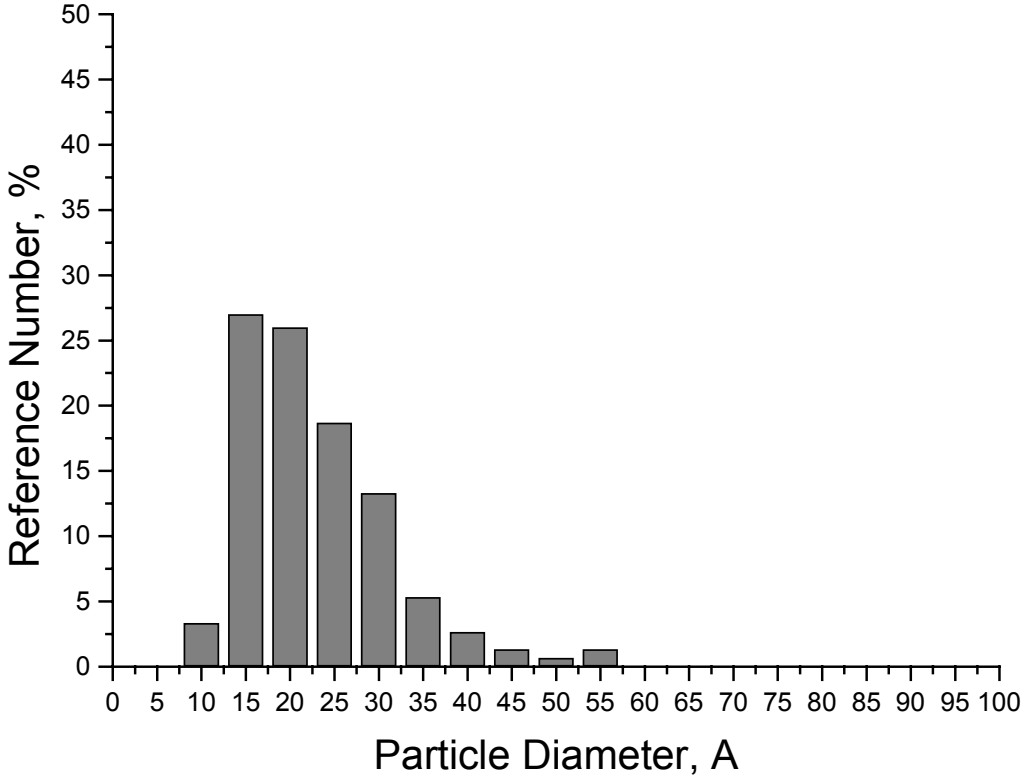

Figure 5. 2 Particle size distribution (Å) for a Pt(Cl, H_2O) catalyst pretreated under standard conditions.

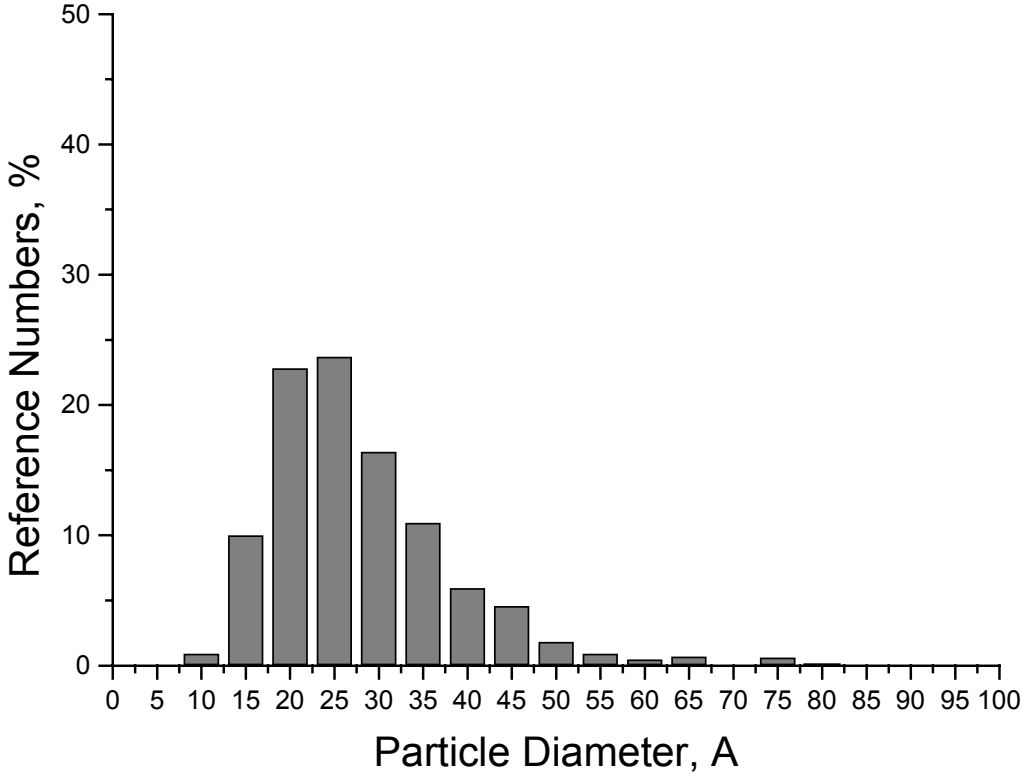

Figure 5. 3 Particle size distribution (Å) for a Pt(Cl) catalyst pretreated under standard conditions then reduced at 400^{o}C.

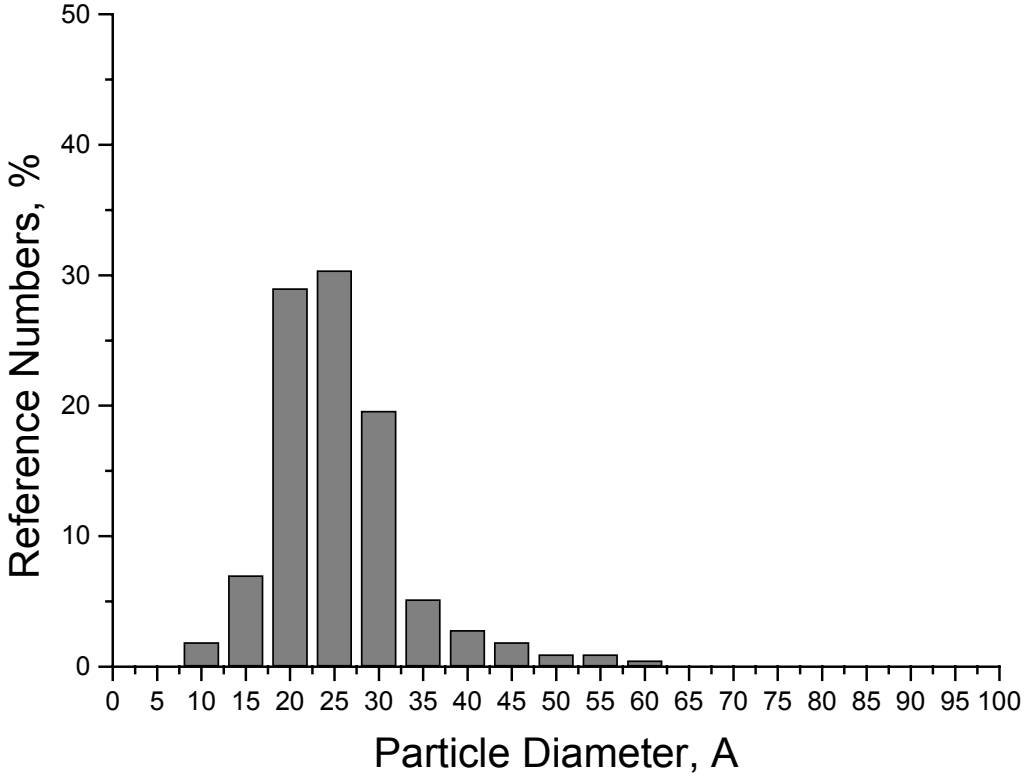

Figure 5. 4 Particle size distribution (Å) for a Pt1Cu1(Cl) catalyst pretreated under standard conditions.

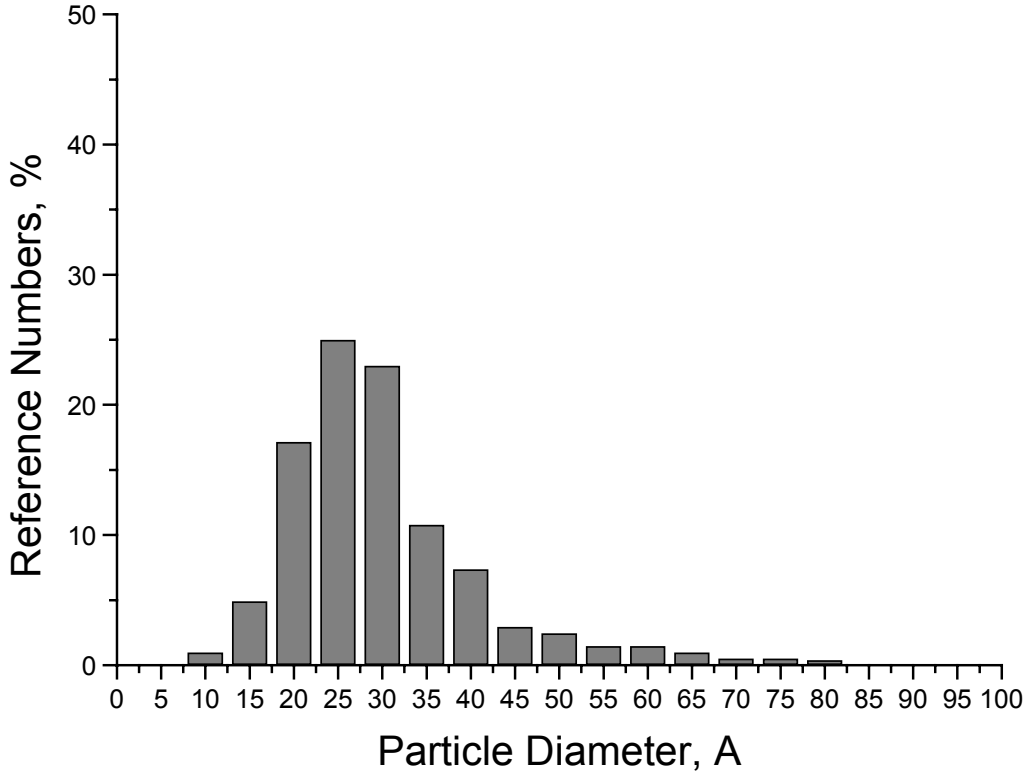

Figure 5. 5 Particle size distribution (Å) for a Pt1Cu1(Cl, H_2O) catalyst pretreated under standard conditions.

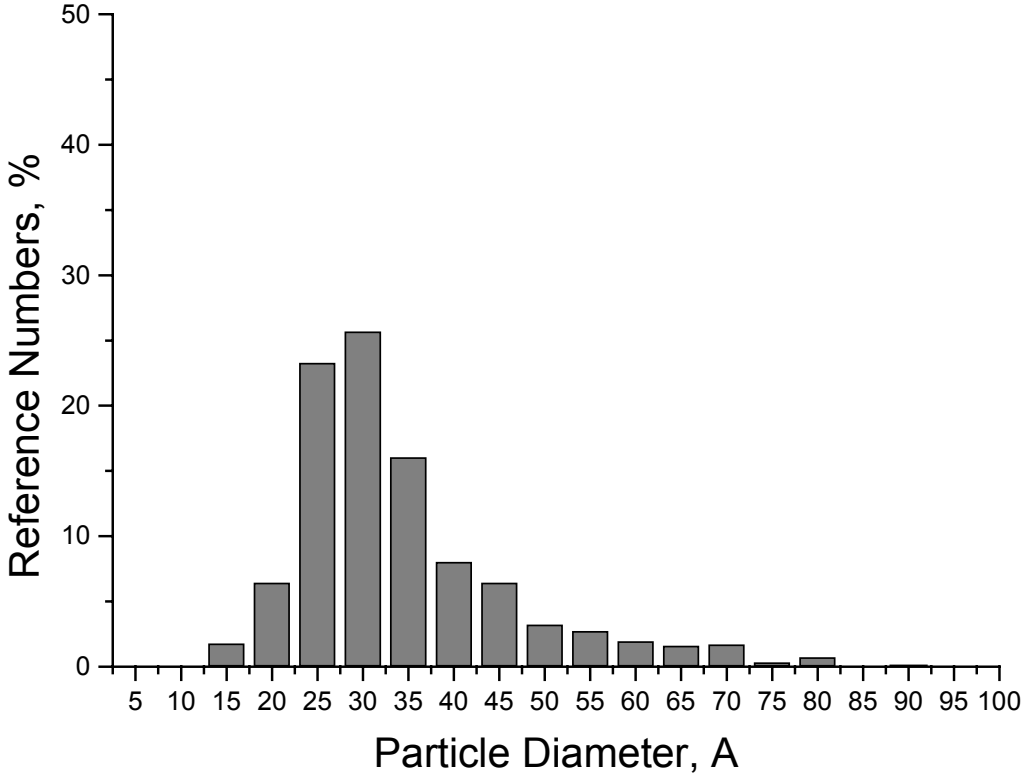

Figure 5. 6 Particle size distribution (Å) for a Pt1Cu1(Cl) catalyst pretreated under standard conditions then reduced at 400^{o}C.

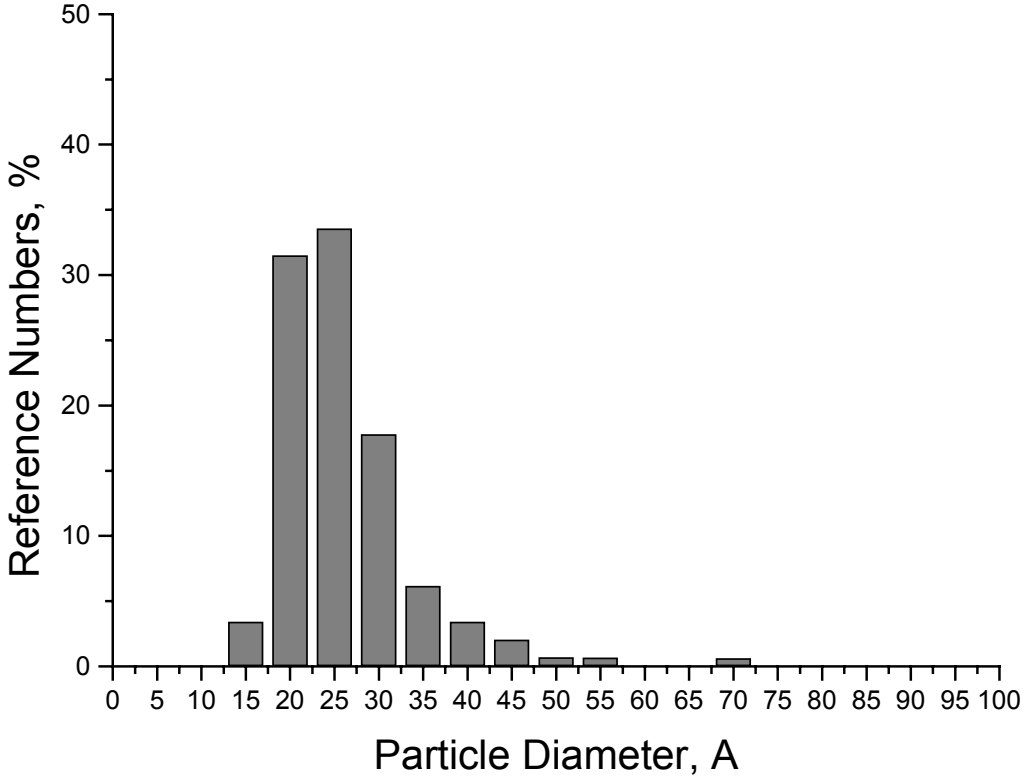

Figure 5. 7 Particle size distribution (Å) for a Pt1Cu3(Cl) catalyst pretreated under standard conditions.

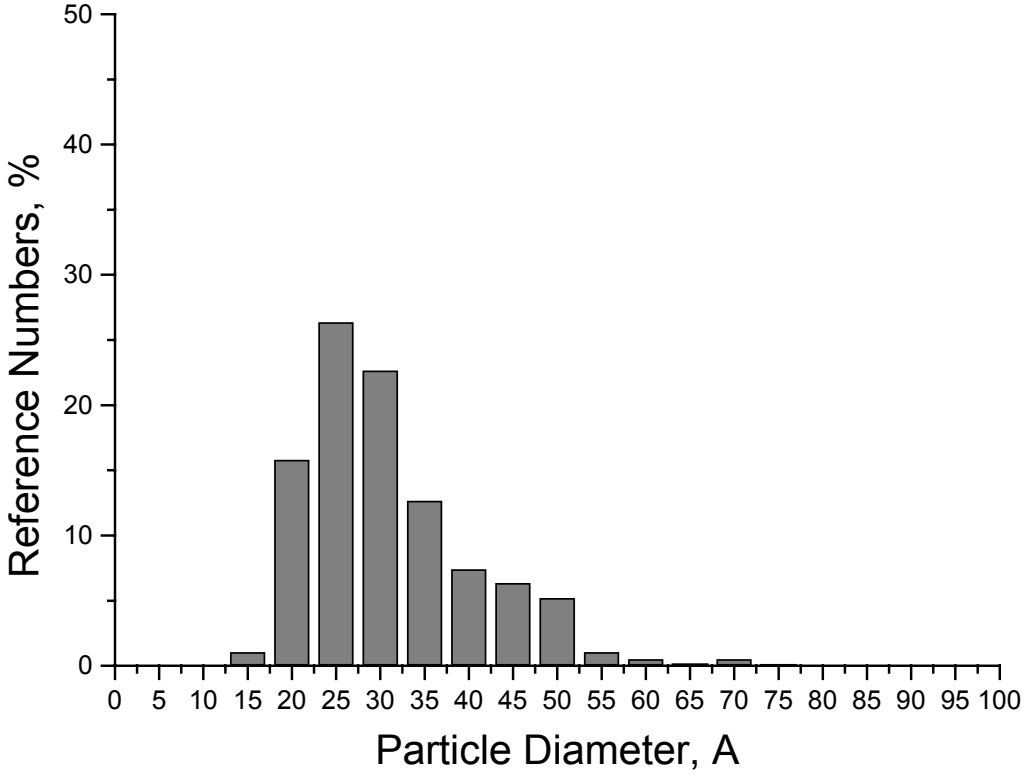

Figure 5. 8 Particle size distribution (Å) for a Pt1Cu3(Cl, H_2O) catalyst pretreated under standard conditions.

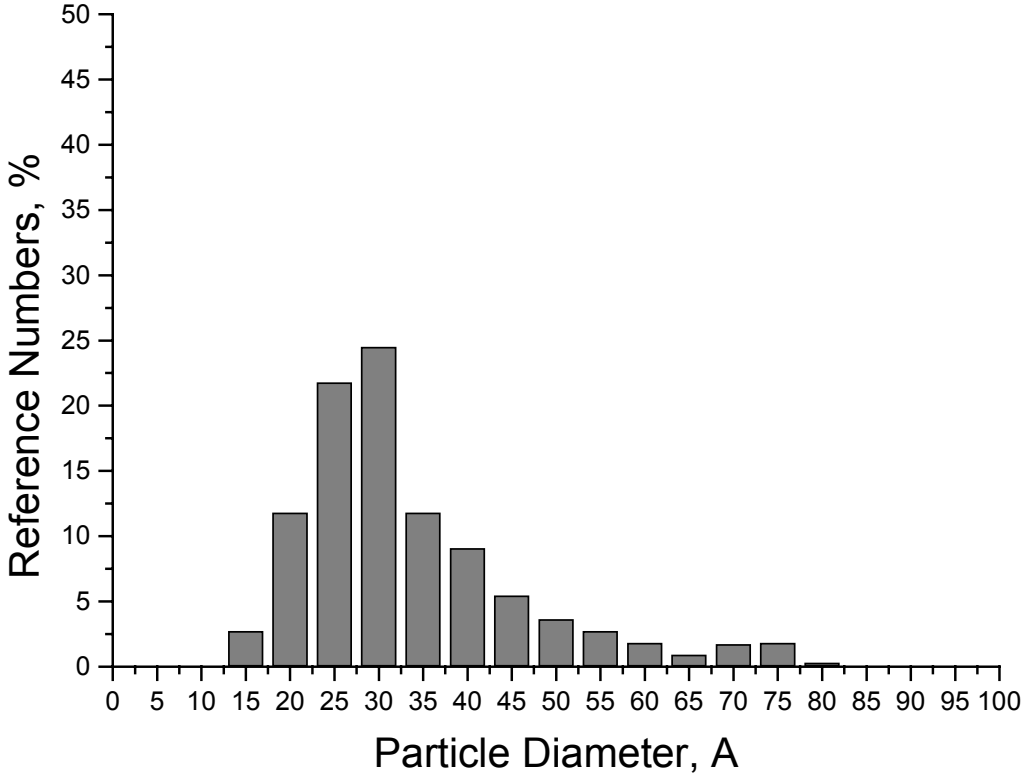

Figure 5. 9 Particle size distribution (Å) for a Pt1Cu3(Cl) catalyst pretreated under standard conditions then reduced at 400^{o}C.

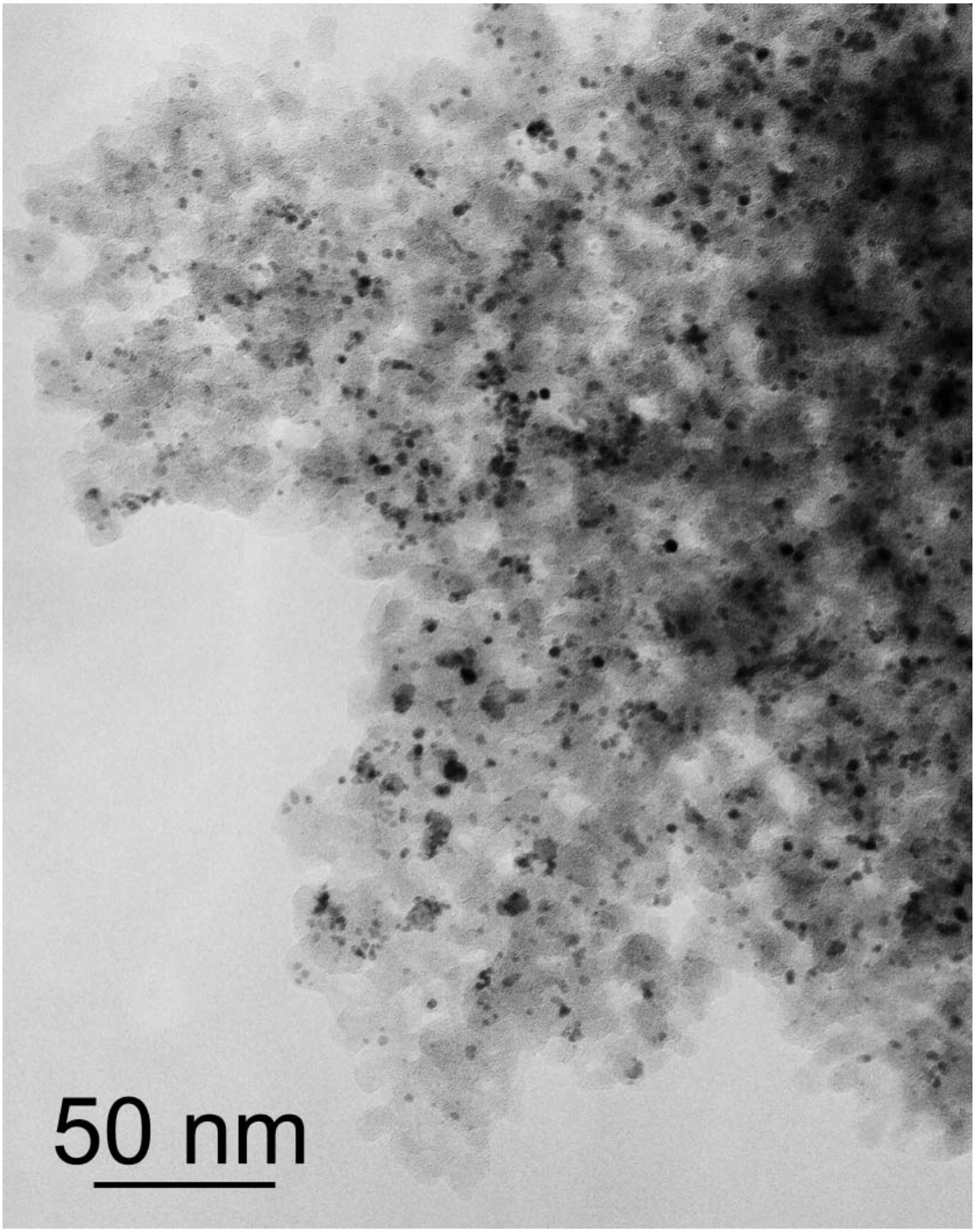

Figure 5. 10 TEM micrograph of 2.3%Pt/SiO_2 reduced at 220°C for 1.5 h.

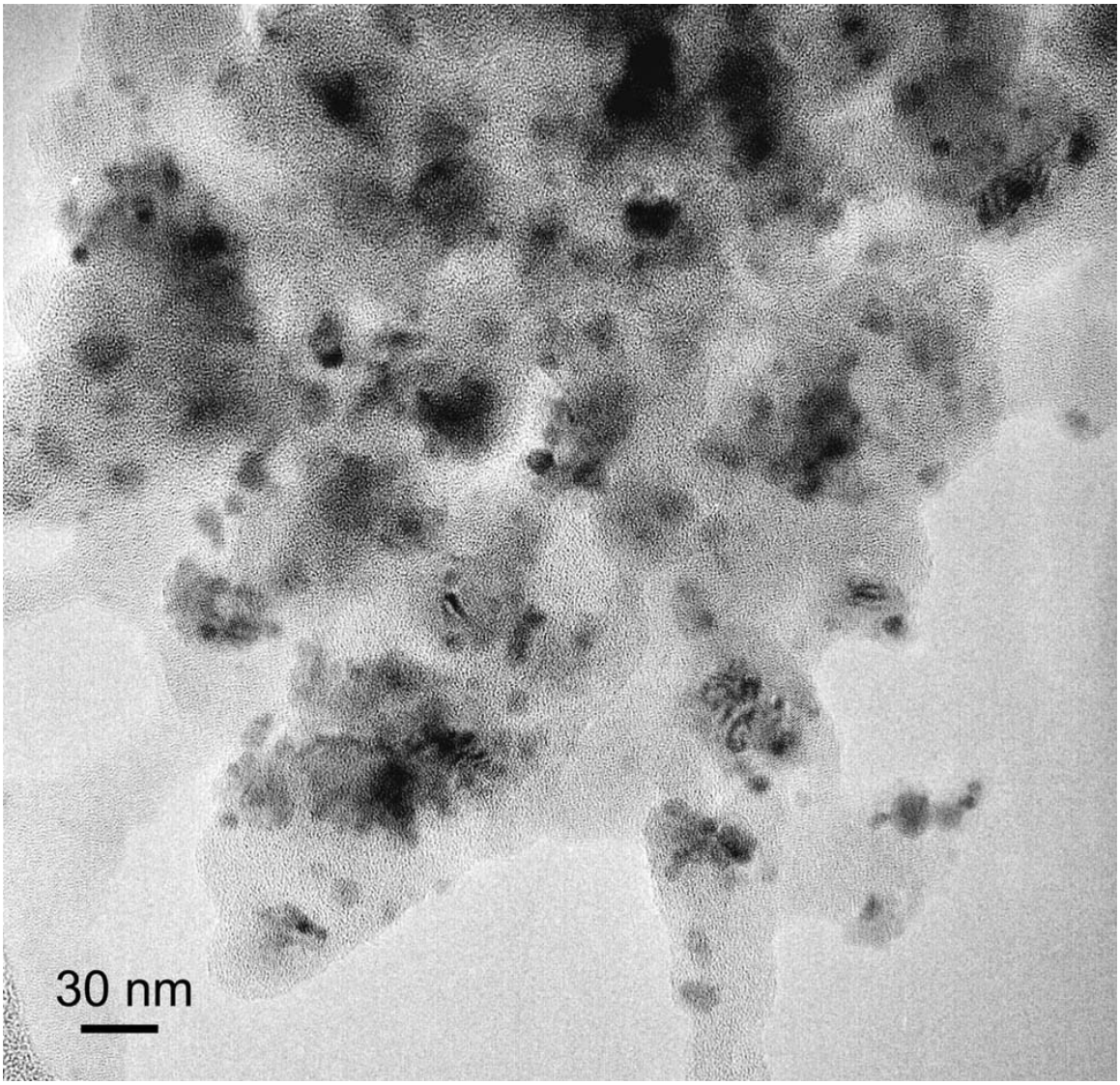

Figure 5. 11 TEM micrograph of (2.7%Pt+0.93%Cu)/SiO_2 reduced at 350°C for 1.5 h.

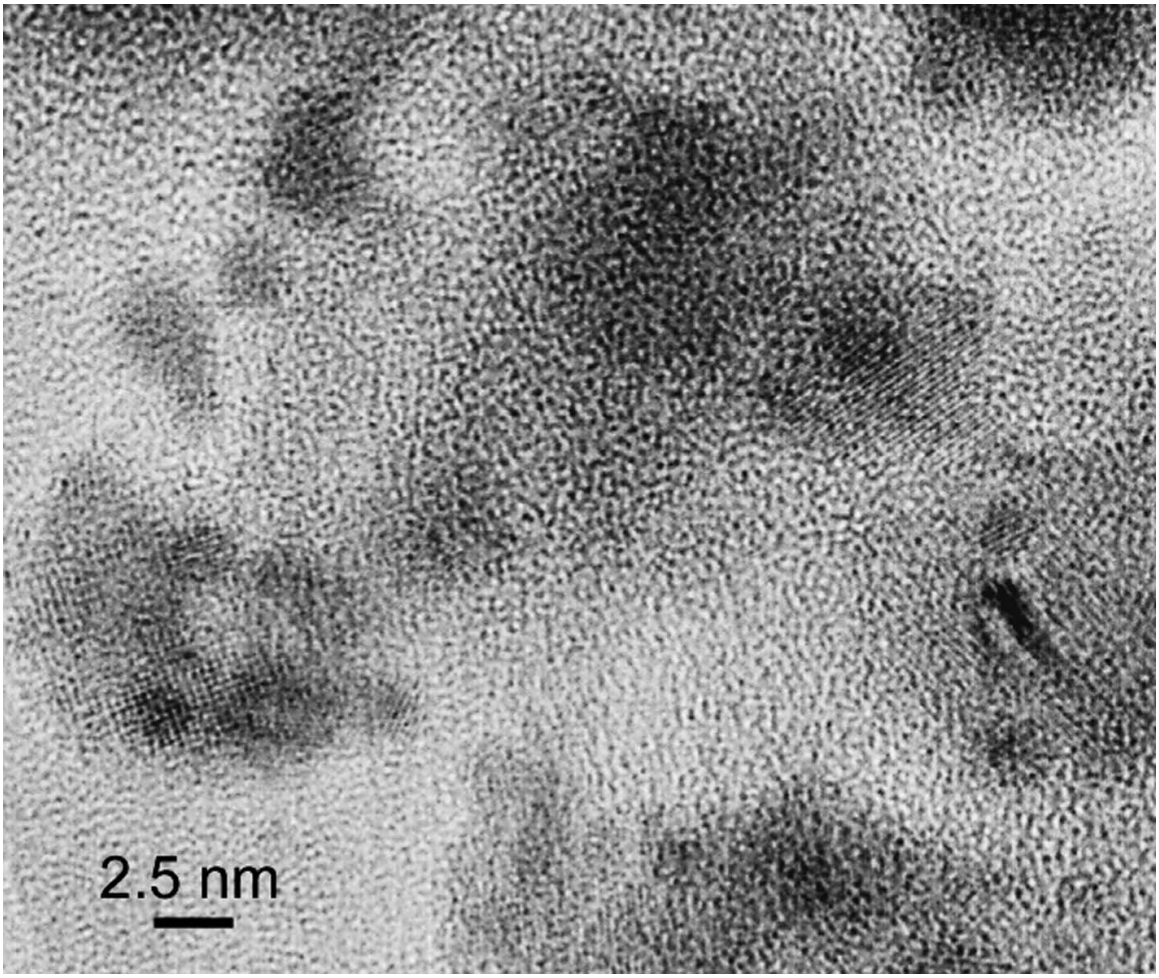

Figure 5. 12 TEM micrograph of (2.7%Pt+0.93%Cu)/SiO_2 reduced at 350°C for 1.5 h.

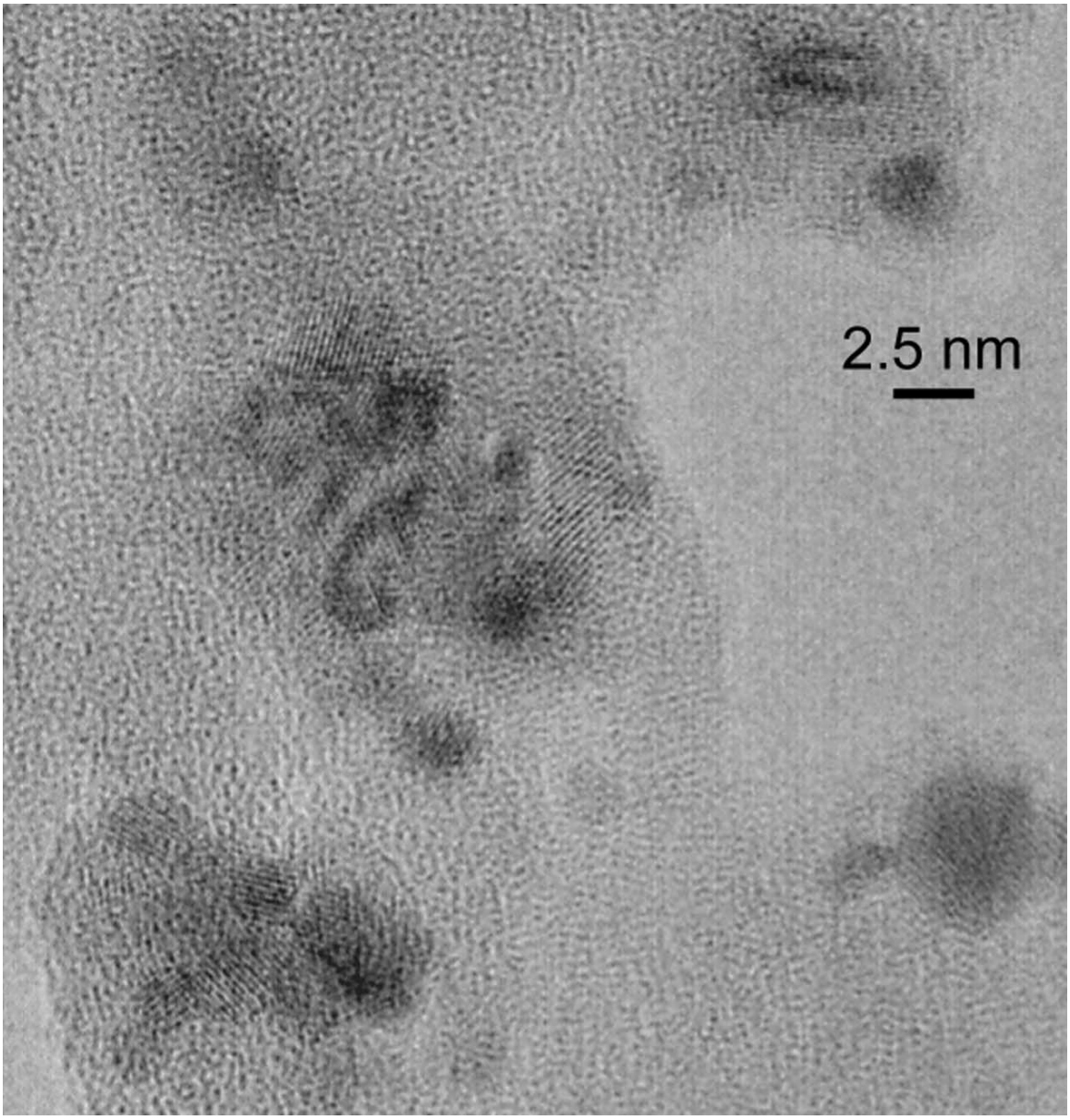

Figure 5. 13 TEM micrograph of (2.7%Pt+0.93%Cu)/SiO_2 reduced at 350°C for 1.5 h.

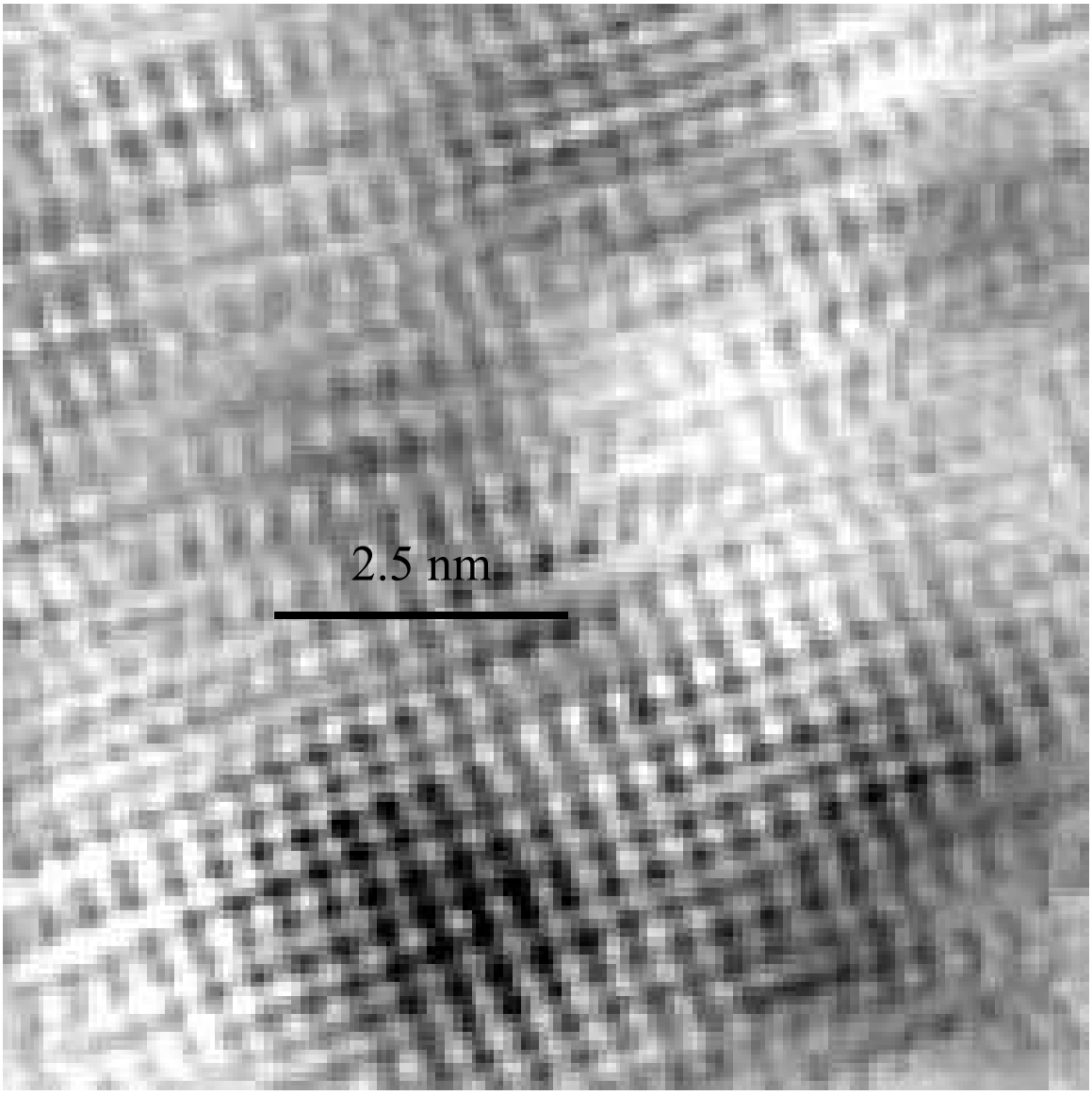

Figure 5. 14 TEM micrograph of (2.7%Pt+0.93%Cu)/SiO_2 reduced at 350°C for 1.5 h after Fourier filtration.

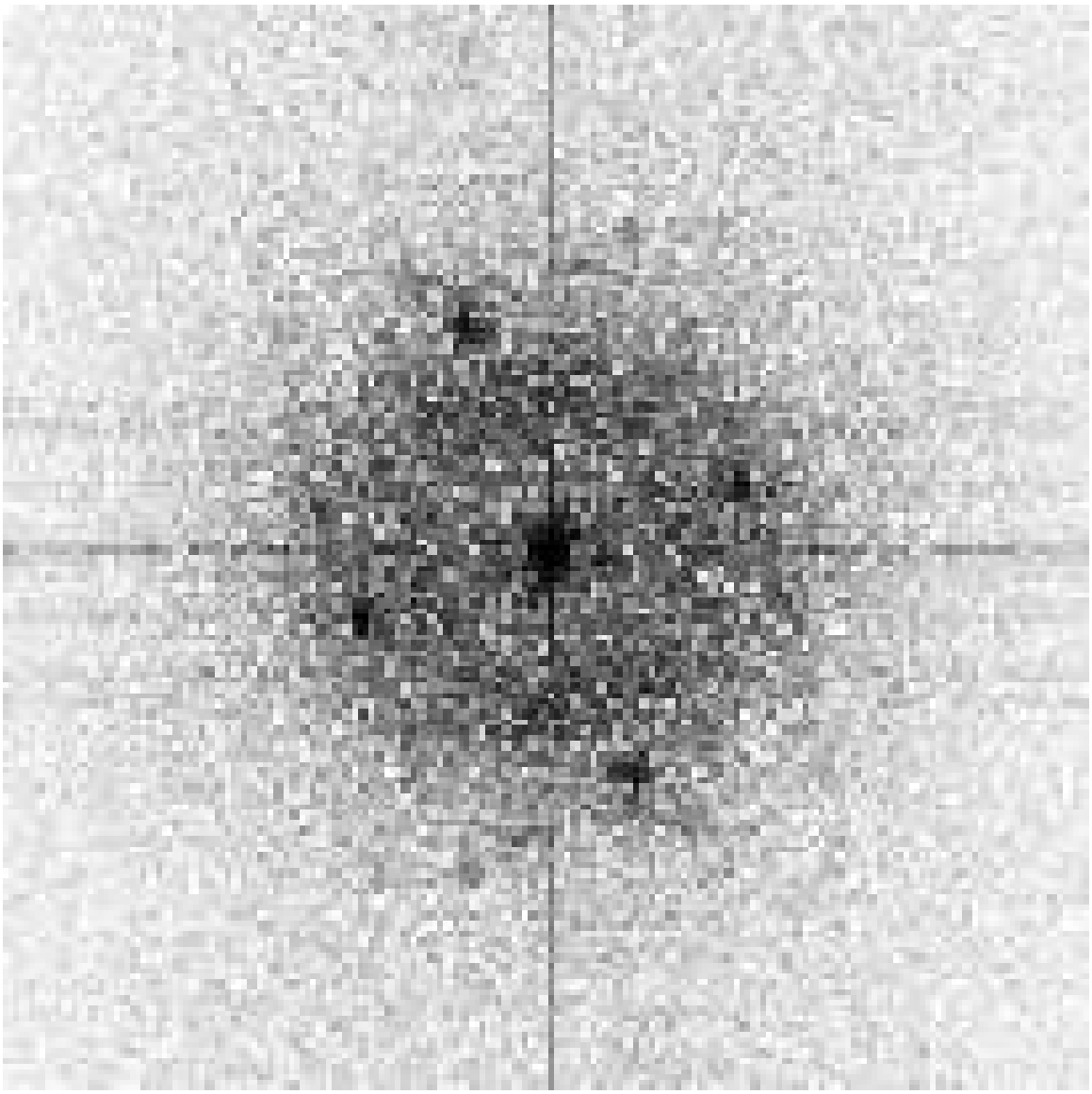

Figure 5. 15 Diffractogram taken of the dark region of Figure 5.14.

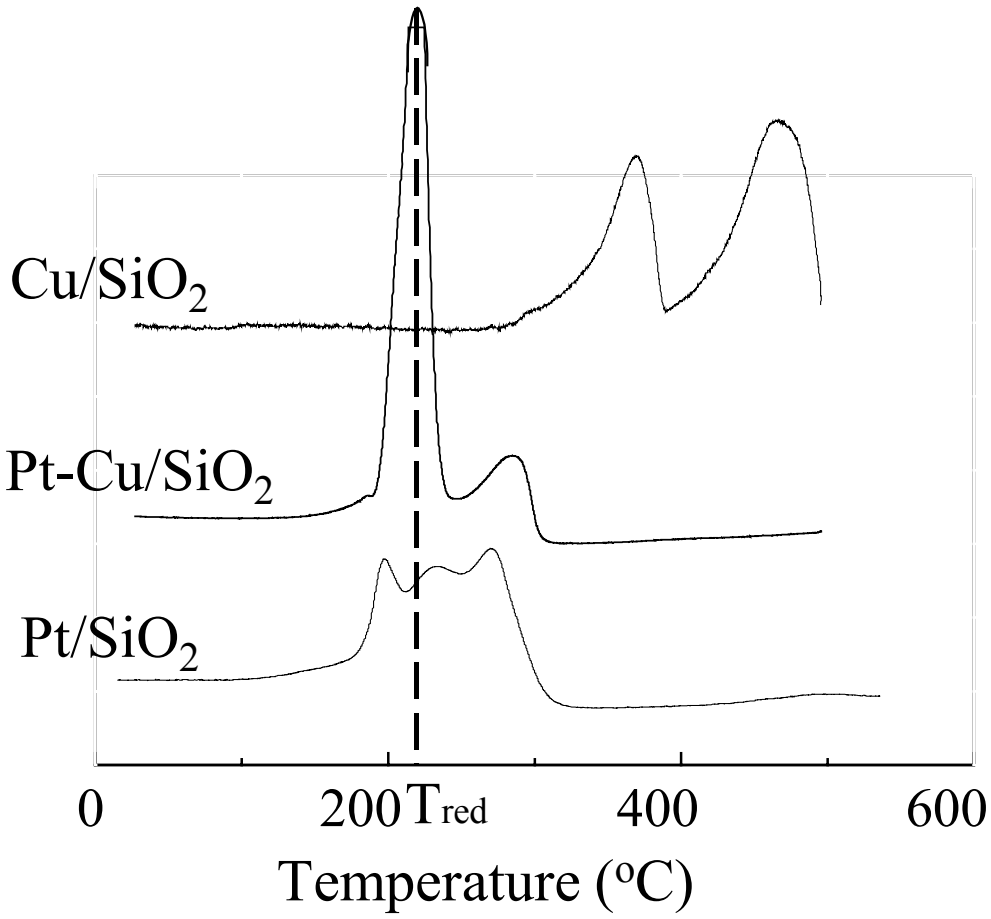

Figure 5. 16 Temperature programmed reduction profiles, β = 8°C/min, for the reduction of precursor species on Cu(Cl), Pt1Cu3(Cl) and Pt(Cl) catalysts.

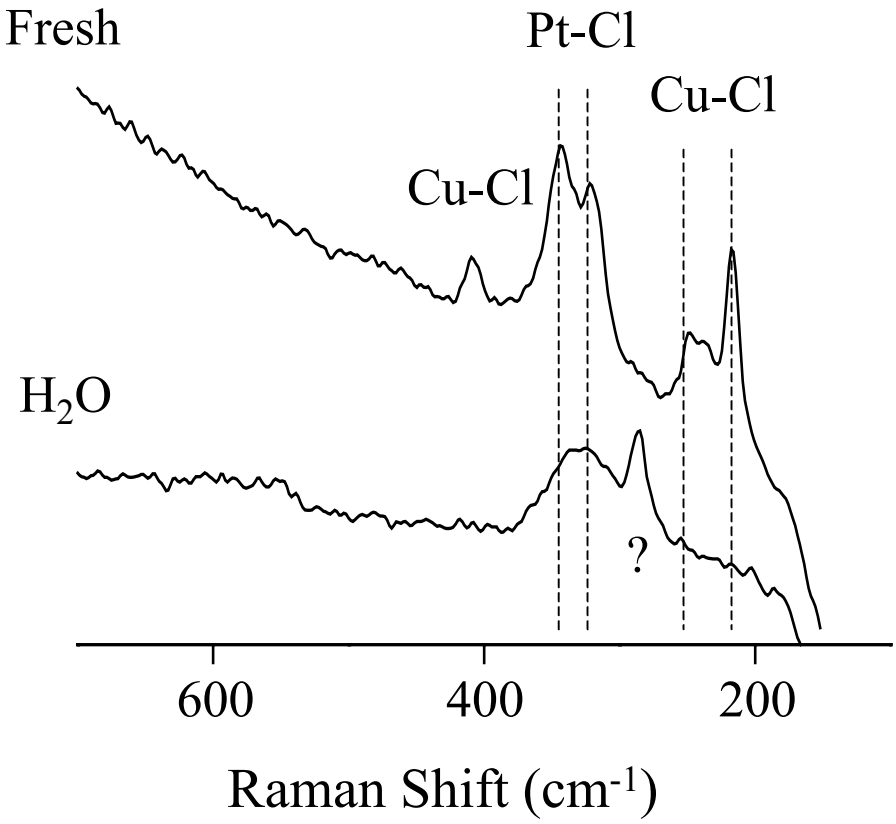

Figure 5. 17 Raman spectra taken at room temperature for dry, Pt1Cu3(Cl) catalysts without reduction both fresh and after addition of water.

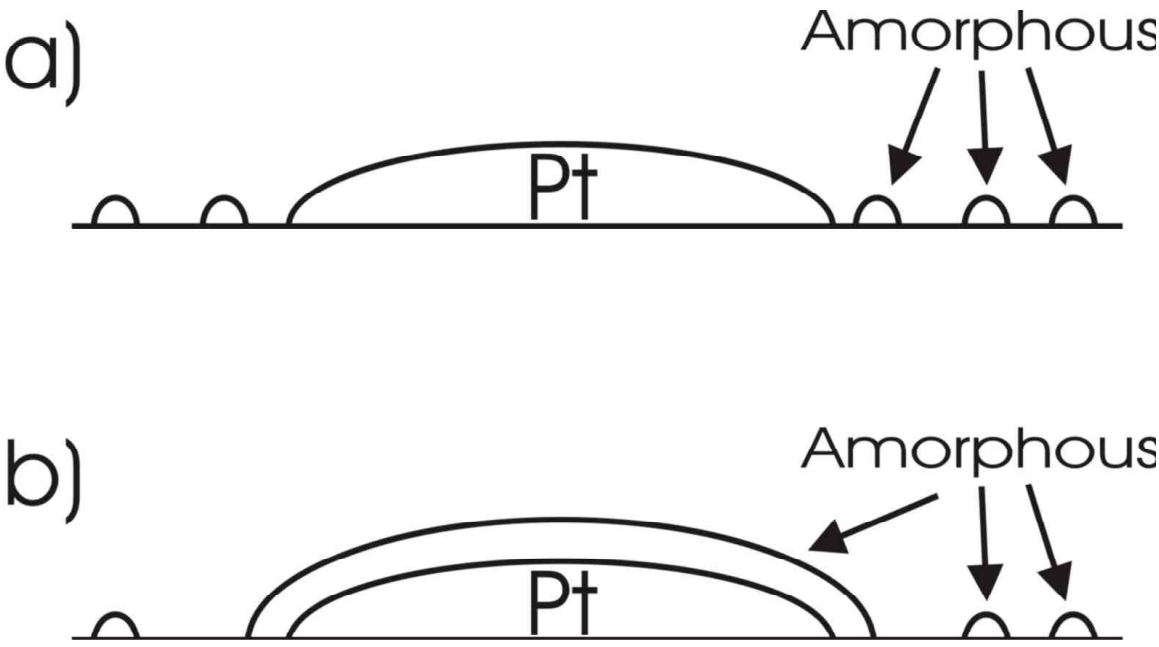

Figure 5. 18 Illustration of the structure of chloride-precursor, Pt-Cu, bimetallic catalysts as observed by microscopy: fresh, showing reduced Pt particles and smaller amorphous objects (a) and after addition of water, showing a similar structure with the addition of an amorphous overlayer on the reduced particles (b).

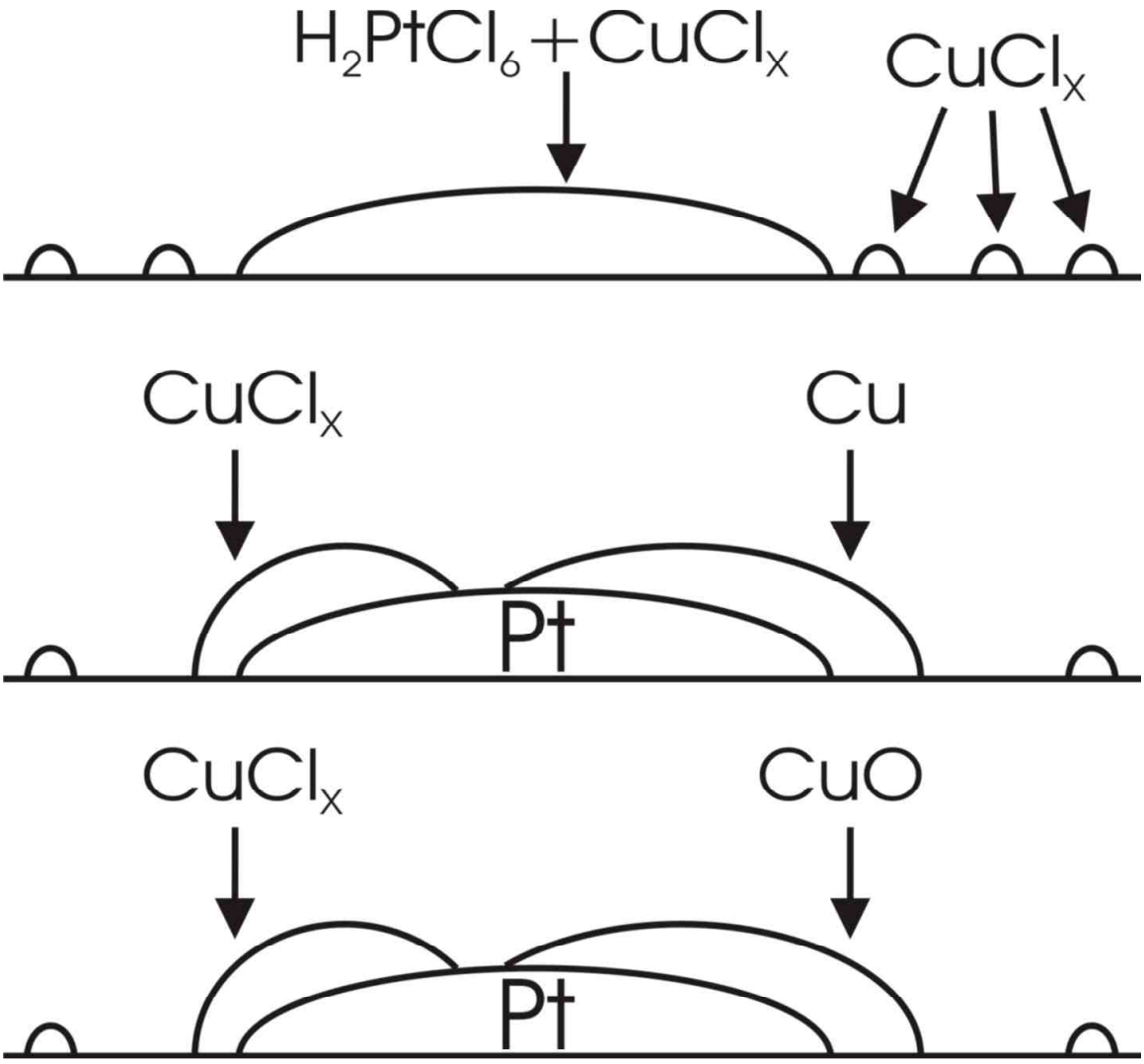

Figure 5. 19 Illustration of possible structures for chloride-precursor, bimetallic, Pt-Cu catalysts after exposure to water, prior to reduction (top), after 220°C, H_2 reduction (center), and after exposure to atmosphere (bottom).

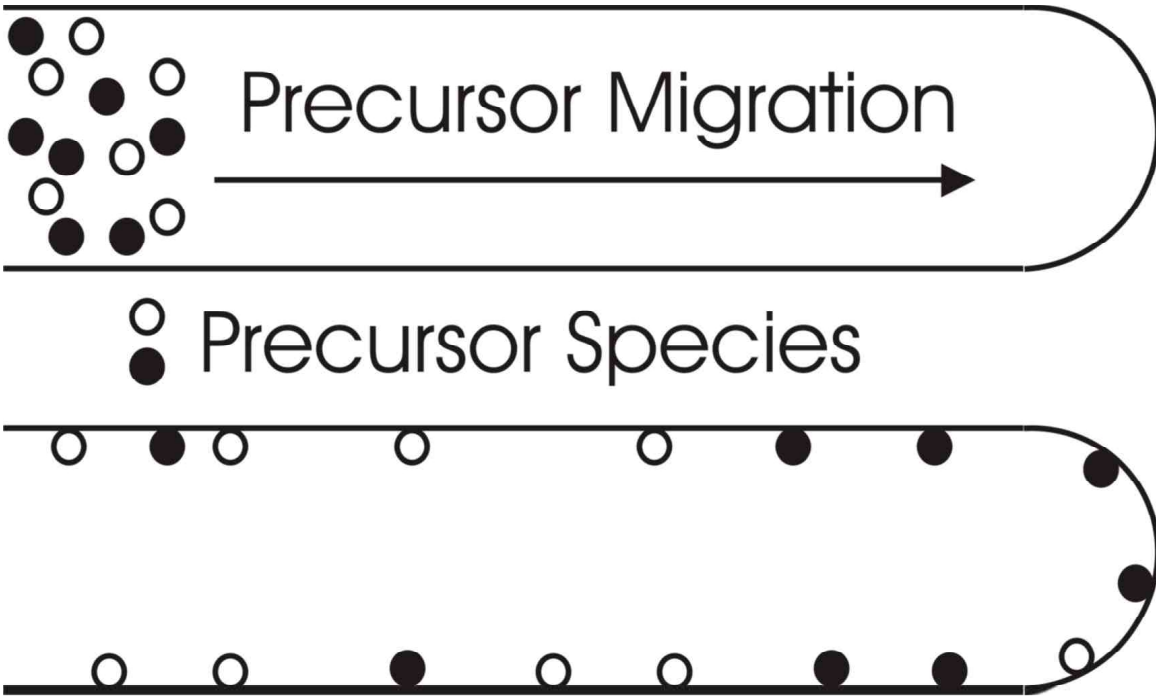

Figure 5. 20 Illustration of the events leading to chromatic separation of Pt and Cu precursor particles in bimetallic catalysts prepared by coimpregnation showing a solution-filled pore (above) and a pore after drying (below).

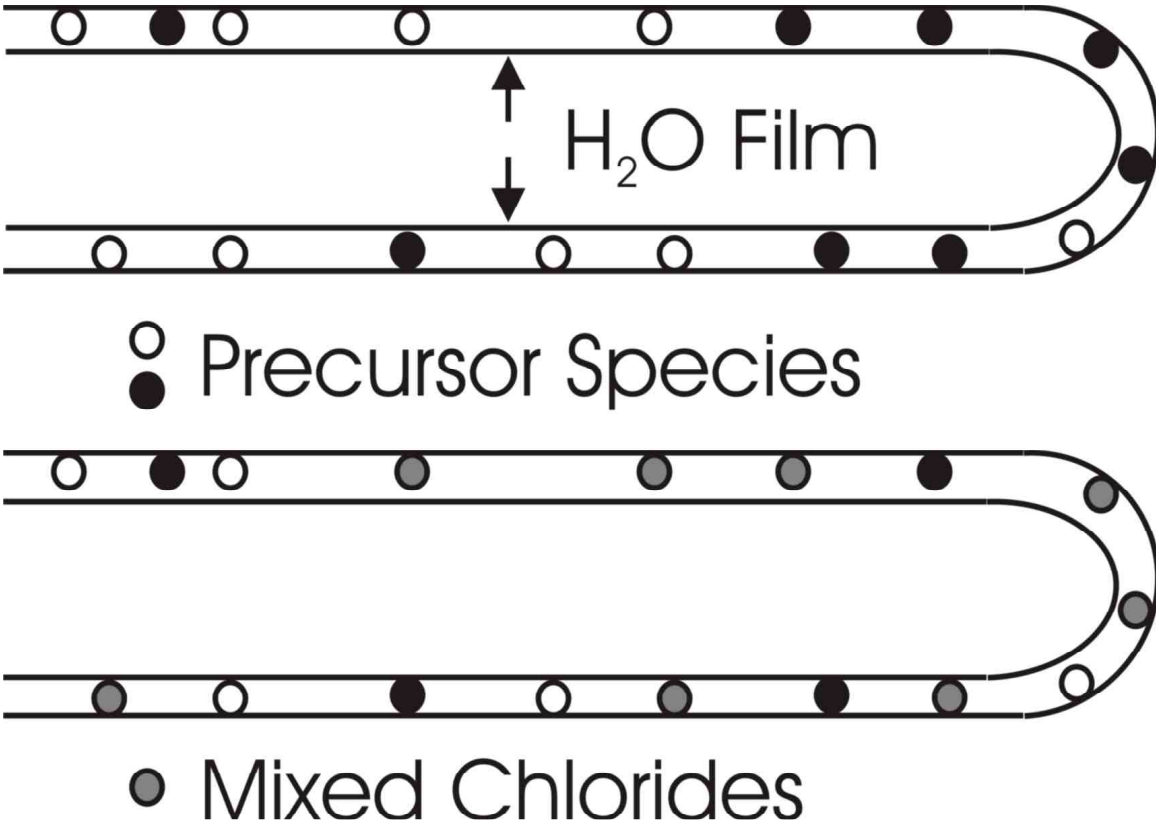

Figure 5. 21 Illustration of the possible effect of atmospheric humidity on chloride-precursor, Pt-Cu, bimetallic catalysts showing the formation of a film of precursor solution inside the pore due to condensation of atmospheric moisture (above) and the alleviation of chromatographic separations and formation of mixed chlorides (below).

6.0 1,2-DICHLOROETHANE HYDRODECHLORINATION CATALYZED BY PT-CU/SIO2 CATALYSTS: EVIDENCE FOR DIFFERENT FUNCTIONS OF PT AND CU SITES

6.1 Introduction

The effects of adding a second metal to a noble metal catalyst are of interest both industrially and academically. In addition to performance characteristics unique to the bimetallic system,[13] industry invariably finds the promise of catalysts containing smaller amounts of expensive metals like Pt attractive. Academics have found these systems exceptionally interesting both for the complexity of the interactions of the metals themselves and the effect those interactions have on the chemistry of catalytic processes.[12,14,17,95]

While the metal-metal interactions are extremely complex, they have traditionally been broken down into two general categories: electronic and geometric interactions. Hall and Emmett were among the first to explain catalytic phenomena based on electronic modification in alloys of group 8 and 1B metals. Referencing the earlier work of Dowden,[96] they interpret changes in catalytic properties in terms of changes in electronic properties altered by donation of electron density from the group 1B metal to the incompletely filled d band of the group 8 metal.[97] The second category, that of geometric interactions, was developed by Satchler and others more recently.[17] These studies, in turn, have their roots in the ideas of Boudart, who was the first to define

structure sensitivity as being present in any reaction in which turn over frequency (TOF) varied with particle size.[98]

One means of effectively probing both electronic and geometric interactions is the examination of CO adsorption using FTIR. This technique has been used extensively particularly in studies of Pt-containing systems.[99-101] The current study employs both FTIR and kinetic techniques in the examination of silica-supported, Pt-Cu catalysts for the dechlorination of 1,2-dichloroethane.

6.2 Experimental

6.2.1 Material Preparation

The catalysts were prepared by pore volume impregnation of SiO_2 (Aldrich, 99+%, 60-100 mesh, 300 m^2 g^{-1}, average pore diameter, 150 Å) with a 0.1 N aqueous HCl solution containing $H_2PtCl_6 \cdot 6H_2O$ (Alfa, 99.9%) or a mixture of $H_2PtCl_6 \cdot 6H_2O$ and $CuCl_2 \cdot 2H_2O$ (MCB Manufacturing Chemists, 99.5%), as described elsewhere.[42] The concentrations of the metal precursors in the impregnating solutions were adjusted to obtain metal weight loadings of 2.4% Pt/SiO_2, 3.0% Pt + 1.0% Cu, and 3.0% Pt + 2.9% Cu. The bimetallic catalysts had Pt/Cu atomic ratios of 1:1 (Pt1Cu1) and 1:3 (Pt1Cu3), respectively. The fraction of exposed Pt atoms after reduction at 493 K, as determined by CO chemisorption,[42] was 43, 6, and 3% for Pt/SiO_2, $Pt1Cu1/SiO_2$, and $Pt1Cu3/SiO_2$, respectively.

6.2.2 FTIR Experiments

The infrared spectra were recorded with a Mattson Research Series II FTIR spectrometer equipped with a liquid N_2 cooled MCT detector. The resolution was 4 cm^{-1} and 400 scans were accumulated per spectrum. The IR cell was similar to that described elsewhere.[60] The cell volume was 200 cm^3 and the light pathlength was approximately 15 cm. The cell was equipped with glass stopcocks connected to gas inlet/outlet ports.

The infrared spectra were collected in the transmission mode which mandated the use of thin wafers of the catalyst sample. The self-supporting catalyst wafers (~ 20 mg/cm^2 thick) were prepared by powdering the catalyst material in an agate mortor and then pressing the powder at 830 atm for 3 min. The wafers were pretreated *in situ* by evacuation at 403 K for 1 h, followed by heating in flowing 5% H_2 + 95% He mixture (80 ml/min) to 493 K at 5 K/min and holding at this temperature for 1 h. Then the gas phase was evacuated at 493 K to a pressure of 10^{-5} Torr.

The dipole-dipole frequency shifts and singleton frequencies of CO adsorbed on the metals were measured using a modified isotopic dilution method.[61] Initially $^{12}C^{16}O$ was adsorbed on the pretreated sample at room temperature at an equilibrium pressure of 8-10 Torr. The spectrum of adsorbed CO was recorded and then the gaseous CO was evacuated at room temperature. Subsequently, 0.1-0.5 Torr of $^{13}C^{18}O$ (Isotec, 99+% ^{13}C, 95+% ^{18}O, primary impurity: $^{12}C^{18}O$, others not exceeding 1 ppm) was admitted into the IR cell and the spectra of adsorbed CO were measured as a function of both $^{13}C^{18}O$ pressure and time. The dipole-dipole shifts for $^{12}C^{16}O$ and $^{13}C^{18}O$ were calculated from the difference between the band position observed at maximum surface concentration and

the singleton frequency observed at the maximum level of exchange at which a band is detectable. The degree of exchange of preadsorbed $^{12}C^{16}O$ for gaseous $^{13}C^{18}O$ was approximated by the formula:

$$D = [(I_o - I)/I_o] \times 100\%,$$

where I_o is the initial band intensity and I is the band intensity at the time of observation in the spectra of $^{12}C^{16}O$ linearly adsorbed on Pt.

The kinetics of 1,2-dichloroethane conversion in the presence of H_2 was studied using both static and continuous flow reactors. The static system was the IR system described, and experiments were conducted at a reaction temperature of 523 K and atmospheric pressure. The reaction mixture consisted of 7-10 Torr of $C_2H_4Cl_2$ and 5 fold excess of H_2. In some cases a small amount of CO (~2 Torr) was admitted to the reaction mixture. The $C_2H_4Cl_2$ conversion and the composition of the reaction products were determined from the IR band intensities of the gas phase species.

In order to determine an approximate mass transfer rate in the FTIR cell to be compared with the observed reaction rate, Fick's Law was integrated for diffusion in a cylinder 1.5 cm in diameter and 45 cm in length which represented the area separating the catalyst sample from the detector. Diffusivities were calculated for reactants and products in H_2 and 1,2-dichloroethane using a correlation, and the lowest value, that for diffusion of ethylchloride in 1,2-dichloroethane, was used for calculations.[103]

6.2.3 Flow Kinetics Experiments

The flow kinetics experiments were conducted in a stainless-steel, differential, flow reaction system equipped with a quartz microreactor (10 mm i.d.) in which the catalyst was supported on a quartz frit. The pretreatment gases and gaseous reactants were metered using mass flow controllers (Brooks, model 5850E) and mixed prior to entering the reactor. All gases except CO were 99.999% pure with impurities of O_2, H_2O, and total hydrocarbons not exceeding 4.0, 3.5, and 0.5 ppm, respectively (Air Products). Carbon monoxide was 99.99% pure with impurities of CO_2, O_2, H_2O, and total hydrocarbons not exceeding 20.0, 0.5, 1.0, and 8.0 ppm, respectively (Praxair). The 1,2-dichloroethane (Sigma-Aldrich, 99.8%, primary impurity: 1,1-dichloroethane) was metered into the system by flowing He through a saturator containing the liquid reactant. A constant inlet concentration was ensured by maintaining the saturator at a constant temperature of 273±1 K using a recirculating cooling system. The catalyst temperature was maintained ±1 K using an electric furnace and a temperature controller (Omega model CN2011). The reaction products were monitored online using a gas chromatograph (Varian 3300 series) equipped with a 10 ft 60/80 Carbopack B/5% Fluorocol packed column (Supelco) and a flame ionization detector. The detection limit for all products was 2 ppm. Hydrogen chloride was not quantified in these experiments.

The catalyst pretreatment consisted of purging the catalyst with He (30 ml/min) for 5 min at 303 K. The He flow was held constant as the catalyst was heated to 403 K at a rate of 6.7 K/min. The catalyst was maintained at these conditions for 1 h before the

flow was switched to 20% H_2 + 80% He (50 ml/min). The catalyst was heated to 493 K at a rate of 6.7 K/min and held at 493 K for 1.5 h. The catalyst was then cooled in He (40 ml/min) to the reaction temperature.

The reaction was conducted at 473 K and atmospheric pressure. The total flow rate of the reaction mixture was 41 ml/min and consisted of 7,000 ppm CH_2ClCH_2Cl, 36,600 ppm H_2, and a balance of He. For some experiments, 1450 ppm He was replaced with an equal volume of CO. The conversion was maintained in the differential range between 3 and 4%. Approximately 200 mg of catalyst was necessary to achieve this conversion given the described flow rates and temperature.

6.3 Results

6.3.1 FTIR Analysis of Adsorbed CO

The exposure of the monometallic Pt catalyst, which had been pre-exposed to $^{12}C^{16}O$, to $^{13}C^{18}O$ resulted in the replacement of adsorbed $^{12}C^{16}O$ by gaseous $^{13}C^{18}O$ (Figure 6.6). The spectrum of $^{12}C^{16}O$ adsorbed on Pt consisted of an intense absorption band at 2082 cm^{-1} and a low intensity band at 1840 cm^{-1} corresponding to linear and bridged modes, respectively.[62,104] As the exchange of adsorbed $^{12}C^{16}O$ for $^{13}C^{18}O$ progressed, the intensities of those two bands decreased, and the high-frequency band position shifted to 2040 cm^{-1}. This shift resulted from of a weakening of dipole-dipole coupling between adsorbed $^{12}C^{16}O$ molecules as the coverage of $^{12}C^{16}O$ decreased due to substitution of $^{13}C^{18}O$ molecules.[61,105] Simultaneously, the vibrational bands attributed

to $^{13}C^{18}O$ adsorbed on metallic Pt in the linear and bridged forms appeared and increased in intensity. The bridged form of adsorption was characterized by a low intensity band at 1750 cm^{-1}. The vibrational frequency of CO linearly adsorbed was 1945 cm^{-1} at a low degree of exchange of $^{12}C^{16}O$ for $^{13}C^{18}O$ and shifted to 1980 cm-1 with increasing degree of exchange. Thus, the singleton frequencies for linearly adsorbed $^{12}C^{16}O$ and $^{13}C^{18}O$ molecules on Pt were equal to 1945 and 2040 cm^{-1}, respectively. The dipole-dipole shifts for both isotopes were equal to 42 cm^{-1}.

When the same exchange experiment was conducted with the Pt1Cu1 catalyst, very different adsorption behavior from that of monometallic Pt was observed (Figure 6.7). In the presence of gas-phase $^{12}C^{16}O$, the spectrum of adsorbed $^{12}C^{16}O$ consisted of two absorption bands with maxima at 2073 and 2133 cm^{-1} corresponding to $^{12}C^{16}O$ adsorbed on metallic Pt and Cu in linear form, respectively.[105-106] The adsorption of CO on Cu was sufficiently weak that the CO desorbed from the copper surface when the sample evacuation at room temperature for less than 30 min. For the Pt1Cu1 catalyst, similar wavenumber shifts to those for the monometallic Pt catalyst were observed during the exchange of preadsorbed $^{12}C^{16}O$ for $^{13}C^{18}O$. As in the case of monometallic Pt-catalyst, the singleton frequencies for linearly adsorbed $^{12}C^{16}O$ and $^{13}C^{18}O$ on Pt were equal to 2040 and 1945 cm^{-1}, but the dipole-dipole shift for both molecules decreased from 41 cm^{-1} to 33 cm^{-1}.

Spectra of $^{12}C^{16}O$ adsorbed on a freshly reduced Pt1Cu3 catalyst were recorded at a range of equilibrium pressures (Figure 6.8). The band at 2032 cm^{-1} corresponded to linearly adsorbed CO on Pt, while the band at 2136 cm^{-1} was attributed to CO adsorbed

on Cu.[106] A strong decrease in the intensity of the Cu band with decreasing equilibrium CO pressure indicated that the CO-Cu species was unstable. As the CO pressure decreased, the band positions for CO adsorbed on both Pt and Cu remained unchanged. Subsequent evacuation of the sample at room temperature for 12 h resulted in the band at 2032 cm^{-1} decreasing substantially in intensity, and the maximum shifting toward the singleton frequency of linearly adsorbed on Pt, 2023 cm^{-1}.

Spectra were collected as $^{13}C^{18}O$ replaced preadsorbed $^{12}C^{16}O$ on a Pt1Cu1 catalyst treated in CO at 473 K (Figure 6.9). While equilibrium with the gas phase CO was maintained, the spectrum of $^{12}C^{16}O$ consisted of two bands at 2052 and 2136 cm^{-1}. These bands corresponded to CO molecules linearly adsorbed on metallic Pt and Cu, respectively. As in the case of the freshly reduced sample, the high-frequency band disappeared after brief sample evacuation at room temperature. During the exchange of preadsorbed $^{12}C^{16}O$ for $^{13}C^{18}O$ the band positions of both linearly adsorbed $^{12}C^{16}O$ and $^{13}C^{18}O$ remained unchanged.

6.3.2 Non-steady State Kinetics of CH2ClCH2Cl+H2 Reaction

It was conservatively estimated that diffusion in the cell limits the transfer of reactants and products to a maximum rate of approximately 0.05 μmol/s. This value exceeds the observed reaction rates by at least two orders of magnitude. It was concluded that mass transfer limitation were not present. However, due to the uncertainty introduced by any theoretical calculation and the easy accessibility and greater sensitivity

of other techniques for measuring activity, the choice was made to consider only product distribution and accumulation trends rather than rigorously evaluating activity.

With a five fold excess of hydrogen, 1,2-dichloroethane was converted exclusively into ethane and HCl over both monometallic Pt and bimetallic Pt1Cu1 catalysts (Figure 6.1). Lowering the Pt:Cu atomic ratio to Pt1Cu3 resulted in the formation of not only ethane and HCl, but also ethylene (Figure 6.2). The selectivity toward formation of ethylene decreased from 76 to 50% after 40 min time on stream.

Both monometallic Pt and Pt1Cu1 showed no selectivity changes upon addition of CO (~2 Torr) to the reaction mixture; only ethane and HCl were formed. With the addition of only 2 Torr of CO to the reaction mixture over the Pt1Cu3 catalyst, only ethylene formed (Figure 6.3).

Exposing the Pt1Cu1 catalyst to 35 Torr of CO at 473 K for 0.5 h dramatically changed the selectivity behavior in comparison to the results obtained for the same catalyst in the absence of CO. In the presence of CO, ethylene was formed predominantly at the beginning of the reaction (Figure 6.4). After 20 min, the mole fraction of ethylene reached a maximum of 4.5% and remained constant thereafter. The mole fraction of ethane increased gradually with reaction time and after 15 min exceeded the concentration of ethylene.

6.3.3 Flow System Kinetics of CH2ClCH2Cl+H2 Reaction

The influence of CO on activity and selectivity was reversible, as shown by the differential, flow kinetics experiment presented in Figure 6.5. For the Pt1Cu1/SiO_2

catalyst in the absence of CO in the reactant stream, ethane was the main product with a selectivity in excess of 95%; monochloroethane (5%) was also observed (Figure 6.5). Upon addition of CO, ethylene was the main product with a selectivity of approximately 90% with the minor product being ethane. No monochloroethane was observed. When the CO was eliminated, initial selectivity was restored. Activity, which was reduced by approximately 25% upon addition of CO, also returned to its original level when CO was removed. The CO was not consumed during the reaction.

6.4 Discussion

The results of this investigation prompt the question of why the addition of Cu suppresses the hydrogenation activity of Pt to the extent that ethylene is the major product formed from CH_2ClCH_2Cl and H_2 instead of ethane. A change in the electronic properties of the Pt is a reasonable interpretation to consider. The singleton frequency associated with CO adsorbed on Pt is essentially the same for the freshly reduced Pt1Cu1 catalyst as for the monometallic Pt sample (2040 cm^{-1}). Both these catalysts produce only ethane. For the Pt1Cu3 catalyst, with which the ethylene selectivity is 76%, the singleton frequency is 8 cm^{-1} less (2032 cm^{-1}) than the Pt1Cu1 and Pt catalyst.

The 8 cm^{-1} shift is indicative of donation of electron density from Cu to Pt.[107-108] Hall and Emmett theorized this sort of interaction between group 8 and 1B metals, i.e. the donation of electrons from the group 1B metal to the incompletely filled d-band of the group 8 metal, was responsible for activity and selectivity changes in Cu-Ni hydrogenation catalysts.[97] Since the development of more direct techniques such as

FTIR spectroscopy, there is disagreement in the literature about whether or not such modification occurs in dispersed catalytic systems. Ponec and coworkers believed that electronic modification of Pt by Cu in these systems was very slight or nonexistent.[105-106] More recent studies by Grunert and coworkers[109] and our own work[43] seem to suggest that electronic modification, if unimportant to catalytic performance, does occur.

A distinctly different change in the electronic properties of Pt occurs when the PtCu1 catalyst is heated in CO at 473 K for 0.5 h. A shift in singleton frequency from 2040 cm^{-1} to 2052 cm^{-1}, indicating electron withdrawl from Pt, was observed. It is well known that Pt is capable of decomposing CO in Boudart type reactions below 473 K.[98,110] The presence of atomic oxygen coadsorbed with CO is known to result in increasing singleton frequency due to removal of electron density from the surface. Yates and coworkers observed this effect in single crystals of Ni.[111] Oxygen is also known to spillover,[74] particularly in cases where adsorption is more favorable on the neighboring site such as Cu sites adjoining Pt with heats of adsorption of 122 and 67 kcal/mol, respectively.[112] Electron density on Pt is likely reduced directly by absorbed atomic oxygen as well as indirectly by the presence of this oxygen on neighboring Cu sites preventing metal-metal electron donation. The Pt1Cu1, previously 100% ethane selective under all conditions, also becomes initially selective to ethylene after treatment at 473 K in CO.

Changes to electronic state of opposite character accompany similar changes in selectivity. Pt in the Pt1Cu3 catalyst is electron-rich while Pt after treatment of PtCu1 in CO is electron poor, yet both catalyst produce ethylene instead of ethane as the main

product. It is particularly difficult to visualize, then, how electronic effects can be important to selectivity change. Other possibilities seem more plausible.

It is well-established that dilution of one metal with another reduces the average size of ensembles containing only one kind of metal atom. This is most easily explored by examination of band frequency due to CO dipole-dipole shifts using FTIR. In work with Pt-Cu systems similar to those considered here, Chandler and Pignolet analyzed CO adsorption on a cluster-derived, silica-supported Pt-Cu catalyst using DRIFTS.[113] The finding of diminished CO dipole-dipole interaction with respect to that observed by others in coimpregnation catalysts was attributed to a more complete alloy state. Grunert and coworkers examined ZSM-5-supported Pt-Cu catalysts using a variety of techniques including FTIR.[109] They interpreted diminishing CO dipole-dipole interactions after repeated oxidation and reduction cycles in terms of alloy formation resulting in diminished Pt ensemble size. In both these works, changes in dipole-dipole interactions of approximately 10 cm^{-1} are considered substantial. Comparison to this work in which monometallic Pt and freshly reduced Pt1Cu1 show dipole-dipole shifts of 33 and 42 cm^{-1}, respectively, and Pt1Cu3 and CO treated Pt1Cu1 display no interaction whatsoever give strong evidence for the formation of alloys.

The absence of dipole-dipole interaction between linearly adsorbed CO on Pt could indicate that on the metal surface Pt ensembles become finely divided through dilution with Cu.[113] The mechanism by which this occurs could be a redistribution of the metals on the support surface due to the formation of oxychloro-Pt complexes resulting in the formation of greater numbers of Pt-Cu alloy particles with surfaces

enriched in Cu. The phenomenon has been thoroughly characterized by Rochester and coworkers for Pt-Re,[114] Pt-Sn,[115-116] and Pt-Ge[117] systems. Surface enrichment of Cu in Pt-Cu bimetallic particles, as observed by Brongersma and Sparnaay in LEIS experiments,[91] would result in significantly reduced Pt ensemble size, fewer CO molecules in close interaction with one another, and, as a result, a decrease in the dipole-dipole shift observed for CO linearly adsorbed on Pt. Both possibilities have been illustrated in Figure 6.10.

The formation of bimetallic particles with finely divided Pt ensembles, clearly more favorable in the presence of greater amounts of Cu, is likely the reason for the absence of dipole-dipole interactions in the Pt1Cu3 catalyst even without CO pretreatment. By combining a CO isotopic dilution method with manipulation of the dimension of CO islands on Pt(001) and Pt(111) single crystals, King and Crossley were able to correlate the number of interacting CO molecules directly to dipole-dipole shift.[118-119] While Crossley and King obtained results for average ensembles no smaller than 11 contiguous Pt atoms, it is possible to extrapolate their work by taking advantage of the fact that no dipole-dipole shift would occur in the case of isolated Pt atoms. Given the lack of dipole-dipole interaction observed in ethylene selective catalysts, it is posible to suggest that the average Pt ensemble consists of an isolated Pt atom. The presence of a strong CO dipole-dipole shift of 33 cm^{-1} in the freshly reduced Pt1Cu1 catalyst, correlating to Pt ensembles of more than 50 members. .

The correlation between the frequency shifts due to dipole-dipole interactions of adsorbed CO and the existing literature have provided estimates of the Pt ensemble size

for the bimetallic catalysts: 50 or more atoms for Pt1Cu1 and one for Pt1Cu3. The primary intermediates of the dechlorination of 1,2-dichloroethane are thought to be di-σ complexes of ethylene ($PtCH_2CH_2Pt$) formed as a result of two-point adsorption of $C_2H_4Cl_2$ due to homolytic dissociation of two C-Cl bonds.[41-42] Koel and coworkers[120-121] and Dumesic and coworkers[122] have shown that di-σ ethylene adsorption on Pt requires a minimum of 4 contiguous Pt atoms and ethylidyne formation a minimum of 6. It has been argued by others on the basis of the lack of size demand in the hydrogenation of ethylene that ethylene can adsorb on a single Pt atom.[123] While this is certainly true, it offers no evidence as to the form of ethylene on the Pt surface. McCrea and Somorjai have recently shown using sum frequency generation-surface specific vibrational spectroscopy that the hydrogenation of ethylene does not occur through either a di-σ bonded ethylene or ethylidyne intermediate. A π-bonded species, present in much lower concentration, is apparently the active intermediate.[124] Given the more demanding nature of 1,2-dichloroethane adsorption, i.e. the breaking to two C-Cl bonds, it seems unlikely that this adsorption would take place on smaller ensembles. When Pt ensembles of sufficient size to dissociate 1,2-dichloroethane are present, as they are in the monometallic Pt catalyst studied, the hydrocarbon intermediated is quickly hydrogenated to form ethane. A similar process was previously observed for trifluoroethylidynes obtained by chemisorption of 1,1-dichlorotetrafluoroethane on metallic Pd supported on alumina.[125] An illustration of the activity of large Pt and Cu ensembles is given in Figure 6.11.

The suggestion that large Pt ensembles are responsible for ethane formation is further substantiated by the effect of CO on selectivity. It was observed both in the static and flow kinetic systems that only a small amount of CO in the reactant mixture is necessary to greatly increase the selectivity toward ethylene. The difference in heat of adsorption for CO on Pt and Cu at room temperature is known to be considerable, 46 kcal/mol and 19 kcal/mol, respectively.[112] The difference is sufficiently great that CO adsorbs strongly on Pt and can be removed from Cu by simple evacuation.[126] When present in the reaction mixture, CO will preferentially adsorb on Pt sites with an effect similar to that shown in Figure 6.10. In this way, the size of Pt ensembles available for dissociative adsorption of 1,2-dichloroethane, apparently to the extent that the selectivity toward ethane is suppressed (Figures 6.3-5).

It can be argued that chemisorbed chlorine atoms formed in the course of CH_2ClCH_2Cl chemisorption due to homolytic cleavage of C-Cl bonds would have the same dilution effect on Pt ensembles as adsorption of CO. If this were the case, one would expect to observe a decrease in ethane selectivity as Cl coverage on the surface changes. Atomic hydrogen on Pt, however, is highly reactive with chemisorbed chlorine forming HCl which evolves into the gas-phase resulting in cleaning of the metal surface.[65] With a barrier to H_2 dissociation of 1 kcal/mol, it is difficult to imagine a surface more resistant to Cl poisoning than Pt.[65] The reversibility of the selectivity change which occurs in the presence of CO is also important. This is observed in the flow kinetics experiment (Figure 6.5). The lack of a permanent change in the catalyst

gives evidence that no global restructuring of the catalyst surface occurs and points again to the dilution of Pt ensembles by simple, reversible adsorption.

When ethylene is the major product, it appears that most Pt ensembles are not sufficiently large for the dissociation of chemisorbed 1,2-dichloroethane, either because of dilution with Cu or site blocking by CO. Indeed, it may be possible that as one approaches the limiting case, one Pt surface atom surrounded by a large excess of Cu atoms, that the dissociative chemisorption of 1,2-dichloroethane occurs on Cu.[69,127]

Given the previously observed low activity of the monometallic Cu catalyst in these reactions,[42] it is difficult to visualize how Cu could be solely responsible for the catalysts activity. The lower activity of the monometallic Cu catalyst is likely due to its larger energy barrier for H_2 dissociation (14 kcal/mol for Cu[64] and 1 kcal/mol for Pt[65]). The lack of ability of Cu to rapidly dissociate H_2 would lead to the accumulation of Cl on the surface and rapid deactivation.

It is clear then that Cu suppresses the hydrogenation ability of Pt by removing the ability of Pt to adsorb 1,2-dichloroethane. The observed activity of the catalyst is not significantly decreased because Cu also has the ability to take over this step because Pt, which can dissociate H_2 regardless of ensemble size,[128] prevents the accumulation of Cl on the surface. An illustration of the process is shown in Figure 6.12.

6.5 Conclusions

The addition of Cu to a silica-supported Pt catalyst modifies it both geometrically and electronically. Strong CO dipole-dipole interactions are observed in the

monometallic Pt and Pt1Cu1 catalysts. The geometric effect of Cu is characterized by the diminished CO dipole-dipole interactions observed in the presence of Cu for the Pt1Cu3 catalyst and the Pt1Cu1 catalyst after high temperature treatment in the presence of CO. Changes in the singleton frequencies observed by the isotopic dilution method of both Pt and Cu show that both are electronically modified.

Silica-supported Pt-Cu catalysts show selectivity toward ethylene only when Pt ensembles are sufficiently small to eliminate the CO dipole-dipole interactions observed in FTIR spectroscopy. The geometric effect is thought to be more important to changes in the ethylene selectivity of the catalyst since the observed changes in electronic state are found in both ethylene and ethane selective catalysts.

The observations are consistent with the idea that smaller Pt ensembles lose the ability to dissociatively adsorb 1,2-dichloroethane forcing this critical step to shift to Cu sites. The Cu sites, having lower H coverage, would then be more likely to desorb rather than hydrogenate the ethylene intermediate. The result is a catalytic cycle in which the only role of Pt is to provide dissociated H_2 to prevent Cl poisoning of the active Cu sites.

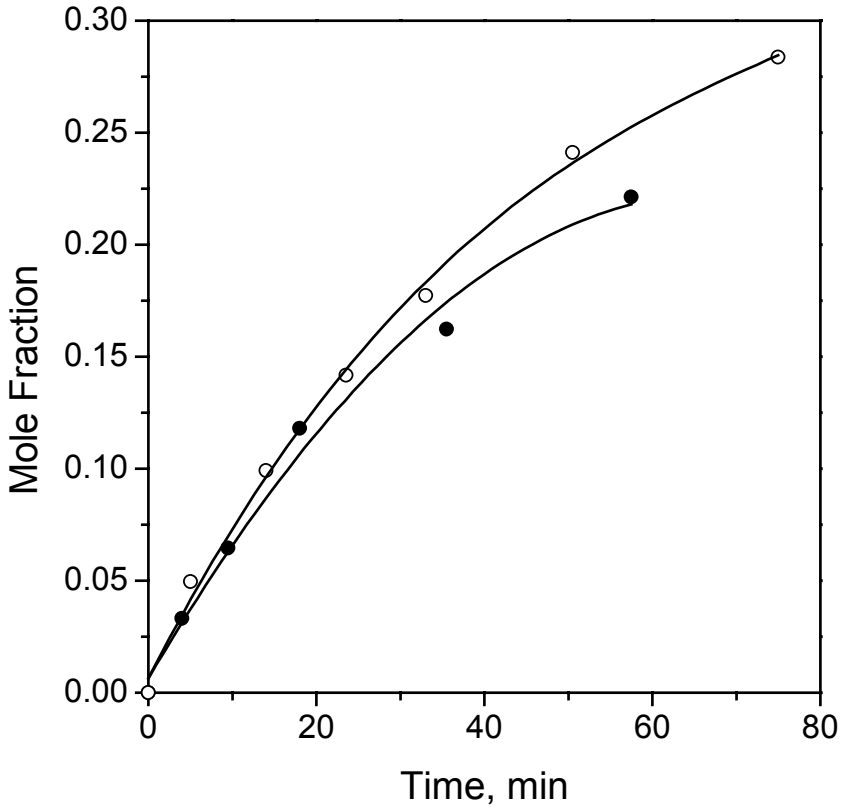

Figure 6. 1 Dynamics of ethane accumulation in the catalyzed $CH_2ClCH_2Cl+H_2$ reaction at 523 K in a static reactor; (●) – Pt/SiO_2, initial pressures of CH_2ClCH_2Cl and H_2 were 10.0 and 50.0 Torr, respectively; (○) – $Pt1Cu1/SiO_2$, initial pressures of CH_2ClCH_2Cl and H_2 were 7.0 and 35.0 Torr, respectively.

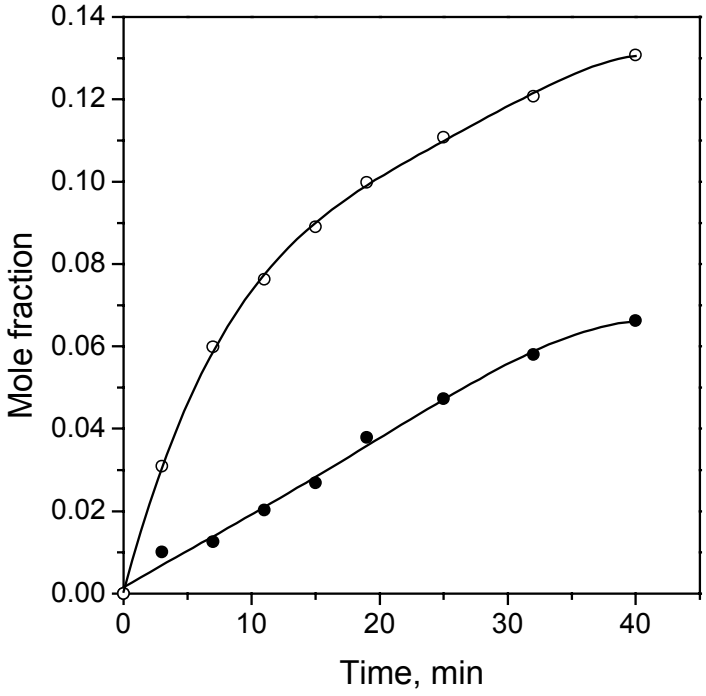

Figure 6. 2 Dynamics of reaction product accumulation in the $CH_2ClCH_2Cl+H_2$ reaction catalyzed by $Pt1Cu3/SiO_2$ at 523 K in a static reactor to form C_2H_4 (○) and C_2H_6 (●). Initial pressures of CH_2ClCH_2Cl and H_2 were 7.8 and 50.0 Torr, respectively.

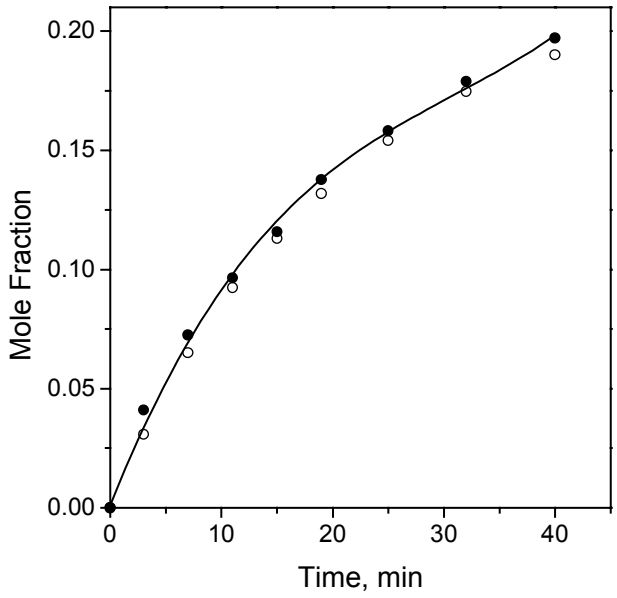

Figure 6. 3 Dynamics of reaction product accumulation in the $CH_2ClCH_2Cl+H_2$ reaction catalyzed by $Pt1Cu3/SiO_2$ at 523 K in a static reactor without (●) and with addition of 1.5 Torr CO (○). Initial pressures of CH_2ClCH_2Cl and H_2 were 7.8 and 50.0 Torr, respectively.

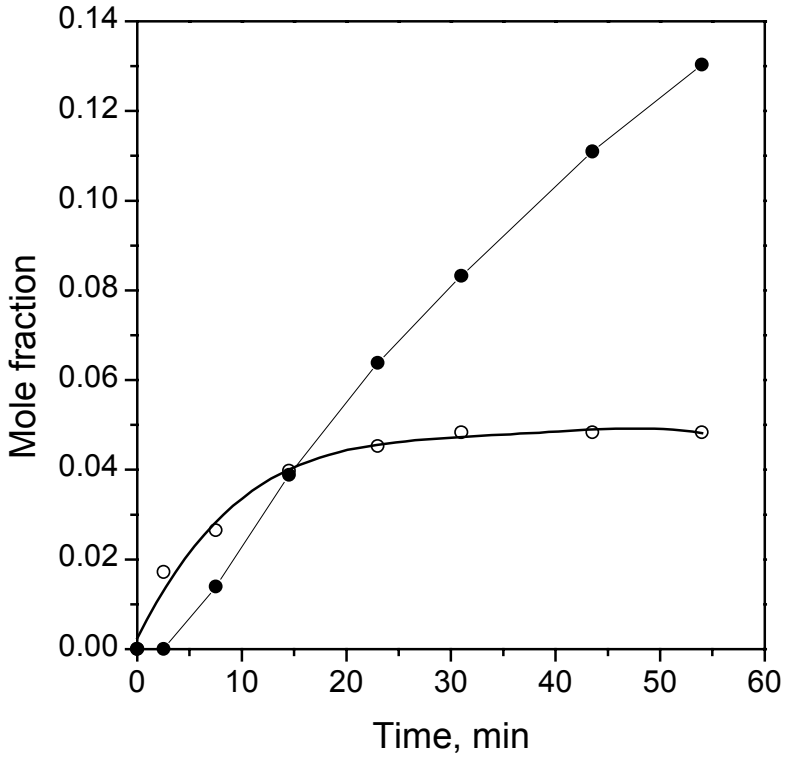

Figure 6. 4 Dynamics of reaction product accumulation, C_2H_4 (○) and C_2H_6 (●), in the $CH_2ClCH_2Cl+H_2$ reaction with CO addition catalyzed by $Pt1Cu1/SiO_2$ at 523 K in a static reactor. Initial pressures of CH_2ClCH_2Cl, H_2, and CO were 9.0, 45.0, and 1.5 Torr, respectively.

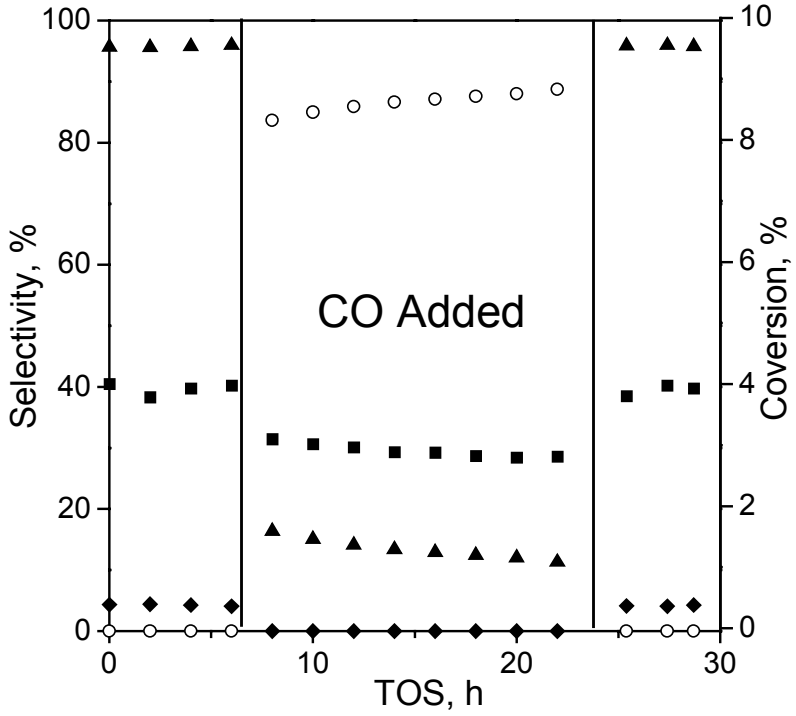

Figure 6. 5 Time on stream performance of the $Pt1Cu1/SiO_2$ in the $CH_2ClCH_2Cl+H_2$ reaction at 473 K in a continuous flow reactor with and without CO in the stream; (○), ethylene, (▲), ethane, (♦), ethyl chloride, (€), conversion.

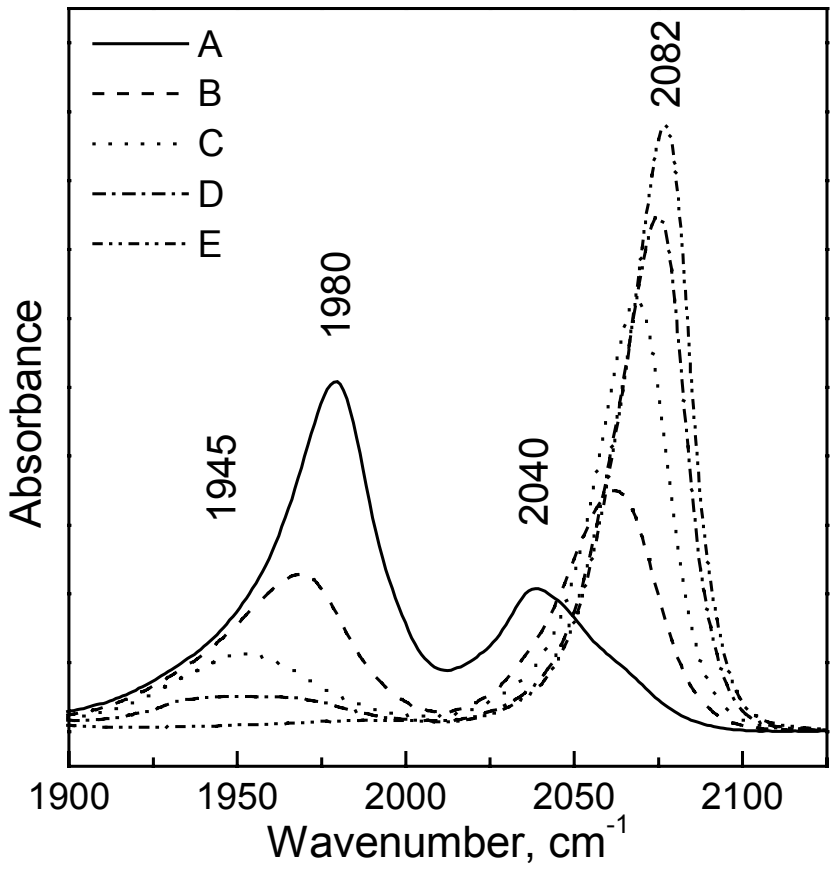

Figure 6. 6 Dynamics of the exchange of $^{12}C^{16}O$ pre-adsorbed on the reduced Pt/SiO_2 with gaseous $^{13}C^{18}O$ at ambient temperature shown as spectra in the presence of gas-phase $^{12}C^{16}O$ (A), after evacuation at room temperature (B), and at 30 (C), 60 (D), and 75% (E) exchange.

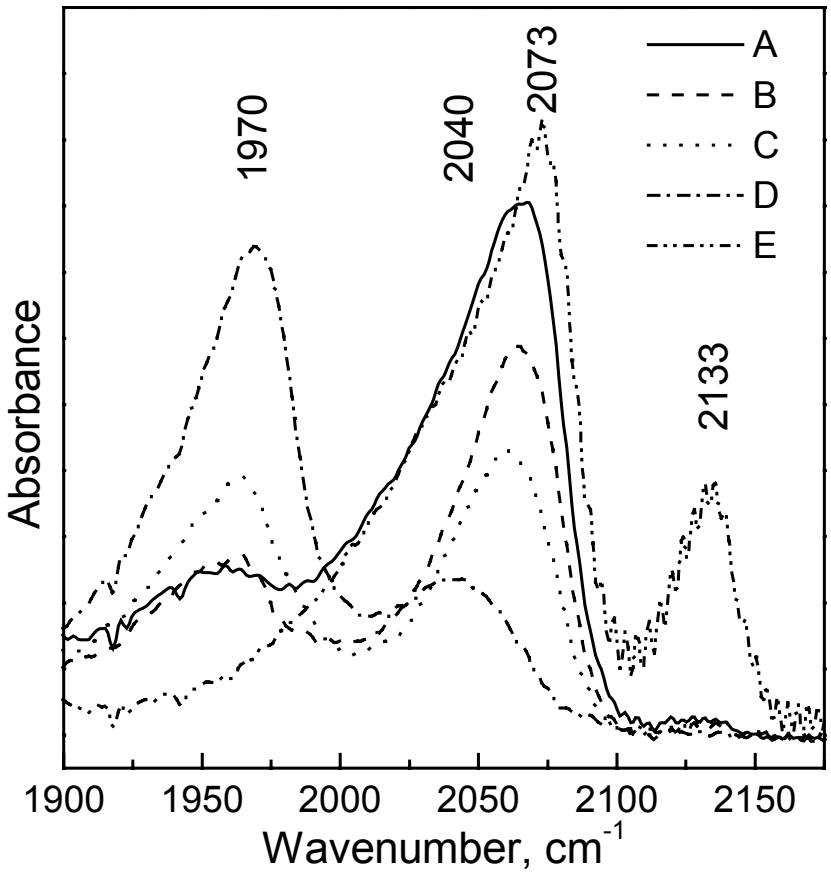

Figure 6. 7 Dynamics of the exchange of $^{12}C^{16}O$ pre-adsorbed on the reduced $Pt1Cu1/SiO_2$ with gaseous $^{13}C^{18}O$ at ambient temperature shown as spectra in the presence of gas-phase $^{12}C^{16}O$ (A), after evacuation at room temperature (B), and at 27 (C), 45 (D), and 70% (E) exchange.

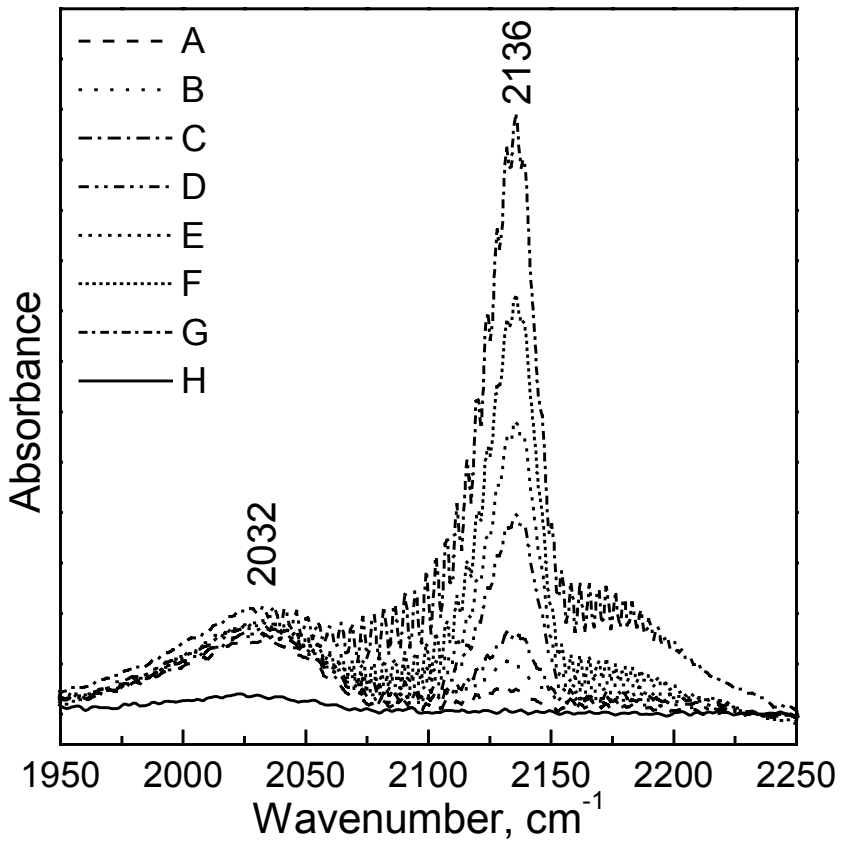

Figure 6. 8 IR spectra of CO adsorbed on reduced Pt1Cu3/SiO_2 at equilibrium pressures of 4.3 (A), 2.15 (B), 1.07 (C), 0.53 (D), 0.26 (E), 0.13 (F), 0.07 (G) Torr, and after evacuation of the sample with pre-adsorbed CO at room temperature for 12h (H).

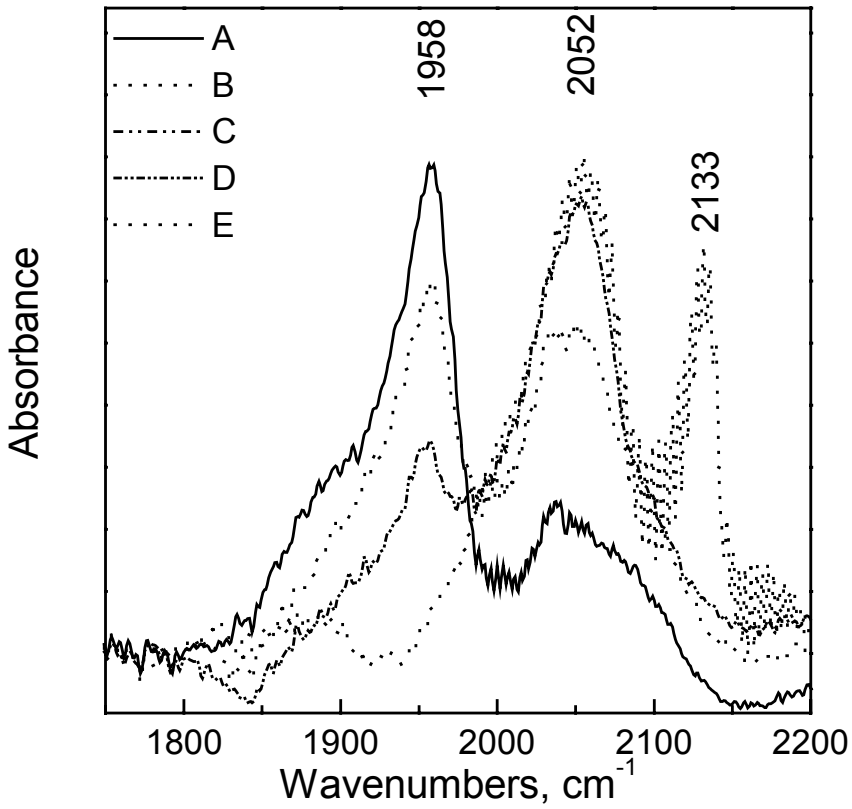

Figure 6. 9 Dynamics of the exchange of $^{12}C^{16}O$ pre-adsorbed on the reduced $Pt1Cu1/SiO_2$ after heating in 35 Torr CO for 0.5 h at 473 K with gaseous $^{13}C^{18}O$ at ambient temperature shown as spectra in the presence of gas-phase $^{12}C^{16}O$ (A), after evacuation at room temperature (B), and at 25 (C), 40 (D), and 65% (E) exchange.

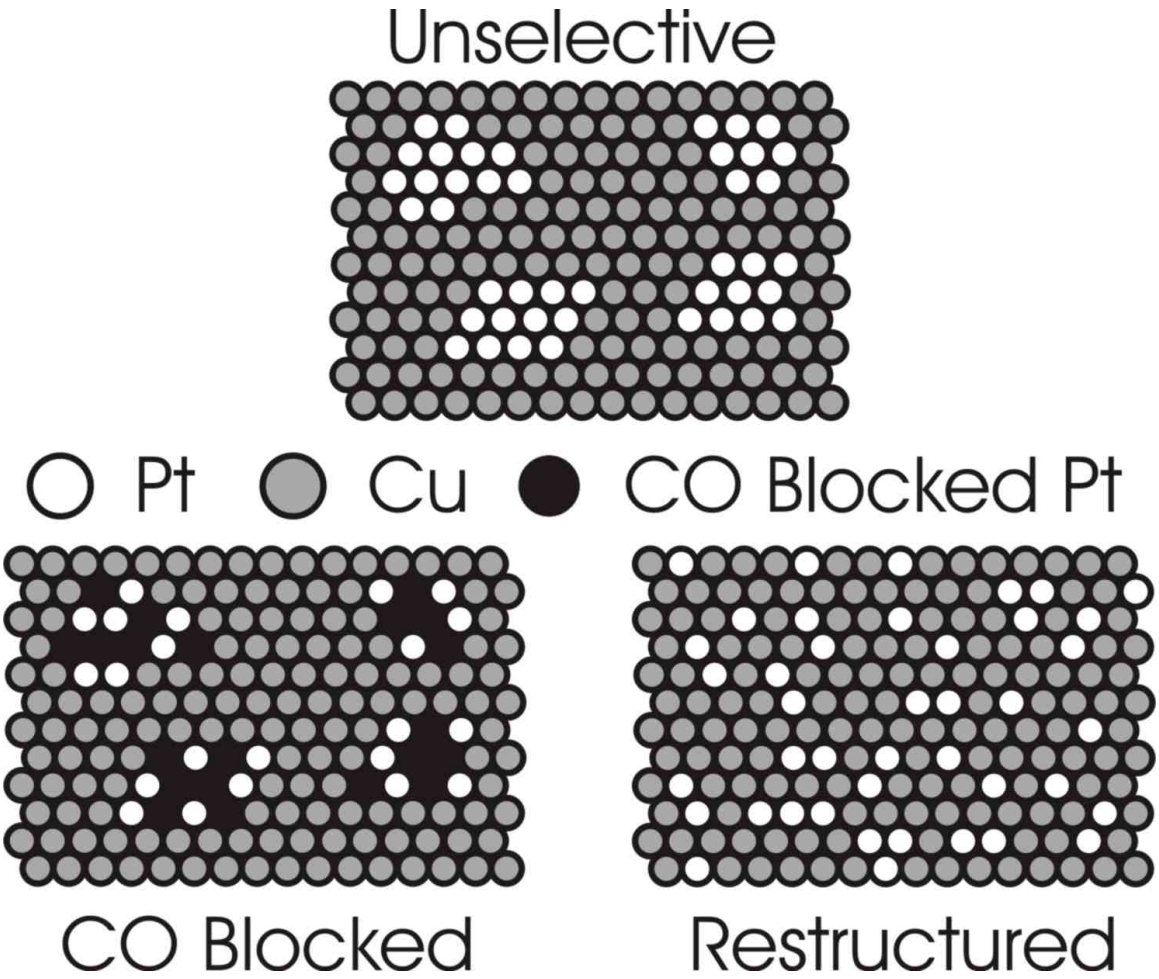

Figure 6. 10 Illustration of possible changes in Pt ensembles associated with CO pretreatment in the $Pt1Cu1/SiO_2$ catalyst showing the fresh catalyst(above), the catalyst after poisoning by Boudart type interactions of CO with the surface(left), and the catalyst after restructuring by metal carbonyl chlorides (right).

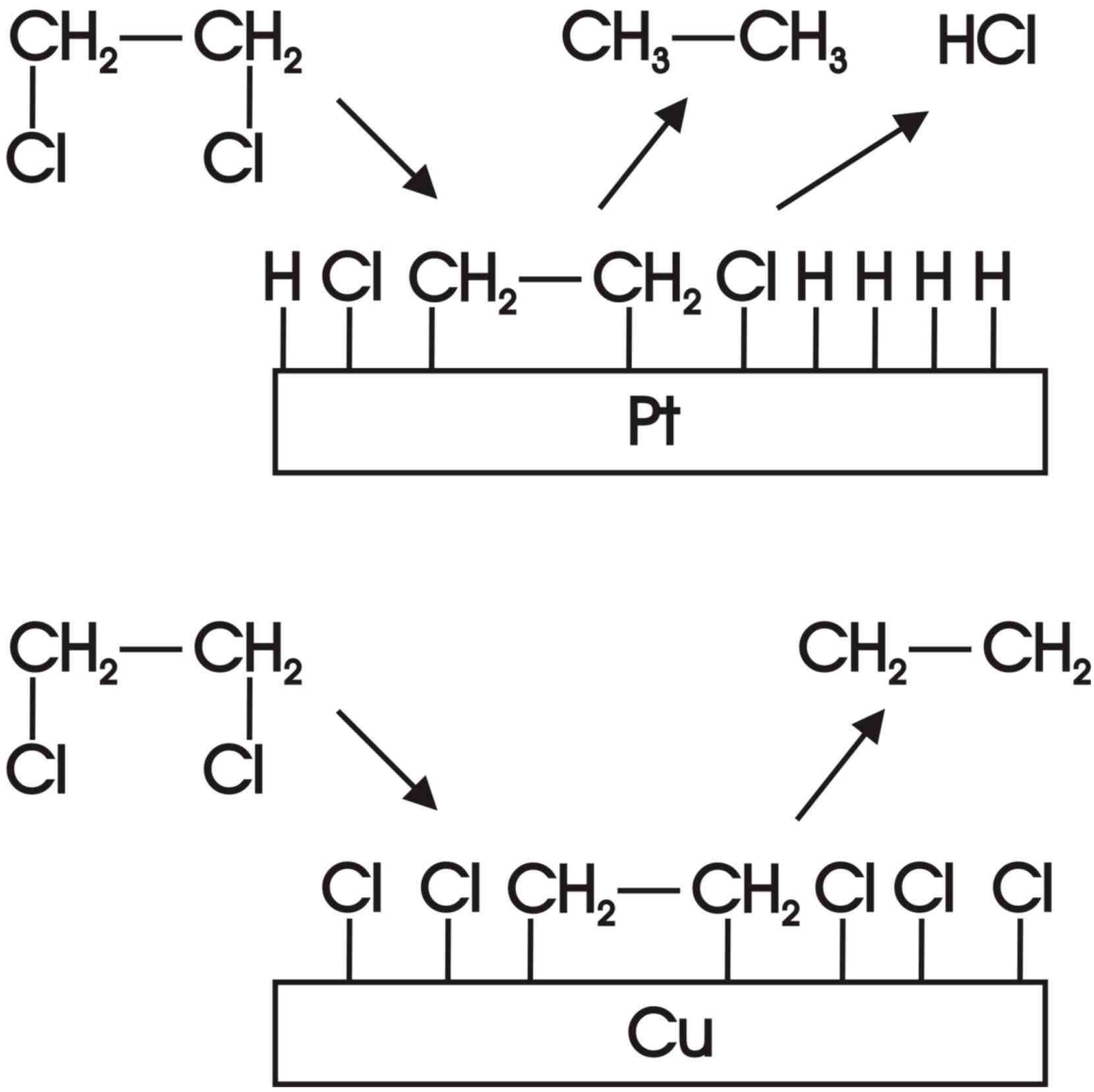

Figure 6. 11 Illustration of a possible reaction scheme for monometallic Pt(above) and Cu(below) which is likely similar to the activity observed in bimetallic catalysts with considerable metal segregation.

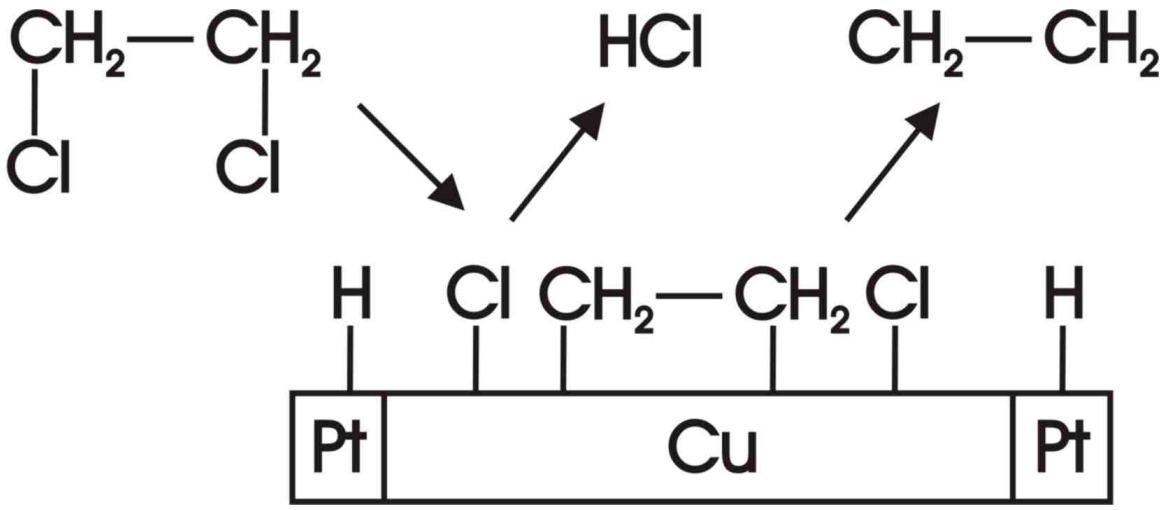

Figure 6. 12 Illustration of a possible reaction scheme for bimetallic catalysts with small Pt ensembles incapable of dissociative adsorption of 1,2-dichloroethane.

7.0 SUMMARY AND FUTURE WORK

The final chapter of this thesis summarizes the contribution of this work to science as perceived by the author.

7.1 Major Results

Kinetic investigation of the transient period in selectivity from ethane as the main product in the dechlorination of 1,2-dichloroethane to ethylene for carbon-supported, Pt-Cu catalysts (Chapter 3) led to a number of interesting revelations about the behavior of these catalysts in the presence of surface Cl. It was discovered that variation of pretreatment to include higher temperature or HCl resulted in the destruction of the transient period. Since the transient period was found to be absent after pretreatments designed to increase (i.e. HCl treatment) and decrease (i.e. 400^{o}C reduction) the amount of surface Cl, it was possible to eliminate the build-up of surface Cl as a possible cause of the change in selectivity. Further evidence for this was given by the lack of effect of successive reduction/reaction cycles on the selectivity transience. By comparing the effect of treatment at 220^{o}C in the presence of the chloride precursors to treatment at 220^{o}C in the reduced state, the suggestion was made that Cl enhanced metal mobility resulting in the formation of alloy particles active in the production of ethylene.

Further insight into these phenomena was given by investigation of silica-supported Pt-Cu catalysts using pulse and flow kinetics techniques as well as FTIR spectroscopic studies (Chapter 4). The indirect role of Cl in determining selectivity was

confirmed by examining the selectivity in pulse experiments which admitted only small amounts of 1,2-dichloroethane every 40 min. In this way, the Cl surface coverage was greatly reduced, and it was possible to examine selectivity in the first minute of reaction. It was shown that even at very early TOS, before equilibrium coverage of Cl has been achieved, some catalysts had high ethylene selectivity.

Examination of the catalyst surface using FTIR spectroscopy and CO adsorption showed the importance of geometric over electronic effects. By observing the similar singleton frequencies of CO adsorbed on Pt in ethylene-selective, Pt1Cu3 catalysts and ethane-selective, Pt1Cu1 catalysts electronic modification of Pt sites was eliminated as a possible cause of ethylene selectivity in Pt-Cu catalysts. Since CO dipole-dipole interaction, caused by CO molecules adsorbed on adjacent Pt atoms, was observed only in ethane selective catalysts, it was concluded that limiting the size of Pt ensembles by alloying with Cu results in ethylene selectivity.

The study of the effect of water on chloride-precursor, Pt-Cu catalysts (Chapter 5) yielded important information about the differences in alloying caused by water and that caused by high temperature treatment. Transmission electron microscopy showed that both 400^{o}C reduction and treatment with water resulted in the formation of bimetallic particles. Only after high temperature reduction, however, did the particles consist of the Pt-Cu solid solution predicted by the system's bulk thermodynamic properties. After treatment with water, each bimetallic particle consisted of a Pt core (diameter ~25 Å) encapsulated in a shell of oxidized Cu (thickness 5-10 Å). Kinetic investigations showed that regardless of the mechanism of bimetallic particle formation catalysts containing

bimetallic particles remained selective to ethylene. Examination of the time required for the effect of water to take place and differences in the effect of water on catalysts prepared from differing precursors allowed the suggestion that reformation of the impregnation solution in the catalyst pores results in the alleviation of chromatographic separations which were artifacts of the original coimpregnation procedure.

By limiting the size of Pt ensembles using CO adsorption (Chapter 6), the mechanism of dechlorination on Pt-Cu catalysts was elucidated. In FTIR studies electronic effects caused by alloying of Pt and Cu were eliminated as the root cause of ethylene selectivity. It was observed that the addition of CO, which preferentially adsorbs on Pt, to the reaction mixture resulted in the formation of ethylene in bimetallic catalysts previously selective toward ethane.

These results allow the suggestion that limiting the size of Pt ensembles results in a shift in dissociative adsorption of 1,2-dichloroethane from Pt to Cu sites. High hydrogen coverage on Pt sites results in the formation of ethane when the 1,2-dichloroethane adsorption takes place there. Lower hydrogen coverage on Cu sites allows desorption of the intermediate to form ethylene. Size demand in dissociation of the C-Cl bond is the most probable reason for the shift in adsorption.

7.2 Future Work

A variety of work remains to be done to fully explore the reactions of 1,2-dichloroethane over Pt-Cu catalysts. A firm foundation of kinetic and basic characterization techniques has been built. Still required is unification of the several

aspects of this work. In the case of alloy effects, direct, in-situ observation of the catalyst state at various times during reaction would serve to bridge all previous observations and allow final conclusions to be drawn about the effect of alloy state on catalyst performance. Any number of techniques would allow this sort of observation, the simplest and most widely available being XPS. A full molecular-level understanding of the events leading to the formation of ethane and ethylene, respectively, on the catalyst surface requires the work discussed in the author's Ph.D proposal. This work, involving the variation of Pt ensemble size by coking reactions and comparison of C-Cl bond scission rates as ensemble size is varied, could serve to confirm the size demanding nature of the C-Cl bond scission and provide the final piece in the proposed reaction scheme.

BIBLIOGRAPHY

BIBLIOGRAPHY

(1) Kawauchi T., Nishiyama K. Environ. Res. 48 (1989) 296.

(2) Fries, A.A. Trans. Am. Electrochem. Soc. (1926) 49.

(3) Guglielminetti, M. Compt. Rend. 143 (1907) 1191.

(4) Risebrough, R.W. Chem. Fallout (1969) 5.

(5) Durham, W.F. J. Dairy Sci. 54 (1971) 701.

(6) Ray, B.T. "Environmental Engineering" PWS: New York, 1995.

(7) Anderson, J.G., Margitan, J.J., Stedman, D.H. Science 198 (1977) 501.

(8) Nemerow, N.L., Agardy, F.J. "Strategies of Industrial and Hazardous Waste Management" VNR: New York, 1998.

(9) Malanchuk, J., Hillier, E., Wallace, L. Environ. Prot. Eng. 27 (2001) 5.

(10) Kim, D.I., Allen, D.T. Ind. Eng. Chem. Res., 36 (1997) 3019 and references therein.

(11) Ponec, V., Bond, G.C. "Catalysis by Metals and Alloys," Elsevier: Amsterdam, 1995.

(12) Bodnariuk, P., Coq, B., Ferrat, G., Figueras, F. J. Catal., 116 (1989) 459.

(13) Sinfelt, J.H. Adv. Catal., 23 (1973) 91.

(14) Campbell, J.S., Kemball, C. Trans. Faraday Soc., 57 (1961) 809.

(15) Burton, J.J., Garten, R.L. *in:* Adv. Mater. Catal. (Burton, J.J. and Garten, R.L., Eds.) Academic Press, New York, 1977. P. 33.

(16) Yermakov, Yu.I., Kuznetsov, B.N., Zakharov, V.A. "Catalysis by Supported Complexes" Elsevier: Amsterdam, 1981.

(17) Sachtler, W.M.H., van Santen, R.A. Adv. Catal., 26 (1977) 69.

(18) Peden, C.H.F., Goodman, D.W. J. Catal., 104 (1987) 347.

(19) Dautzenberg, F.M., Helle, J.N., Biloen, P., Sachtler, W.M.H. J. Catal., 63 (1980) 119.

(20) Carter, J.L., McVicker, G.B., Weissman, J., Kmak, W.S., Sinfelt, J.H. Appl. Catal., 3 (1982) 327.

(21) Dowden, D.A., Reynolds, P.W. Discussions Faraday Soc. 184 (1950) 189.

(22) Hall, W.K., Emmett, P.H. J. Phys. Chem. 62 (1958) 816.

(23) Hall, W.K., Emmett, P.H. J. Phys. Chem. 63 (1959) 1102.

(24) Sinfelt, J.H. Acc. Chem. Res. 10 (1977) 15.

(25) Rodriguez, J.A., Campbell, R.A., Goodman, D.W. Surf. Sci. 307 (1994) 377.

(26) Rodriguez, J.A., Campbell, R.A., Goodman, D.W. J. Phys. Chem. 95 (1991) 5716.

(27) Rodriguez, J.A., Goodman, D.W. Science 257 (1992) 897.

(28) Natal-Santiago, M.A., Podkolzin, S.G., Cortright, R.D., Dumesic, J.A. Catal. Lett. 45 (1997) 155.

(29) Shen, J., Hill, J.M., Watwe, R.M., Spiewak, B.E., Dumesic, J.A. J. Phys. Chem. B 103 (1999) 3923.

(30) Che, M., Bennett, C.O. Adv. Catal. 36 (1989) 55.

(31) De Jongste, H.C., Ponec, V., Gault, F.G., J. Catal. 63 (1980) 395.

(32) Paffett, M.T., Gebhard, S.C., Windham, R.G., Koel, B.E. Surf. Sci. 223 (1989) 449.

(33) Tsai, Y.L., Xu, C., Koel, B.E. Surf. Sci. 385 (1997) 37.

(34) Larsen, J.H., Chorkendorff, I. Surf. Sci. 405 (1998) 62.

(35) Larsen, J.H., Chorkendorff, I. Catal. Lett. 52 (1998) 1.

(36) Nerlov, J.; Chorkendorff, I. Catal. Lett. 54 (1998) 171.

(37) Nerlov, J.; Chorkendorff, I. J. Catal. 181 (1999) 271.

(38) Nerlov, J., Sckerl, S., Wambach, J., Chorkendorff, I. App. Catal. A 191 (2000) 97.

(39) Greenlief, C.M., Berlowitz, P.J., Goodman, D.W., White, J.M. J. Phys. Chem. 91 (1987) 6669.

(40) Ito, L.N., Harley, D.A., Holbrook, M.T., Smith, D.D., Murchison, C.B., Cisneros, M.D. Eur. Patent 0 640 574 A1 (1994), to The Dow Chemical Company.

(41) Heinrichs, B., Delhez, P., Schoebrechts, J., Pirard, J. J. Catal. 172 (1997) 322.

(42) Vadlamannati, L.S., Kovalchuk, V.I., d'Itri, J.L. Catal. Lett. 58 (1999) 173.

(43) Vadlamannati, L.S., Luebke, D.R., Kovalchuk, V.I., d'Itri, J.L. Stud. Surf. Sci. Catal. 130A (2000) 233.

(44) Early, K.O., Rhodes, W.D., Kovalchuk, V.I., d'Itri, J.L. Appl. Catal. B 26 (2000) 257.

(45) Heinrichs, B., Noville, F., Schoebrechts, J., Pirard, J. J. Catal. 192 (2000) 108.

(46) Stevenson, S.A., Dumesic, J.A., Baker, R.T.K., Ruckenstein, E. (Eds.), Metal-Support Interactions in Catalysis, Sintering, and Redispersion, Van Nostrand Reinhold, New York, 1987.

(47) Yang, M.X., Sharkar, S., Bent, B.E., Bare, S.R., Holbrook, M.T. Langmuir 13 (1997) 229.

(48) Anderson, J.R. Structure of Metallic Catalysts, Academic Press, London et al., 1975.

(49) CRC Handbook of Chemistry and Physiscs, 73rd Edition, CRC Press, Boca Raton et al., 1992.

(50) Borovkov, V. Yu, Unpublished results.

(51) Hultgren, R., Desai, P.D., Hawkins, D.T., Gleiser, M., Kelley, K.K. Selected Values of the Thermodynamic Properties of Binary Alloys, American Society for Metals, Metal Park, OH, 1973.

(52) Cotton, F.A., Wikinson, G. Advanced Inorganic Chemistry, Wiley, New York et al., 1988.

(53) Erley, W. Surf. Sci. 94 (1980) 281.

(54) Erley, W. Surf. Sci. 114 (1982) 47.

(55) Takeuchi, A., Ken-ichi, T., Isamu, T., Koshiro, M. J. Catal. 40 (1975) 94 and references therein.

(56) Shin, E.J., Spiller, A., Tavoularis, G., Keane, M.A. Phys. Chem. Chem. Phys. 1 (1999) 3173.

(57) Peden, C.H.F., Goodman, D.W. J. Catal., 104 (1987) 347.

(58) Dautzenberg, F.M., Helle, J.N., Biloen, P., Sachtler, W.M.H. J. Catal., 63 (1980) 119.

(59) Carter, J.L., McVicker, G.B., Weissman, J., Kmak, W.S., Sinfelt, J.H. Appl. Catal., 3 (1982) 327.

(60) Deshmukh, S.S.; Borovkov, V.Yu.; Kovalchuk, V.I.; d'Itri, J.L. J. Phys. Chem. B 104 (2000) 1277.

(61) Hammaker, R.M.; Francis, S.; Eischens, R.P. Spectrochim. Acta 21 (1965) 1295.

(62) Sheppard, N.; Nguyen, T.T. Adv. in Infrared and Raman Spectr., 5 (1978) 67.

(63) Dandekar, A.; Vannice, M.A. J. Catal., 178 (1998) 621 and references therein.

(64) Campbell, J. M., Campbell, C.T. Surf. Sci. 259 (1991) 1.

(65) Salmeron, M.; Gale, R.J.; Somerjai, G.A. J. Chem. Phys. 70 (1979) 2807.

(66) F. Stoop, F.; Toolenaar, F.J.C.M.; Ponec, V. J. C. S. Chem. Comm. (1981) 1024.

(67) Trapnell, B. M. W. Proc. Soc. London A, 218 (1953) 566.

(68) Passos, F.B.; Schmal, M.; Vannice, M.A. J. Catal., 160 (1996) 118.

(69) Yang, M.X.; Sarcar, S.; Bent, B.E. Langmuir, 13 (1997) 229.

(70) Walter, W.K.; Jones, R.G.; Waugh, K.S.; Bailey, S. Catal. Lett. 24 (1994) 333.

(71) Anderson, J.R.; Avery, N.R. Catal., 5 (1966) 446.

(72) Primet, M. J. Catal., 88 (1984) 273 and references therein.

(73) Fouilloux, P.; Cordier, G.; Colleuille, Y. Stud. Surf. Sci. Catal., 11 (1982) 369.

(74) Conner, W.C., Jr.; Falconer, J.L. Chem. Rev. 95 (1995) 759-788.

(75) Ichikawa, M. Adv. Catal. 38 (1992) 283.

(76) Lesage, P.; Clause, O.; Moral, P.; Didillon, B.; Candy, J.P.; Basset, J.M. J. Catal. 155 (1995) 238-248.

(77) Ferretti, O.A.; Siri, G.J.; Humblot, F.; Candy, J.P.; Didillon, B.; Basset, J.M. React. Kinet. Catal. Lett. 63 (1998) 115-120.

(78) Margitfalvi, J.L.; Borbath, I.; Tfirst, E.; Tompos, A. Catal. Today 43 (1998) 29-49.

(79) Michel, C.G., Bambrick, W.E., Ebel, R.H. Fuel Process. Technol. 35 (1993) 159.

(80) Prestvik, R., Moljord, K., Grande, K., Holmen, A. J. Catal. 174 (1998) 119.

(81) Gjervan, T., Prestvik, R., Totdal, B., Lyman, C.E., Holmen, A. Catal. Today 65 (2001) 163.

(82) Anderson, J.H., Conn, P.J., Brandenberger, S.G. J. Catal. 16 (1970) 326.

(83) Luebke, D., Vadlamannati, L., Kovalchuk, V., d'Itri, J. Appl. Catal. B, 35 (2002) 211.

(84) Beattie, I.R., Gilson, T.R., Ozin, G.A. J. Chem. Soc. A (1969) 534.

(85) Debeau, M., Krauzman, M. C. R. Hebd. Seances Acad. Sci. 92 (1970) 3645.

(86) Person, I., Sandstrom, M., Steel, A.T., Zapetero, M.J., Aakesson, R. Inorg. Chem. 30 (1991) 4075.

(87) Nakamoto, K. "Infrared and Raman Spectra of Inorganic and Coordination Compounds," Wiley: New York, 1997.

(88) Kawashima, T., Takai, K., Aso, H., Manabe, T., Takizawa, K., Kachi-Terajima, C., Ishii, T., Miyasaka, H., Matsuzaka, H., Yamashita, M., Okamoto, H., Kitagawa, H., Shiro, M., Toriumi, K. Inorg. Chem. 40 (2001) 6651.

(89) Kozakevitch, P.P., Urbain, G. C. R. Paris 253 (1961) 2229.

(90) Giorgio, S., Graoui, H., Chapon, C., Henry, C.R. Met. Clusters Chem. 2 (1999) 1194.

(91) Brongersma, H.H., Sparnaay, M.J. Surf. Sci. 71 (1978) 657.

(92) Wilkins, F.J. Phil. Mag. 11 (1931) 422.

(93) Bird, R.B., Stewart, W.E., Lightfoot, E.N. "Transport Phenomena," Wiley: New York, 1960.

(94) Lide, D.R. edt. "CRC Handbook of Chemistry and Physics," CRC Press: Boca Raton, 1992.

(95) Sinfelt, J.H. Acc. Chem. Res. 10 (1977) 15.

(96) Dowden, D.A., Reynolds, P.W. Discussions Faraday Soc. 184 (1950) 189.

(97) Hall, W.K., Emmett, P.H. J. Phys. Chem. 62 (1958) 816.

(98) Boudart, M. Adv. Catal. 20 (1969) 153.

(99) Anderson, J.A. J. Catal. 142 (1993) 153.

(100) Zanier-Szydlowski, N., Moisson, B., Blejean, F., Didillon, B. Proc. SPIE-Int. Soc. Opt. Eng. 2089 (1993) 410.

(101) de Menorval, L., Chaqroune, A., Coq, B., Figuerast, F. J. Chem. Soc. Faraday Trans. 93 (1997) 3715.

(102) Chandler, B. D.; Schabel, A. B.; Rubinstein, L. I.; Pignolet, L. H. Chem. Ind. 75 (1998) 607.

(103) Slattery, J.C., Bird, R.B., AIChE. J., 4 (1958) 137.

(104) De La Crus, C.; Sheppard, N. Spectrochim. Acta A50 (1994) 271.

(105) Toolenaar, F.J.C.M.;Stoop, F.; Ponec, V. J. Catal. 82 (1983) 1.

(106) Toolenaar, F.J.C.M.; Reinalda, D.; Ponec, V. J. Catal. 64 (1980) 110.

(107) Severson, M.W., Stuhlmann, C., Villegas, I., Weaver, M.J. J. Chem. Phys. 103 (1995) 9832.

(108) Balakrishnan, K., Schwank, J. J. Catal. 138 (1992), 491.

(109) Shpiro, E.S., Tkachenko, O.P., Jaeger, N.I., Schulz-Ekloff, G., Grunert, W. J. Phys. Chem. B 102 (1998) 3798.

(110) McCrea, K.R., Parker, J., Chen, P., Somorjai, G. Abstr. Pap. - Am. Chem. Soc. (2001), 221st COLL-183.

(111) Xu, Z., Surnev, L., Uram, K.J., Yates, J.T. Surf. Sci. 292 (1993) 235.

(112) Somorjai, G.A. *Introduction to Surface Chemistry and Catalysis* (Wiley, New York, 1994).

(113) Chandler, B.D., Pignolet, L.H. Catal. Today 65 (2001) 39.

(114) Malet, P., Munuera, G., Caballero, A. J. Catal. 115 (1989) 567.

(115) Arteaga, G.J., Anderson, J.A., Becker, S.M., Rochester, C.H. J. Mol. Catal. A 145 (1999) 183.

(116) Anstice, P.J.C., Becker, S.M., Rochester, C.H. Catal. Lett. 74 (2001) 9.

(117) Arteaga, G.J., Anderson, J.A., Rochester, C.H. J. Catal. 189 (2000) 195.

(118) Crossley, A., King, D.A. Surf. Sci. 95 (1980) 131.

(119) King, D.A Springer Ser. Chem. Phys. 15 (1980) 179.

(120) Windham, R.G., Koel, B.E., Paffett, M.T. Langmuir 4 (1988) 1113.

(121) Paffett, M.T., Gebhard, S.C., Windham, R.G., Koel, B.E. Surf. Sci. 223 (1989) 449.

(122) Cortright, R.D., Dumesic, J.A. J. Catal. 148 (1994) 771.

(123) Osborn, J.A., Jardine, F.H., Young, J.F., Wilkinson, G. J. Chem. Soc. A (1966) 1711.

(124) McCrea, K.R., Somorjai, G.A. J. Mol. Catal. A Chem. 163 (2000) 43.

(125) Borovkov, V.Yu.; Lonyi, F.; Kovalchuk, V.I.; d'Itri, J.L. J. Chem. Phys. B 104 (2000) 5603.

(126) Sokolova, N. A.; Barkova, A. P.; Furman, D. B.; Borovkov, V. Yu.; Kazansky, V. B. Kinet. Catal. 36 (1995) 434.

(127) Walter, W.K.; Jones, R.G.; Waugh, K.S.; Bailey, S. Catal. Lett. 24 (1994) 333.

(128) Linke, R. Schneider, U., Busse, H., Becker, C., Schroder, U., Castro, G.R., Wandelt, K. Surf. Sci. 307 (1994) 407.